

Compensatory movement simulation of subacromial impingement syndrome
kinematics using an asymptomatic group for rehabilitative shoulder exercises

by

Daniel Fournier

A thesis

presented to the University of Waterloo

in fulfillment of the

thesis requirement for the degree of

Master of Science

in

Kinesiology

Waterloo, Ontario, Canada, 2021

© Daniel Fournier 2021

Author's Declaration

I hereby declare that I am the sole author of this thesis. This is a true copy of the thesis, including any required final revisions, as accepted by my examiners.

I understand that my thesis may be made electronically available to the public.

Abstract

Rotator cuff tears are a common source of shoulder pain that requires conservative management or surgical intervention to heal and regain proper function. During both interventions, prescribed exercise programs are given to patients as they increase range of motion (ROM) and improve patient outcome scores. However, when tasked with completing exercises in the home, patient adherence usually decreases and is subjectively monitored by the patient themselves. Wearable sensor devices, such as smartwatches, demonstrate feasibility to objectively track shoulder exercise adherence using machine learning, but these algorithms require a broad range of training data in order to accurately classify exercise type. Further, to monitor shoulder exercise rehabilitation, sensor training data should include compensatory exercise performance associated with symptomatic individuals. However, capturing this movement data from a symptomatic population presents a number of challenges. To address this problem, the objective of this study was to determine if asymptomatic individuals can simulate compensatory movement cues associated with subacromial impingement during various rehabilitative shoulder exercises.

Seventeen participants (10 asymptomatic and 7 symptomatic for subacromial impingement) performed twenty repetitions of six evidence-based shoulder exercises following standard and compensatory movement cues based on their group classification. Kinematics of the torso and upper limbs were collected to identify changes in maximum angle and ROM for torso, thoracohumeral and elbow joint angles. Time-series joint angle data were compared for the standard and compensatory conditions performed by the asymptomatic group using statistical parametric mapping (SPM). Symptomatic and asymptomatic (compensatory) were compared using maximum angle and ROM measures.

Asymptomatic participants were successful in simulating compensatory movement cues based on changes in their time-series data. Differences occurred in the middle portion of the thoracohumeral elevation time-series profile during the flexion ($p < 0.05$), scaption ($p < 0.05$), and abduction ($p < 0.05$) exercises. Further, these simulated compensatory movements were similar to the movement patterns of some symptomatic participants. Overall, these results suggest that asymptomatic individuals can execute both standard and compensatory movement cues. The variability of the data collected represents a spectrum between worst-case compensatory and best-case proper movement for the six shoulder exercises performed. Further research is needed to better understand the range of symptomatic exercise performance in order to refine the movement cue instructions for asymptomatic individual performance. Data and findings from this work provide crucial groundwork towards the development of improved machine learning algorithms for sensor-based tracking of rehabilitative shoulder exercise program adherence and progression.

Acknowledgements

This thesis could not have been completed without the support and advice from numerous individuals. First, I would like to thank my supervisors Dr. Clark Dickerson and Dr. Stewart McLachlin for their continued support throughout my degree. Your expertise and love of biomechanics research always brought a source of positivity and encouragement during each step of the process. I am grateful for the opportunity to have worked with you both and will always cherish my time as a graduate student.

A sincere thank you to Dr. Steven Fischer and Dr. Robyn Ibey for sitting on my thesis committee. I am thankful for your time and valuable feedback as it has pushed me to think more critically and to be a better researcher.

I would also like to thank my DIESEL lab mates Alicia, Jackie, Cristina, Paula, Jacklyn, Bhillie, Tea, Alan, Alison and all the co-op students that I had to opportunity to work and interact with. Whether it was grabbing coffee, discussing problems/issues we were facing or solving the world's problems outside of the lab, I truly appreciate the impact you all have had on this project and on me as an individual. Further, I would like to thank my ORTHOtron lab mates for their feedback, support and encouragement during my time as a graduate student.

To Rachel Whittaker, thank you so much for your belief in me! The feedback and reassurance you provided me over the last two and a half years does not go unnoticed. To Chris Moore, from undergrad to graduate school, you have always been down to run, workout or simply grab a beer, which allowed me to decompress and maintain my sanity. I am grateful for our friendship and look forward to many more running adventures together! To Patrick Naylor, thank you for being my go-to guy to grab coffee with at C&D. Without your mathematical knowledge and wisdom, I don't think I would have ever figured out rotation matrix math. To Tom Hoshizaki, thanks for being a great friend since the start of my grad school journey. I don't think I would have made it through 612/613 without our study/work sessions.

Last, but definitely not least, thank you to my family and my partner Diane Russel. Thank you for supporting me throughout the ups and downs of this degree. Although I kept the majority of things to myself and never went into great detail on what I was working on, I could always tell that you were by my side every step of the way. That is what kept me moving forward.

TABLE OF CONTENTS

Author’s Declaration.....	ii
Abstract.....	iii
Acknowledgements.....	v
LIST OF FIGURES	ix
LIST OF TABLES.....	xii
LIST OF ABBREVIATIONS.....	xiii
1.0 INTRODUCTION	1
1.1 Research Objectives.....	4
1.2 Hypotheses.....	5
1.3 Relevance.....	5
2.0 LITERATURE REVIEW	7
2.1 The Shoulder Complex.....	7
2.2 The Rotator Cuff.....	9
2.3 Rotator Cuff Tears	13
2.4 Treatment & Rehabilitation	15
2.5 Wearables & Machine Learning for Rehabilitation.....	19
3.0 METHODOLOGY	21
3.1 Participants.....	21

3.2 Instrumentation	22
3.2.1 Motion Capture	22
3.3 Experimental Protocol	24
3.3.1 Collection Protocol	25
3.4 Data Analysis	29
3.4.1 Motion Capture Processing.....	29
3.4.2 Statistical Analysis.....	35
3.4.2.1 Statistical Parametric Mapping	35
3.4.2.2 Mann-Whitney U Test	35
4.0 Results.....	36
4.1 Active Assisted Shoulder Flexion.....	36
4.2 Active Assisted Shoulder Scaption.....	40
4.3 Shoulder Abduction	43
4.4 Internal Rotation	47
4.5 External Rotation	50
4.6 Standing Row.....	53
5.0 Discussion.....	56
5.1 Hypotheses.....	57
5.1.1 Hypothesis #1.....	57
5.1.2 Hypothesis #2.....	58

5.2 Kinematics	58
5.2.1 Time-Series Data	58
5.2.2 Maximum Angle & ROM Measures.....	60
5.3 Research Contributions and Applications.....	62
5.4 Limitations	63
5.4.1 Kinematic Data Reduction.....	63
5.4.2 Participant Sample	63
5.5 Future Directions	64
6.0 Conclusions.....	66
References.....	67
Appendix A: QuickDASH Questionnaire.....	80
Appendix B: Individual Participant Results	83

LIST OF FIGURES

Figure 1: An anterior view of the bones and ligaments of the shoulder complex (Engin, 1980)..	8
Figure 2: The anatomy of the rotator cuff muscles (Cooper & Ali, 2013).....	10
Figure 3: Interaction between load and elevation angle for the anterior supraspinatus in abduction (Cudlip & Dickerson, 2018).....	10
Figure 4: Mean integral electromyography (iEMG) of teres minor during flexion and abduction movements (Hamada et al., 2017).....	12
Figure 5: VICON marker placement on the anterior and posterior upper extremities and torso. Blue dots represent individual markers and triangles represents marker clusters	24
Figure 6: Overview of the experimental data collection protocol	25
Figure 7: Visual representation of the angle calculated to represent the shoulder shrug cues	32
Figure 8: Averaged participant group thoracohumeral elevation angle (left), torso lateral flexion angle (middle) and shoulder shrug angle (right) for asymptomatic participants performing active assisted shoulder flexion.....	38
Figure 9: Thoracohumeral elevation maximum angle for the active assisted shoulder flexion exercise at the 5th, 10th and 15th repetitions	39
Figure 10: Torso lateral flexion ROM for the active assisted shoulder flexion exercise at the 5th, 10th and 15th repetitions	39
Figure 11: Shoulder shrug ROM for the active assisted shoulder flexion exercise at the 5th, 10th and 15th repetitions	40
Figure 12: Averaged participant group thoracohumeral elevation angle (left), torso lateral flexion angle (middle) and shoulder shrug angle (right) for asymptomatic participants performing active assisted shoulder scaption.....	41
Figure 13: Thoracohumeral elevation maximum angle for the active assisted shoulder scaption exercise at the 5th, 10th and 15th repetitions	42
Figure 14: Torso lateral flexion ROM for the active assisted shoulder scaption exercise at the 5th, 10th and 15th repetitions	42
Figure 15: Shoulder shrug ROM for the active assisted shoulder scaption exercise at the 5th, 10th and 15th repetitions	43
Figure 16: Averaged participant group thoracohumeral elevation angle (top left), thoracohumeral internal/external rotation (top right), elbow internal/external rotation (bottom left) and shoulder shrug angle (bottom right) for asymptomatic participants performing shoulder abduction	44
Figure 17: Thoracohumeral elevation maximum angle for the shoulder abduction exercise at the 5th, 10th and 15th repetitions.....	45
Figure 18: Thoracohumeral axial rotation ROM for the shoulder abduction exercise at the 5th, 10th, and 15th repetitions	45
Figure 19: Forearm axial rotation ROM for the shoulder abduction exercise at the 5th, 10th, and 15th repetitions.....	46
Figure 20: Shoulder shrug ROM for the shoulder abduction exercise at the 5th, 10th and 15th repetitions.....	46
Figure 21: Averaged participant group thoracohumeral elevation angle (left), torso axial rotation angle (middle) and shoulder shrug angle (right) for asymptomatic participants performing shoulder internal rotation	48

Figure 22: Thoracohumeral elevation maximum angle for the shoulder internal rotation exercise at the 5 th , 10 th and 15 th repetitions	49
Figure 23: Torso axial rotation ROM for the shoulder internal rotation exercise at the 5 th , 10 th and 15 th repetitions	49
Figure 24: Shoulder shrug ROM for the shoulder internal rotation exercise at the 5 th , 10 th and 15 th repetitions.....	50
Figure 25: Averaged participant group thoracohumeral elevation angle (left), torso axial rotation angle (middle) and shoulder shrug angle (right) for asymptomatic participants performing shoulder external rotation.....	51
Figure 26: Thoracohumeral elevation maximum angle for the shoulder external rotation exercise at the 5 th , 10 th and 15 th repetitions	52
Figure 27: Torso axial rotation ROM for the shoulder external rotation exercise at the 5 th , 10 th and 15 th repetitions	52
Figure 28: Shoulder shrug ROM for the shoulder external rotation exercise at the 5 th , 10 th and 15 th repetitions.....	53
Figure 29: Averaged participant group elbow flexion/extension angle (left) and shoulder shrug angle (right) for asymptomatic participants performing standing row	54
Figure 30: Elbow flexion ROM for the standing row exercise at the 5 th , 10 th and 15 th repetitions.....	55
Figure 31: Shoulder shrug ROM for the standing row exercise at the 5 th , 10 th and 15 th repetitions.....	55
Figure 32: Mean thoracohumeral elevation maximum angle for the active assisted shoulder flexion exercise of all participants.	57
Figure 33: Mean torso lateral flexion ROM for the active assisted shoulder flexion exercise of all participants	83
Figure 34: Mean shoulder shrug ROM for the active assisted shoulder flexion exercise of all participants	83
Figure 35: Mean thoracohumeral elevation maximum angle for the active assisted shoulder scaption exercise of all participants	84
Figure 36: Mean torso lateral flexion ROM for the active assisted shoulder scaption exercise of all participants	84
Figure 37: Mean shoulder shrug ROM for the active assisted shoulder scaption exercise of all participants	85
Figure 38: Mean thoracohumeral elevation maximum angle for the shoulder abduction exercise of all participants.....	85
Figure 39: Mean thoracohumeral axial rotation ROM for the shoulder abduction exercise of all participants	86
Figure 40: Mean forearm axial rotation ROM for the shoulder abduction exercise of all participants	86
Figure 41: Mean shoulder shrug ROM for the shoulder abduction exercise of all participants..	87
Figure 42: Mean thoracohumeral elevation maximum angle for the internal rotation exercise of all participants	87
Figure 43: Mean torso axial rotation ROM for the internal rotation exercise of all participants	88
Figure 44: Mean shoulder shrug ROM for the internal rotation exercise of all participants.....	88
Figure 45: Mean thoracohumeral elevation maximum angle for the external rotation exercise of all participants	89

Figure 46: Mean torso axial rotation ROM for the external rotation exercise of all participants 89
Figure 47: Mean shoulder shrug ROM for the external rotation exercise of all participants 90
Figure 48: Mean elbow flexion ROM for the standing row exercise of all participants 90
Figure 49: Mean shoulder shrug ROM for the standing row exercise of all participants..... 91

LIST OF TABLES

Table 1: Classification of Rotator Cuff Tears (Vollans & Ali, 2016).....	14
Table 2: Summary of rehabilitative shoulder exercises and the muscles activated during exercise performance.....	17
Table 3: Participant demographics (mean \pm SD). R indicates right-hand dominant and L indicates left-hand dominant. F indicates female participants and M indicates male participants	21
Table 4: VICON marker placement based on recommendations from Wu et al. (2005)	23
Table 5: Standard and compensatory movement cues for six common rotator cuff rehabilitation exercises	27
Table 6: Local coordinate systems for the thorax, humerus and forearm segments as outlined by Wu et al. (2005).....	30
Table 7: Rotation sequences for joint angle calculations with clinical interpretations as outlined by Wu et al. (2005) for rotation axes as denoted by e1, e2 and e3	33
Table 8: Selected compensatory movement cues and their associated joint angles used for comparison between standard and simulated compensatory exercise performance by the asymptomatic group	34

LIST OF ABBREVIATIONS

AC.....	Acromioclavicular
ACR.....	Acromion
ADL.....	Activities of Daily Living
ANOVA.....	Analysis of Variance
CRNN.....	Convolutional Recurrent Neural Network
EMG.....	Electromyography
fMRI.....	Functional Magnetic Resonance Imaging
GCS.....	Global Coordinate System
GH.....	Glenohumeral
iEMG.....	Integrated Electromyography
ISB.....	International Society of Biomechanics
IMU.....	Inertial Measurement Unit
JRF.....	Joint Reaction Forces
k-NN.....	k-Nearest Neighbors
LCS.....	Local Coordinate System
MRI.....	Magnetic Resonance Imaging
MVC.....	Maximum Voluntary Contraction
MVIC.....	Maximum Voluntary Isometric Contraction
ML.....	Machine Learning
PET.....	Positron Emission Tomography
RCT.....	Rotator Cuff Tears
RF.....	Random Forest
ROM.....	Range of Motion
SAS.....	Subacromial Space
SAIS.....	Subacromial Impingement Syndrome
SC.....	Sternoclavicular
SD.....	Standard Deviation
SS.....	Suprasternal Notch
SPM.....	Statistical Parametric Mapping
SVC.....	Support Vector Machine Classifier

1.0 INTRODUCTION

Rotator cuff tears (RCT) are a common source of shoulder pain in older adults. The occurrence of partial-thickness and full-thickness tears increases after the age of 50, with a 13% likelihood of adults in their fifties developing a rotator cuff tear. This incidence increases to 20%, 31% and 51% as adults age into their sixties, seventies and eighties, respectively (Tempelhof et al., 1999). RCT account for approximately 33% of all shoulder referrals made for rotator cuff disease (Cooper & Ali, 2013). Further, these injuries can severely impact an individual's ability to perform activities of daily living (ADL) (Hall et al., 2011, Vidt et al., 2016), cause decreases in overall shoulder strength, and negatively impact an individual's perception of their quality of life (MacDermaid et al., 2004).

The progression of rotator cuff tears is quite complex and involves intrinsic and extrinsic factors. The intrinsic theory, described by Codman (1934), attributes poor blood supply to the tendon of the supraspinatus. The lack of blood flow to a specific area of the supraspinatus tendon (1cm from the insertion on the humeral head) results in an area that is highly vulnerable to degeneration with a reduced ability to heal. The extrinsic theory describes the process of subacromial impingement in which the supraspinatus tendon is compressed and damaged in the subacromial space (SAS), consisting of the acromion, the coracoacromial ligament and the humeral head. According to Vollans & Ali (2016), a combination of intrinsic and extrinsic factors leads to the development of RCT with contributions from age-related degeneration and injuries.

Many interventions are used to treat rotator cuff tears, from conservative management strategies (*i.e.*, physical therapy) to surgical interventions. No strong evidence suggests that one treatment option is more advantageous over the other (Ryösä et al., 2017). Therefore,

conservative management is usually suggested as an initial treatment modality, as it is less costly to the individual and the healthcare system while obtaining similar outcomes to surgical interventions. An issue that arises from the conservative management approach is the patient's adherence to at-home exercise protocols, which contributes to the improvement of shoulder function and outcome scores. A study done by Kuhn et al. (2013) found that 75% of patients with atraumatic full-thickness RCT, who adhered to a 12-week physical therapy program, had improvements in range of motion (ROM) and patient reported outcome scores. Adherence to evidence-based exercise protocols has been reported around 50% but this decreases drastically when the patient's physical therapy goes unsupervised in the home setting (Holden et al., 2014). At the moment, current strategies for tracking at-home exercise program adherence consist of discussions with a physiotherapist during appointment attendance, patient exercise diaries or journals, and patient self-reports. All of these adherence methods are subjective resulting in questionable validity for the therapist.

A potential solution to objectively monitor physical therapy adherence is use of wearable devices; these devices contain inertial measurement unit (IMU) sensors which can recognize human activity (Garcia-Ceja et al., 2014; Attal et al., 2015; Nguyen et al., 2015; Picerno et al., 2015). The majority of commercial smartwatches contain an IMU, making them candidate tools for therapists and clinicians to monitor patient progress. Burns et al. (2018) reported that a wrist-worn smartwatch paired with machine learning (ML) algorithms could recognize seven different rotator cuff exercise movements with 99.4% accuracy for a trained and labeled subject-specific dataset of healthy subjects. For new subjects (not in the training data set), the classification performance decreased to 88.9%. This proof-of-concept study demonstrated that a smartwatch could be a feasible method to objectively monitor at-home shoulder physiotherapy exercises; yet,

with only small number of subjects examined, the ML model's classification performance could be improved by training with a broader spectrum of shoulder kinematic profiles. However, prior to implementing such improvements, there is a need to better understand individual differences in shoulder kinematics during rehabilitative exercise performance, specifically between symptomatic and asymptomatic individuals. Previous studies evaluating upper extremity kinematics of asymptomatic and symptomatic populations have focused on the performance of activities of daily living (Kelly et al., 2005; Hall et al., 2011; Vidt et al., 2016). Since most individuals recovering from RCT injuries will follow an exercise program in order to regain normal function, understanding the kinematic differences during their exercises can provide insight into a patient's recovery progression while reaffirming good movement patterns for functional movements, exercises and ADL.

Despite previous studies demonstrating that wearable devices and IMU sensors are effective at tracking and recognizing human activities such as activities of daily living and a variety of exercises (Garcia-Ceja et al., 2014; Attal et al., 2015; Nguyen et al., 2015; Picerno et al., 2015, Burns et al., 2018), these studies used a healthy asymptomatic group as their sample population and generalize results for all individuals based on asymptomatic movements. Typically, there has been little to no representation of symptomatic individuals who will likely have different and possibly compensatory movements. These compensatory movements can include higher ROM and various maximum and minimum joint angles at different segments (McClure et al., 2006; Kasten et al., 2009) to allow a symptomatic individual to complete a task or movement while minimizing pain at the location of their injury. With previous literature describing different compensatory movements in the context of ADL, there is a gap in knowledge when it comes to compensatory movement during rehabilitative shoulder exercises which further confirms the

need to collect and quantify these movements between asymptomatic and symptomatic groups. When it comes to experimental studies, it is often challenging to include symptomatic participants as recruitment of symptomatic subjects can be difficult as they may not want to worsen their injury, or they may simply have difficulty completing the experimental protocols during their visit. In order to build a robust dataset of IMU and kinematic data that could be used to train a ML algorithm, it is crucial to include both asymptomatic and symptomatic movements. Due to challenges with recruitment of symptomatic individuals, an alternative solution to collecting and capturing movements between asymptomatic and symptomatic subjects, as well as those progressing in their rehabilitation, could be to have an asymptomatic group perform both proper and compensatory movement patterns to generate a large spectrum of data representing expected differences between these groups. However, the effectiveness of this approach is currently unknown.

1.1 Research Objectives

The goal of this thesis was to examine whether a healthy asymptomatic group can simulate compensatory shoulder exercise movement cues associated with subacromial impingement rotator cuff pathology. This will be assessed by comparing time-series joint angle profiles of the asymptomatic individuals performing a series of shoulder exercises under guided instruction of movement cues for standard and simulated compensatory exercise performances. A secondary goal of this thesis was to determine if specific compensatory movements cues simulated by an asymptomatic group best depicts exercise movements of a symptomatic population. This will be done by comparing the maximum angle and ROM measures at the 5th,

10th, and 15th repetitions of the asymptomatic simulated compensatory performance and the symptomatic group's exercise performance. The related research questions are as followed:

- 1) Can healthy asymptomatic participants simulate instructed compensatory movement cues associated with a symptomatic rotator cuff population during various rehabilitative shoulder exercises?
- 2) Are the compensatory movement cues simulated by the asymptomatic group similar to the exercise movements of a symptomatic rotator cuff population during a set of various rehabilitative shoulder exercises?

1.2 Hypotheses

- 1) There will be detectable differences in trunk, thoracohumeral and elbow kinematic patterns between standard exercise movements and simulated compensatory exercise movements performed by the asymptomatic group.
- 2) Asymptomatic individuals performing simulated compensatory shoulder exercise movement cues will have similar measures in maximum angle and ROM for trunk, thoracohumeral and elbow movements, compared to symptomatic individuals performing the same shoulder exercises.

1.3 Relevance

Outcomes from this work provide an initial attempt to quantify differences in asymptomatic and symptomatic movement patterns and evaluate the ability to simulate compensatory movement during rehabilitative shoulder exercises. To date, prior work has only examined similar measures with regards to performance of activities of daily living. As such, this

work is crucial to better understanding movement patterns of patients suffering from rotator cuff injuries and how performing simple functional movements such as shoulder exercises, can be used to assess a patient's progress in their rehabilitation. Furthermore, if the kinematics are able to provide evidence that asymptomatic individuals can perform simulated compensatory exercise movements that represent a symptomatic population, we would be able to generate a dataset encompassing a spectrum of movement variability depicting individuals with asymptomatic and symptomatic RCT while avoiding the ethical dilemma of exposing an injured population to movements outside of their current ability. The dataset generated by an asymptomatic population could be used to improve training of ML algorithms to more accurately recognize both rehabilitative shoulder exercises along with the quality of performance based on wrist-worn IMU sensor data. This could potentially drive future work to develop ML models which can better assist tracking exercise adherence and evaluating exercise performance using wearable devices in the home setting, ultimately improving exercise adherence and the outcomes for those suffering from rotator cuff tears.

2.0 LITERATURE REVIEW

2.1 The Shoulder Complex

The shoulder complex is composed of the thorax, sternum, clavicle, scapula, and humerus. These bones articulate to form the sternoclavicular (SC), acromioclavicular (AC), and glenohumeral (GH) joints (Figure 1). These joints allow the coordination of upper extremity movement with a high degree of mobility and the capability to exert forces in many directions. The sternoclavicular joint is defined as a saddle joint with the medial aspect of the clavicle articulating with the clavicular notch of the manubrium and surrounded by the sternoclavicular ligament. Clavicular movements of elevation and depression are both limited by the lower and upper portions of the joint capsule respectively (Engin, 1980). The acromioclavicular joint is the articulation between the lateral aspect of the clavicle and the acromion of the scapula. The joint is surrounded by a fibrous capsule and is supported by the acromioclavicular ligaments. The sternoclavicular and acromioclavicular joints play a role in clavicular elevation, retraction during arm elevation and axial rotation, while the glenohumeral joint and scapulothoracic-gliding plane allow arm elevation and axial rotation of the humerus (Veeger & van der Helm, 2007). Veeger and van der Helm (2007) define the shoulder as a closed-chain mechanism where the humeral head is positioned by the chain formed by the thorax, scapula and clavicle. Changes to the mechanism due to pain or anatomical changes result in decreases in shoulder strength and function. Due to the functional complexity of the glenohumeral joint, its high degree of mobility comes at the cost of reduced inherent stability, requiring the intricate coordination of the muscles, ligaments, tendons and connective tissues for functional movements (Huegel et al., 2015). In order to compensate for the laxity of the glenohumeral capsule and provide sufficient stability, the surrounding ligaments and stabilizing muscles are required to compress the head of

the humerus or redirect any translational forces towards the articular surface of the glenoid fossa. The main ligamentous structures that contribute to glenohumeral stability are the coracohumeral ligament, the superior, middle and inferior glenohumeral ligaments (Burkart & Debski, 2002).

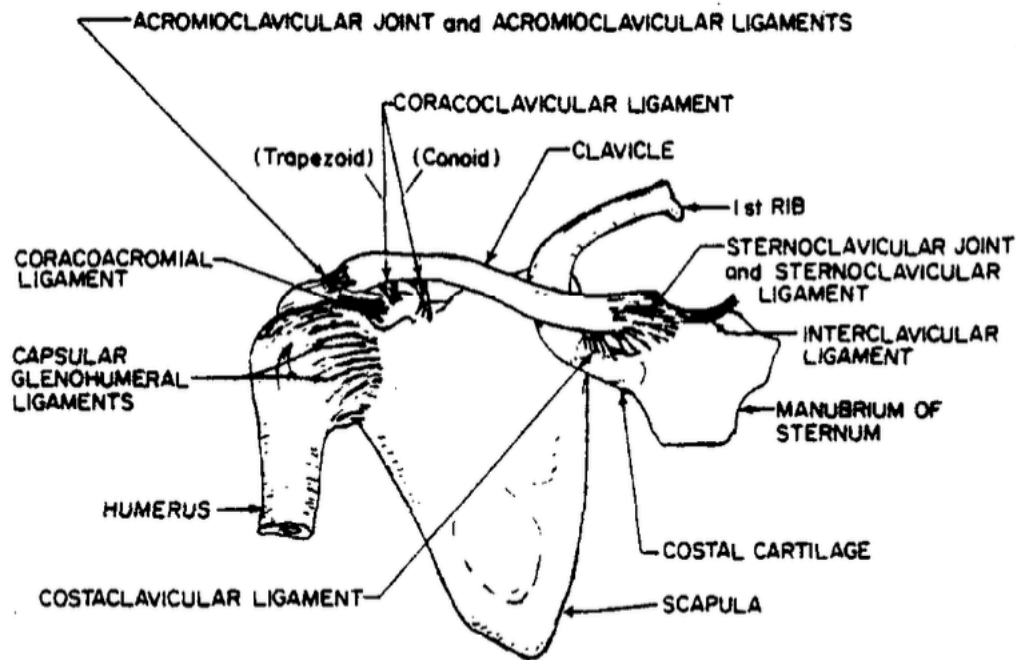


Figure 1: An anterior view of the bones and ligaments of the shoulder complex (Engin, 1980).

In addition to the support from ligamentous structures, the glenohumeral joint relies on the surrounding musculature to keep the resulting joint reaction forces (JRF) directed into the glenoid (Blasier et al., 1997). The muscles contributing to glenohumeral joint stability include the muscles of the rotator cuff, deltoid, pectoralis major and latissimus dorsi. Due to the size and anatomical arrangement of the rotator cuff muscles around the glenohumeral joint, they are primarily responsible for maintaining glenohumeral joint stability. Stability is achieved by pulling the head of the humerus towards the glenoid fossa, resulting in an increase of the compressive joint reaction force (Veeger & van der Helm, 2007). Assistance from the

musculature helps maintain the resulting JRF within the glenoid cavity and ensures that the joint does not experience instability in the form of dislocations or subluxations.

2.2 The Rotator Cuff

The rotator cuff consists of four muscles: supraspinatus, infraspinatus, teres minor and subscapularis (Figure 2). These muscles originate on the body of the scapula and insert on the tuberosities of the proximal humerus. The main roles of the rotator cuff muscles are providing stability to the glenohumeral joint throughout a wide range of motion and producing humeral relative motion. The supraspinatus assists with abduction and external rotation movements of the shoulder (Malanga et al., 1996). This muscle has been studied extensively, as it is commonly the first muscle of the rotator cuff to become injured. The supraspinatus can be divided into an anterior and posterior region with two different functions. The anterior region acts to perform glenohumeral movement while the posterior region serves as a stabilizer for the glenohumeral joint (Cudlip & Dickerson, 2018; Alenabi et al., 2019). When performing tasks that have various working heights and loads, the muscle activation of the supraspinatus increases with workload, and as the elevation angle increases from 5° to 90° (Figure 3).

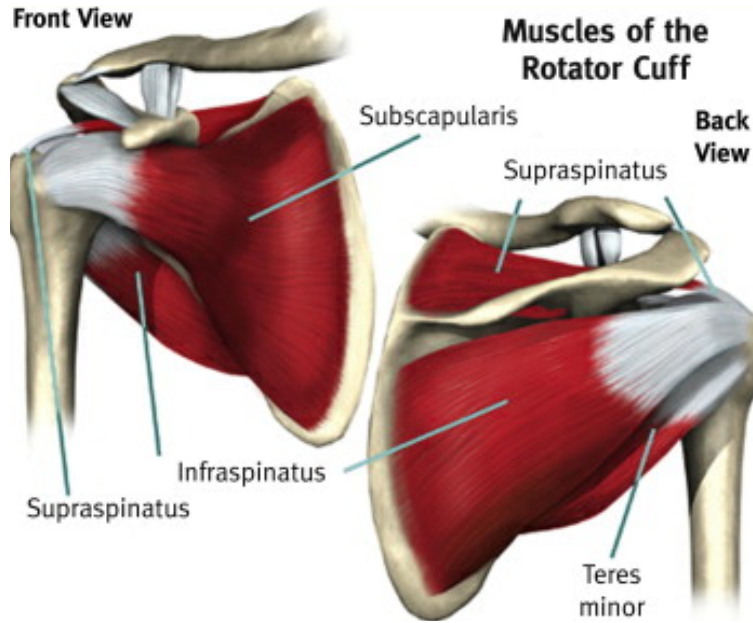


Figure 2: The anatomy of the rotator cuff muscles (Cooper & Ali, 2013).

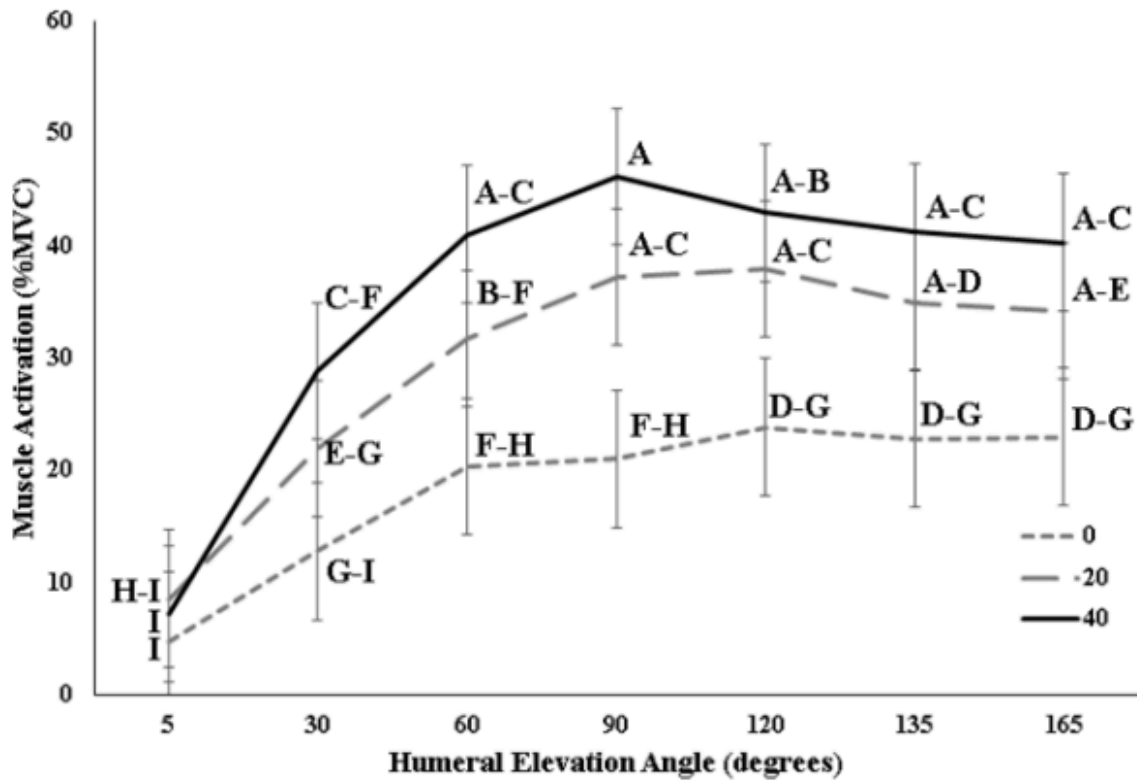


Figure 3: Interaction between load and elevation angle for the anterior supraspinatus in abduction (Cudlip & Dickerson, 2018).

The infraspinatus is involved in external rotation, abduction and flexion movements of the shoulder. It can be divided into the superior, middle and inferior regions of the infraspinatus. As an external rotator of the shoulder, it has been suggested that 0° of humeral abduction is the optimal position for isolating infraspinatus and maximizing force production (Otis et al., 1994; Kelly et al., 1996). Alenabi et al. (2018) reported postural modulation of regional activation of infraspinatus in isometric contractions. The superior region was more active when participants performed external rotation and extension in a prone position, while the middle region of infraspinatus was more active during: 1) seated full can test (arm elevated to 60° and 90° in the scapular plane), 2) seated empty can test (arm elevated to 60° and 90° in the scapular plane) and 3) seated flexion with the arm at 90° of elevation. Similar to the infraspinatus, the teres minor also acts as an external rotator of the humerus. At angles greater than 60° of abduction, the teres minor takes over as the dominant muscle in external rotation of the shoulder (Otis et al., 1994). Like other muscles of the rotator cuff, the teres minor can be divided into an upper and lower portion, separated by tendinous-like fascia. Hamada et al. (2017) found that the upper and lower portion had distinct origin and insertion points with separate innervations from branches of the axillary nerve. The upper portion originates from the lateral edge of the scapula and inserts on the posterior impression of the greater tuberosity, while the lower portion originates from the fascia (between teres minor and infraspinatus) and the inferior surface of the lateral edge of the scapula and inserts in the surgical neck of the humerus (Hamada et al., 2017). Although, the teres minor is primarily considered an external rotator, it experiences similar activation patterns in flexion and abduction as elevation angle increases (Figure 4). This reaffirms the role of teres minor as the dominant external rotator of the shoulder when the humerus begins to reach angles of elevation greater than 60°.

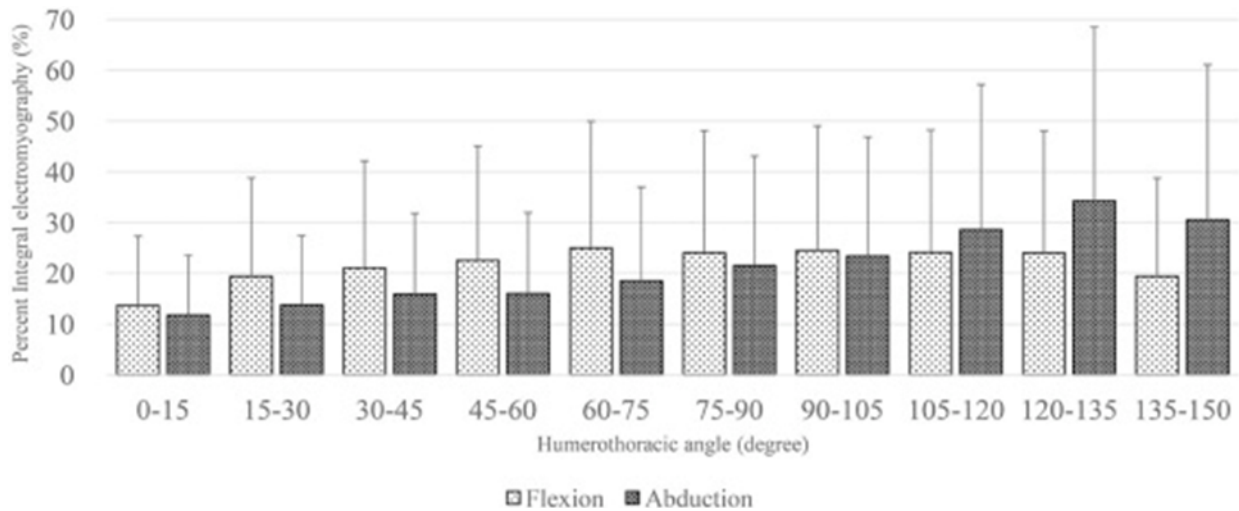


Figure 4: Mean integral electromyography (iEMG) of teres minor during flexion and abduction movements (Hamada et al., 2017).

Lastly, the subscapularis acts primarily as an internal rotator of the humerus but also contributes to abduction movements and stability of the glenohumeral joint. It is the largest muscle of the rotator cuff originating from the subscapular fossa of the anterior scapula and inserts into two locations. As the muscle of the superior two-thirds merges into the subscapularis tendon, it inserts onto the lesser tuberosity, bicipital groove and greater tuberosity of the humeral head. The inferior third of the muscle forms a muscular attachment that inserts onto the inferior aspect of the lesser tuberosity and the anterior aspect of the humeral metaphysis (Morag et al., 2011). Subscapularis can therefore be divided into an upper and lower segment. Each segment is innervated by the upper and lower subscapularis nerves, respectively. With separate innervations, the roles of subscapularis can be assigned based on the electromyography (EMG) activity of the upper and lower segments. A study performed by Rathi et al. (2017) found that during maximum voluntary isometric contractions (MVIC), upper subscapularis showed higher activation during internal rotation and lower subscapularis showed higher activation during external rotation. These findings suggest that the upper segment of subscapularis is primarily involved in internal

rotation movements while the lower segment is more involved in the stabilization of the glenohumeral joint.

2.3 Rotator Cuff Tears

Rotator cuff tears can be diagnosed with a clinical examination of a patient's shoulder. Confirming the diagnosis is typically done using an ultrasound or magnetic resonance imaging (MRI) scan (Cooper & Ali, 2013; Vollans & Ali, 2016). Patients who suffer from RCT can be classified as asymptomatic or symptomatic. Patients who are asymptomatic have shown little to no pain (below 3 on a visual analog scale), no loss in ROM and are able to rely on the surrounding musculature to maintain normal shoulder function (Kelly et al., 2005). Symptomatic patients report pain scores above 3 on a visual analog scale, have decreased ROM of their injured arm compared to their unaffected arm and continue to rely on the torn tendon which compromises shoulder function (Kelly et al., 2005). With the majority of RCT being posterosuperior, meaning they occur more frequently to the supraspinatus and infraspinatus tendons, there are three classification systems used to describe the location and size of the tear and to assist with the management of the injury. The first system classifies the tear based on its size (<1cm = small and >5cm = massive). The second classifies the tear based on its retraction in the frontal plane. Lastly, the tear is classified based on the extent of fatty muscle atrophy shown on the MRI. These classification systems are summarized in Table 1.

Table 1: Classification of Rotator Cuff Tears (Vollans & Ali, 2016).

Classification of rotator cuff tears	
Classification by tear size (Cofield)	
Small	<1 cm
Medium	1–3 cm
Large	3–5 cm
Massive	>5 cm
Classification by cuff tear retraction in the frontal plane (Patte)	
Stage 1	Proximal stump lies close to its bony insertion
Stage 2	Proximal stump retracted to level of the humeral head
Stage 3	Proximal stump retracted to level of glenoid
Classification by extent of fatty muscle atrophy originally on computed tomography (CT) but now more applicable to MRI (Goutallier)	
Stage 0	Normal muscle
Stage 1	some fatty streaks
Stage 2	<50% fatty muscle atrophy
Stage 3	50% fatty muscle atrophy
Stage 4	>50% fatty muscle atrophy

As mentioned previously, RCT develop from the culmination of intrinsic and extrinsic factors, such as aging and the development of subacromial impingement, resulting in pain and weakness of the shoulder. With RCT positively correlating with aging (Milgrom et al., 1995; Tempelhof et al., 1999) and over 50% of asymptomatic adults over the age of 60 experiencing some form of tear (partial- or full-thickness) (Sher et al., 1995), it is crucial to understand the progression of pathology in order to minimize the risk of developing a tear as a population ages. Subacromial impingement syndrome (SAIS) is a common symptom that typically precedes a partial- or full-thickness tear and is composed of three progressive stages: 1) edema & hemorrhage, 2) fibrosis & tendinitis, and 3) tears of the rotator cuff, bicep ruptures, and bone

changes (Neer, 1983). SAIS is triggered when there is a reduction in the subacromial space, which produces an increase in compressive forces on the structures within the space. Reduction in the SAS can occur from the development of fatigue in the rotator cuff muscles during activities of work and sport that require a large demand of rotator cuff muscle activity. As fatigue develops, changes occur to the kinematics of the upper extremity joints, specifically at the glenohumeral and scapulothoracic joints in the form of superior humeral head translation and scapula reorientation respectively. These changes often result in the reduction of the subacromial space and increase the risk of impingement (Chopp et al., 2010; Chopp-Hurley & Dickerson, 2015; Chopp-Hurley et al., 2016). Ultimately, the damage occurring from SAIS on these interposed structures leads to various rotator cuff pathologies.

2.4 Treatment & Rehabilitation

When a patient experiences an asymptomatic or symptomatic RCT, they are typically recommended two possible routes for treatment. The first option is non-operative conservative management through physical therapy exercises, electrotherapy, acupuncture, injection therapy, etc. (Osborne et al., 2016). When a patient with a rotator cuff injury visits a physical therapist, it is almost certain that an exercise program consisting of passive ROM, active ROM and strengthening exercises will be prescribed in order to progressively improve the patient's ROM, increase strength and restore normal function. Improved outcomes are dependent on the patient's ability to properly perform and execute the exercise program not only in the clinic but in the home setting as well. An obstacle that patients may need to overcome are the changes in muscle activation and tendency towards compensatory movement patterns that an injury such as RCT or the preceding symptoms of shoulder impingement may cause. Ludewig & Cook (2000) reported

that participants with symptoms of impingement showed decreased scapular upward rotation, increased anterior tipping, increased scapular medial rotation, increased trapezius and decreased serratus anterior muscle activity during humeral elevation with different loads. So, for an exercise program to be effective, it is crucial to ensure patients are avoiding any compensatory movement that may alter their movement patterns and utilize different musculature to compensate for the injury.

Since there are many rotator cuff exercises that can be added to a program to help improve ROM and strength, selection of the proper exercises to fit the needs of the patient must be considered while targeting the rotator cuff muscles and surrounding musculature. The goal for passive ROM exercises is to reduce post-operative stiffness in the joints and promote tendon-bone healing (Kluczynski et al., 2014). Exercises such as forward flexion, abduction, scaption can be done passively using a cane, broom stick, etc., driven by the uninjured arm to gain motion in different planes. Next, active motion and strengthening are needed to progress the rehabilitation of the muscles and surrounding structures to prevent a reoccurring injury. To target the supraspinatus muscle, exercises such as the empty can (abduction with internal rotation), full can (abduction with external rotation) and forward flexion have shown high levels of activation in maximal muscle tests at 74%, 64%, 67%, respectively (Hintermeister et al., 1998; Burke et al., 2002). These exercises will also activate the anterior and middle deltoid and the subscapularis muscles. Burke et al. (2002) notes caution from previous studies that the empty can should be avoided as a rehabilitation exercises by populations with subacromial impingement or RCT due to the increased risk of impingement as the subacromial space is reduced when elevating the arm between 70-120° and internally rotating the humerus. They suggest the full can as an alternative as the external rotation clears the greater tuberosity from under the acromion during elevation

and minimizes the risk of impingement. In order to strengthen the infraspinatus and teres minor muscles, variations of external rotation exercises (*i.e.*, external rotation with resistance band at 0° abduction and diagonals) have been shown to maximally activate these muscles. Myers et al. (2005) reported muscle activations of 84% and 46% for teres minor and infraspinatus during an external rotation exercise at 0° of abduction. Lastly, the subscapularis can be strengthened by performing exercises involving internal rotation and movements like rows that require increased glenohumeral stability. Levels of activation have been reported around 74% for the subscapularis when performing internal rotation at 0° of abduction and 88% when performing rows with a middle grip posture (Hintermeister et al., 1998; Myers et al., 2005). In summary, there are a variety of rehabilitative shoulder exercises that can be performed in order to strengthen the shoulder and help individuals return to normal function after suffering a RCT injury. A summary of the exercises and different muscles activated during each are found in Table 2.

Table 2: Summary of rehabilitative shoulder exercises and the muscles activated during exercise performance.

Exercise	Activated Muscles
Full Can (Scaption/Abduction)	Supraspinatus, Anterior & Middle Deltoid, Subscapularis, Infraspinatus
Forward Flexion	Supraspinatus, Infraspinatus
Rows	Supraspinatus, Infraspinatus, Subscapularis, Trapezius
External Rotation	Infraspinatus, Teres Minor
Diagonals	Infraspinatus, Teres Minor, Posterior Deltoid
Internal Rotation	Subscapularis, Pectoralis Major

If initial conservative management is unsuccessful, the second option is surgical intervention through arthroscopic rotator cuff repair. This treatment has been shown to have a lower risk of stiffness, deltoid injury and infections, and allows for earlier ROM post-operation due to its minimal invasiveness. Proper execution of this method results in a good suture to the tendon and suture to bone fixation, minimal suture abrasion, good knot security and optimizes footprint coverage to allow tendon to bone healing (Osborne et al., 2016). The post-surgical protocol usually consists of an immobilization period of 4-6 weeks that includes some limited passive ROM exercises, followed by a 6-week period of progressive passive and active ROM and strengthening exercises that resembles the conservative management through exercise alternative. Previous studies have evaluated the use of different protocols at different times post-surgery and it still remains unclear what combination and timing may be the most effective due to the individualization of each RCT injury. For example, Raschhofer et al. (2017) compared early isometric loading of the rotator cuff to primary passive motion after arthroscopic repair. They reported reduction of maximal pain, improvements in Constant-Murley scores after 6 weeks post-surgery and higher active internal rotation after 12 weeks for the isometric loading group. On the contrary, a study done by Longo et al. (2019) evaluated two different post-operative rehabilitation protocols for two groups that underwent arthroscopic rotator cuff repair. One group was excluded from performing passive external rotation, anterior elevation ROM and active pendulum exercises during the first two weeks while the other began performing them the day after surgery. They reported no significant differences in clinical scores, muscle strength, or passive and active ROM between both groups. Additionally, a meta-analysis done by Chang et al. (2015) concluded that early passive ROM accelerated recovery from post-operative stiffness but was likely to result in improper tendon-bone healing. Thus, the literature remains

inconclusive about which post-surgical interventions for rehabilitation may or may not assist in quicker return to normal function after surgery and each treatment plan must be tailored to each individual patient's needs in order to maximize their recovery.

2.5 Wearables & Machine Learning for Rehabilitation

In recent years, devices such as smartphones, fitness bracelets, and smartwatches have been used to track and recognize human performance during simple and complex activities. Within these devices, there are several sensors embedded in order to collect different types of data such as acceleration, heart rate, rotation, position, magnetic field and light sensitivity (Garcia-Ceja et al., 2014). Inertial measurement unit sensors found in smartwatches contain an accelerometer, gyroscope and, in some devices, a magnetometer for each axis, allowing it to track a person's acceleration, angular velocity, and change in magnetic field respectively. The data being collected provides opportunities for human performance evaluation for activities performed in sport, rehabilitation and everyday life. Prior to doing any performance evaluations, a critical need is the ability to recognize different activities based on the collected data. Simple activities such as running, walking, sitting, etc., can be successfully recognized since they do not depend on context, whereas complex and long-term activities (*i.e.*, cooking, shopping, exercising, etc.) may be composed of numerous simple activities and require contextual information (Garcia-Ceja et al., 2014). In order to track activity outside of a clinical setting, it is important to minimize the number of sensors worn by an individual due to inconvenience and possible discomfort while maintaining the accuracy of activity recognition. Previous studies collecting data from a set of sensors on multiple body locations (*i.e.* wrist, chest, hip, ankle) reported accuracies above 85% for recognition of activities (Maurer et al., 2006; Riboni &

Bettini, 2011; Lara et al., 2012). When considering the use of only one wrist-worn sensor, a study done by Nguyen et al. (2015) reported that acceleration data was sufficient for ambulation activity recognition as accuracy was 91.92% when using a Random Forest (RF) classifier individually and 91.98% when using a combination of Random Forest and k-nearest neighbors (k-NN) classifiers. Similarly, accuracies for a single wrist-worn sensor have been reported by Burns et al. (2018) as mentioned in Section 1.0 of this proposal. Therefore, depending on the type of classifier used (individually or some combination of two or more), it is possible to achieve high rates of accuracy for activity recognition.

In order to train ML algorithms to accurately distinguish between different types and qualities of movement associated with human activity during rehabilitation, large and robust data sets are required. These large data sets may contain a wide range of variability in movement patterns associated with performance of different rehabilitation exercises. For supervised learning algorithms, it is essential that the labels and inputs from these data sets are well defined to identify the relevant features in the dataset for accurate classification performance. Some data sets are made publicly available through the University of California, Irvine Machine Learning Repository (*i.e.*, the OPPORTUNITY Activity Recognition Dataset (2010)) in order to test and compare performance of human activity recognition algorithms. Examples of supervised ML algorithms that are frequently compared in the literature consist of RF, k-NN, support vector machine classifier (SVC) and convolutional recurrent neural network (CRNN) (Maurer et al., 2006; Lara et al., 2012; Nguyen et al., 2015; Burns et al., 2018). Therefore, the creation of a robust data set involving a range of movement patterns for individuals with asymptomatic and symptomatic RCT can assist development of ML algorithms for tracking shoulder rehabilitation.

3.0 METHODOLOGY

3.1 Participants

Seventeen adults (ten asymptomatic and seven symptomatic for subacromial impingement syndrome) participated in this study. An *a priori* power analysis determined a minimum sample of 16 participants (8 participants per group) were required to detect significant differences using a repeated-measures analysis of variance (ANOVA) with an alpha (α) value of 0.05 and a power value ($1-\beta$) of 0.8 (Cohen, 1992). Participants were screened and initially classified into the asymptomatic or symptomatic group based on self-reported upper extremity injuries within the last six months. Classification was finalized for each arm following the completion of the Neer impingement test and Hawkins-Kennedy test. All clinical impingement tests were performed by the lead researcher to ensure consistency in the evaluation of SAIS. Based on the approved study design, University of Waterloo Office of Research Ethics (ORE#: 23205), participants provided informed written consent prior to participating in the experimental data collection. Participant demographics are presented in Table 3.

Table 3: Participant demographics (mean \pm SD). R indicates right-hand dominant and L indicates left-hand dominant. F indicates female participants and M indicates male participants.

Group	Sex	Handedness	Age (years)	Height (cm)	Weight (kg)	QuickDASH Score
Asymptomatic (n = 10)	4F, 6M	10R	47.9 \pm 18.9	174.9 \pm 9.2	68.4 \pm 12.0	10.6 \pm 11.2
Symptomatic (n = 7)	2F, 5M	5R, 2L	55.9 \pm 26.8	176.0 \pm 8.7	78.4 \pm 13.5	17.9 \pm 10.1

3.2 Instrumentation

3.2.1 Motion Capture

Three-dimensional kinematic data of the right and left upper limbs and torso were collected using a 13-camera VICON MX20 passive optoelectronic motion capture system (VICON, Oxford, UK) at a sample rate of 50 Hz. Prior to the participants' arrival, the collection space was calibrated with the origin set to ensure that movements will be performed in the positive axes during the experiment. The global coordinate system (GCS) was set to International Society of Biomechanics (ISB) standards, where +Y represents up, +X represents forward and +Z represents to the right of the origin (Wu & Cavanaugh, 1995). Eighteen individual reflective markers were placed on bony landmarks of the right and left upper limbs and torso, following ISB recommendations (Table 4, Figure 5) (Wu et al., 2005). In addition to the individual reflective markers, six clusters consisting of three markers each were attached to the forearms, upper arms and torso. A five second static calibration trial, with the participant standing in a "T-pose", was taken prior to the beginning of the experimental trials.

Table 4: VICON marker placement based on recommendations from Wu et al. (2005).

Body Segment	Anatomical Landmark
Thorax	Spinous Process of the 7 th Cervical Vertebra (C7)
	Spinous Process of the 8 th Thoracic Vertebra (T8)
	Suprasternal Notch (SS)
	Xiphoid Process (XP)
	Left & Right Acromion Process (ACR)
	Chest Cluster (CHEST1, CHEST2, CHEST3)
	Back Cluster (BACK1, BACK2, BACK3)
Left & Right Humerus	Upper Arm Cluster (UA1, UA2, UA3)
	Medial Epicondyle (ME)
	Lateral Epicondyle (LE)
Left & Right Forearm	Forearm Cluster (FA1, FA2, FA3)
	Radial Styloid Process (RS)
	Ulnar Styloid Process (US)
Left & Right Hand	2 nd Metacarpal Joint (MCP2)
	5 th Metacarpal Joint (MCP5)

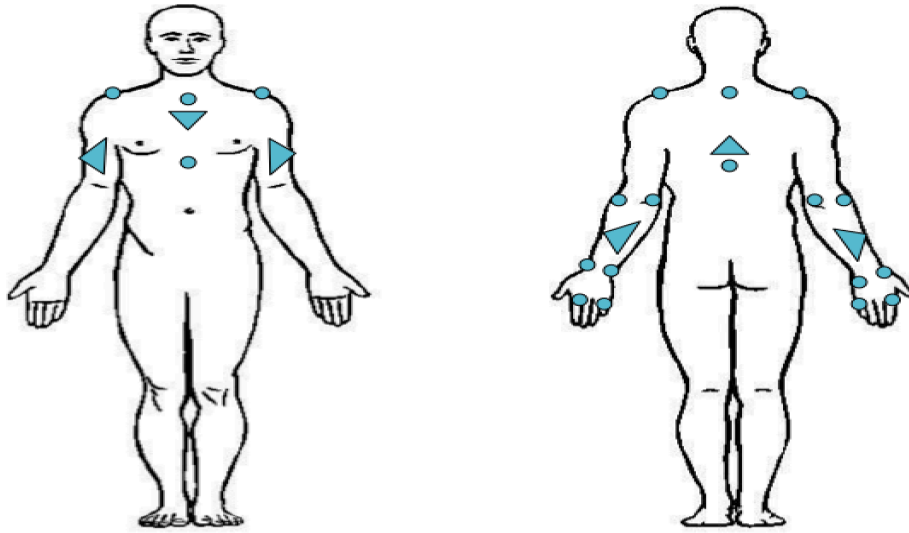


Figure 5: VICON marker placement on the anterior and posterior upper extremities and torso. Blue dots represent individual markers and triangles represents marker clusters.

3.3 Experimental Protocol

For this study, participants were required to attend one session in the lab lasting approximately one and a half to two hours. During this time, they were evaluated for signs of impingement and performed 20 repetitions of six common rotator cuff rehabilitation exercises consisting of standard and compensatory movement cues with each arm independently. For a parallel investigation (outside the scope of this work), the participants wore a smartwatch, containing an IMU, on the wrist of the arm performing the exercise. Depending on the outcome of the impingement evaluation, participants followed 1 of 2 protocols. The experimental protocols are outlined in Figure 6.

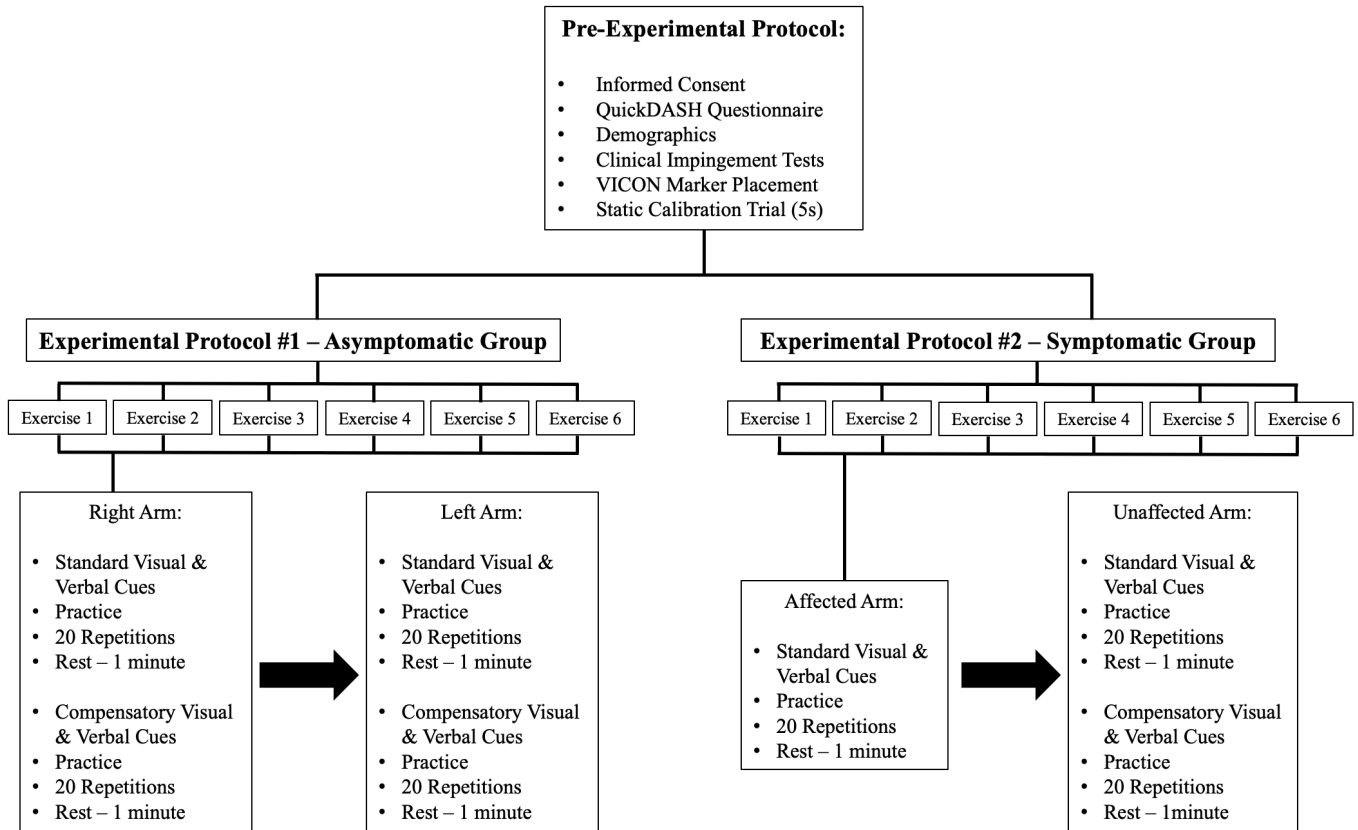


Figure 6: Overview of the experimental data collection protocol. Both groups underwent the same pre-experimental protocol. After being classified in the asymptomatic or symptomatic group from the clinical impingement tests, both groups performed 20 repetitions of 6 rotator cuff exercises. Protocol #1 began with exercise 1, following the steps for the right arm and repeating them for the left arm prior to moving on to the next exercise. Protocol #2 followed the same methodology, but symptomatic participants only performed standard exercise movements with their affected arm followed by standard and compensatory movements for their unaffected arm.

3.3.1 Collection Protocol

Upon arrival, participants reviewed the information and consent forms, provided written informed consent and completed the QuickDASH questionnaire (Appendix A). Participant demographics (*i.e.* age, handedness, etc.) were taken following the completion of the questionnaire. Next, participants were evaluated for subacromial impingement syndrome using the Neer’s and Hawkins-Kennedy clinical impingement tests (Neer, 1983; Hawkins & Kennedy,

1980). Participants who did not show signs of impingement were categorized as asymptomatic and completed protocol one for both the left and right arms. If a participant tested positive for signs of impingement in both tests, they were categorized as symptomatic. These participants followed protocol two that excluded exercises completed with compensatory movement cues for their affected arm. Following the clinical impingement tests, individual reflective markers and marker clusters were placed on the bony landmarks and segments of participants. Markers and clusters were secured using double-sided adhesive tape.

Before beginning any of the experimental trials, a five second static calibration trial was taken with the participant standing in a “T-pose”. For the purpose of this thesis, cues and exercise movements indicating ideal exercise performance will be labeled as “standard”, while cues and exercise movements indicating compensatory exercise performance will be labeled as “compensatory” for the asymptomatic group. Prior to each exercise and condition (standard and compensatory), participants who did not test positive for symptoms of impingement received verbal and visual cues on how to complete each of the six exercises with standard movement cues followed by compensatory movement cues (Table 5). Participants who were classified as symptomatic only received verbal and visual cues for standard movement prior to performing each of the exercises with their affected arm. Next, they completed the exercises with standard and compensatory movement cues with their unaffected arm. Cues associated with standard and compensatory movement were compiled from findings in the literature outlining performance cues (Hintermeister et al., 1998; Myers et al., 2005; Haberle et al., 2018) and from discussions with health professionals who specialize in RCT injuries. For the selected exercises, the goal was to have participants focus on completing all movements with the instructed cues, while minimizing fatigue and exertion throughout the protocol. To achieve this, a minimum weight of

one pound and a light resistance band was used to provide minor resistance during the strengthening exercises. Practice time was given to participants to ensure that they were comfortable performing each condition of each exercise with its associated cues. The order of the performed exercises followed a standard physiotherapy progression starting with ROM exercises and moving into muscle strengthening exercises with light weight and resistance bands. Asymptomatic participants followed protocol one and performed 20 repetitions of each exercise with standard and compensatory movement cues for the left and right arms (totaling 480 movements), while symptomatic participants followed protocol two and excluded the performance of compensatory movement cues for their affected arm (totaling 240-360 movements). Participants were given a minimum of one minute to rest between trials in order to reduce the effects of fatigue from any of the exercises.

Table 5: Standard and compensatory movement cues for six common rotator cuff rehabilitation exercises.

Exercise	Standard Movement Cues	Compensatory Movement Cues
Active Assisted Shoulder Flexion	<ul style="list-style-type: none"> • place hand of the ‘affected’ arm on top of the cane • keep ‘affected’ arm straight • maintain neutral posture • use the opposite arm to raise the ‘affected’ arm as high as possible in the sagittal plane 	<ul style="list-style-type: none"> • begin in the same position as described in proper movement • raise the ‘affected’ arm to 90° of shoulder flexion • shrug the shoulder of the ‘affected’ arm when approaching 90° • bend the trunk laterally towards the arm used to raise the ‘affected’ arm
Active Assisted Shoulder Scaption	<ul style="list-style-type: none"> • hold a cane across the pelvis with arms slightly wider than shoulder width • let the hand of the ‘affected’ arm rest on top of the cane • maintain neutral posture • raise the ‘unaffected’ arm in scaption and let the other follow passively 	<ul style="list-style-type: none"> • begin in the same position as described in proper movement • raise the arms to 90° of elevation, leading with the ‘unaffected’ arm • shrug the shoulder of the ‘affected’ arm when approaching 90° • bend the trunk laterally towards the arm used to raise the ‘affected’ arm

<p>Shoulder Abduction with Weight</p>	<ul style="list-style-type: none"> • maintain neutral posture • keep the moving arm straight and thumb pointed towards the ceiling • raise the arm in the frontal plane as high as possible while maintaining control on the ascent and descent 	<ul style="list-style-type: none"> • begin in the same position as described in proper movement • raise the arm to 90° of shoulder abduction • shrug the shoulder of the moving arm when approaching 90° • internally rotate the upper arm and forearm
<p>Internal Rotation with Resistance Band</p>	<ul style="list-style-type: none"> • start with the elbow bent at 90° and tucked against the torso, thumb pointing upward • maintain neutral wrist position and posture • start with a fist pointing forward and bring the forearm towards the stomach, keeping the elbow tucked • maintain control on the return 	<ul style="list-style-type: none"> • begin in the same position as described in proper movement • when bringing the forearm towards the stomach, let the elbow come off the torso • shrug the shoulder of the arm performing the movement • rotate the torso in the same direction as the forearm movement
<p>External Rotation with Resistance Band</p>	<ul style="list-style-type: none"> • start with the elbow bent at 90° and tucked against the torso, thumb pointing upward • maintain neutral wrist position and posture • start with a fist pointing forward and rotate the forearm outward, keeping the elbow tucked • maintain control on the return 	<ul style="list-style-type: none"> • begin in the same position as described in proper movement • when rotating the forearm outwards, let the elbow come off the torso • shrug the shoulder of the arm performing the movement • rotate the torso in the same direction as the forearm movement
<p>Standing Rows with Resistance Band</p>	<ul style="list-style-type: none"> • maintain neutral posture • start with the arms slightly extended, thumbs pointing upward and pull the band straight back • retract the scapula • maintain control on the return 	<ul style="list-style-type: none"> • begin in the same position as described in proper movement • pull the band upwards in a diagonal motion towards the shoulders • shrug the shoulders • avoid retracting the scapula during the movement

3.4 Data Analysis

3.4.1 Motion Capture Processing

Raw three-dimensional kinematic data was visually inspected and labeled using the VICON Nexus 1.8.5 software (VICON, Oxford, UK). If gaps (50 frames or less) were found in a marker's trajectory due to marker drop-out, they were gap-filled using the pattern fill function in the VICON software. This function copies the movement pattern of another marker on the same segment that has no gaps and fills the trajectory with that same movement pattern. To remove high frequency noise content, all kinematic data was filtered with a dual pass, second order, low-pass Butterworth filter with a cutoff frequency set to 4Hz, since human movement occurs between 0-6Hz (Winter, 2009). The static calibration trial was used to develop rotation matrices between the anatomical axis systems and the cluster axis systems of the torso, upper arms and forearms. These rotation matrices allow the use of three-dimensional position data from the cluster markers to compute joint angles, which are less sensitive to skin motion artifact compared to the anatomical markers (Leardini et al., 2005; Winter, 2009). During the calibration trial, local coordinate systems (LCS) were calculated using the anatomical markers of the torso, humeri, and forearms, following ISB recommendations (Table 6) (Wu et al., 2005). LCS were also calculated for the marker clusters placed on the back, upper arms, and forearms. The segment rotation matrix between the cluster axis [M] and anatomical systems [A], the "[M to A] rotation matrix", was computed for each segment cluster relative to its respective anatomical frame of reference. It is assumed that the relationship between the cluster and anatomical axis systems remained constant during a repetitive task (Winter, 2009).

Table 6: Local coordinate systems for the thorax, humerus and forearm segments as outlined by Wu et al. (2005).

Segment	Origin	Local Coordinate System
Thorax	SS	Y_t – The line connecting the midpoint between XP and T8 and the midpoint between SS and C7, pointing up. Z_t – The line perpendicular to the plane formed by SS, C7, and the midpoint between XP and T8, pointing to the right. X_t – The common line perpendicular to the Z_t and Y_t axes, pointing forward.
Humerus	GH	Y_h – The line connecting GH and the midpoint of LE and ME, pointing to GH. X_h – The line perpendicular to the plane formed by LE, ME, and GH, pointing forward. Z_h – The common line perpendicular to the Y_h and Z_h axes, pointing to the right.
Forearm	US	Y_f – The line connecting US and the midpoint between LE and ME, pointing proximally. X_f – The line perpendicular to the plane through US, RS, and the midpoint between LE and ME, pointing forward. Z_f – The common line perpendicular to the X_f and Y_f axes, pointing to the right.

During each exercise trial, the glenohumeral joint center position was calculated by subtracting 60mm from the acromion marker along the Y-axis of the torso segment (Nussbaum & Zhang, 2000). The elbow and wrist joint centers were calculated from the midpoint between the medial and lateral epicondyles and the radial and ulnar styloid processes, respectively. To compute joint angles for the torso (thorax to global), thoracohumeral (humerus to torso), and elbow (forearm to humerus) segments, a time varying rotation matrix was constructed between the GCS [G] and the cluster LCS, “[G to M] rotation matrix”, using the position data from the back, upper arm, and forearm marker clusters. Next, a rotation matrix between the GCS and the anatomical coordinate system, “[G to A] rotation matrix”, was calculated for each segment by

finding the dot product of the time varying [G to M] matrix and the constant [M to A] matrix for the back, upper arm, and forearm clusters. With the LCS of each segment, rotation matrices were calculated between the distal LCS and the proximal LCS to extract joint angles for the thorax, thoracohumeral and elbow joints. This was done by multiplying the transpose of the distal LCS (transpose of [G to A] matrix = [A to G] matrix) by the proximal LCS [G to A] matrix. The created direction cosine matrices were decomposed based on the recommended Euler/Cardan rotation sequences and clinical interpretations from Wu et al. (2005) (Table 7) to extract joint angles. For the thorax and elbow, the ZXY rotation sequence (Equation 1) was used for all exercises. A YXY' rotation sequence (Equation 2) was used to calculate thoracohumeral joint angles for the internal rotation, external rotation, and standing row exercises since participants were unlikely to raise their humerus above 90°. For the shoulder flexion, shoulder scaption, and shoulder abduction exercises, an alternative rotation sequence of XZY (Equation 3) was used to calculate thoracohumeral joint angles since gimbal lock occurs when approaching 0° and 180° of glenohumeral elevation with the YXY' rotation sequence (Phadke et al., 2011). Finally, to quantify the shoulder shrug cue, a “clavicle” vector was created using the line connecting the suprasternal notch (SS) and the right or left acromion (ACR) anatomical markers (Figure 7). The dot product of the “clavicle” vector and the vector of the y-axis of the thorax local coordinate system was calculated and the arccosine was computed to obtain the time-series angle between these vectors. This method defined a shrug movement, alternatively it has been quantified by tracking scapular movement using the acromion cluster method (van Andel et al., 2009; Lempereur et al., 2014).

$$\begin{bmatrix} \cos(\gamma) \cos(\alpha) - \sin(\beta) \sin(\alpha) & \cos(\gamma) \sin(\alpha) + \sin(\gamma) \sin(\beta) \cos(\alpha) & -\sin(\gamma) \cos(\beta) \\ -\cos(\beta) \sin(\alpha) & \cos(\beta) \cos(\alpha) & \sin(\beta) \\ \sin(\gamma) \cos(\alpha) + \cos(\gamma) \sin(\beta) \sin(\alpha) & \sin(\gamma) \sin(\alpha) - \cos(\gamma) \sin(\beta) \cos(\alpha) & \cos(\gamma) \cos(\beta) \end{bmatrix} \quad (Eq. 1)$$

$$\begin{bmatrix} \cos(\gamma) \cos(\alpha) - \sin(\gamma) \cos(\beta) \sin(\alpha) & \sin(\gamma) \sin(\beta) & -\cos(\gamma) \sin(\alpha) - \sin(\gamma) \cos(\beta) \cos(\alpha) \\ \sin(\alpha) \sin(\beta) & \cos(\beta) & \cos(\alpha) \sin(\beta) \\ \sin(\gamma) \cos(\alpha) + \cos(\gamma) \cos(\beta) \sin(\alpha) & -\cos(\gamma) \sin(\beta) & -\sin(\gamma) \sin(\alpha) + \cos(\gamma) \cos(\beta) \cos(\alpha) \end{bmatrix} \quad (Eq. 2)$$

$$\begin{bmatrix} \cos(\gamma) \cos(\alpha) & \cos(\gamma) \sin(\alpha) \cos(\beta) + \sin(\gamma) \sin(\beta) & \cos(\gamma) \sin(\alpha) \sin(\beta) - \sin(\gamma) \cos(\beta) \\ -\sin(\alpha) & \cos(\alpha) \cos(\beta) & \cos(\alpha) \sin(\beta) \\ \sin(\gamma) \cos(\alpha) & \sin(\gamma) \sin(\alpha) \cos(\beta) - \cos(\gamma) \sin(\beta) & \sin(\gamma) \sin(\alpha) \sin(\beta) + \cos(\gamma) \cos(\beta) \end{bmatrix} \quad (Eq. 3)$$

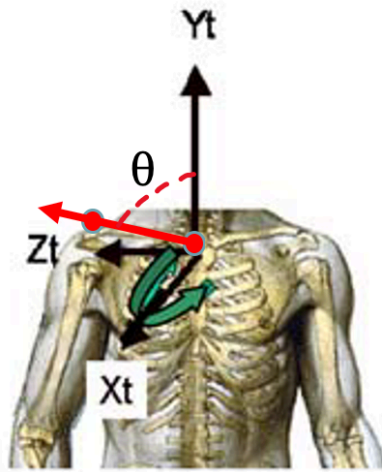


Figure 7: Visual representation of the angle calculated to represent the shoulder shrug cue. The red arrow represents the “clavicle” vector (ACR – SS), the black arrow (Yt) represents the y-axis vector of the thorax LCS, and theta (θ) represents the angle calculated by the arccosine of the dot product of both vectors.

Table 7: Rotation sequences for joint angle calculations with clinical interpretations as outlined by Wu et al. (2005) for rotation axes as denoted by e1, e2 and e3.

Joint	Rotation and Clinical Interpretations
Thorax to Global	Rotation Sequence: Z-X-Y e1: Z-axis of the global coordinate system. Rotation (α_{GT}): flexion (-) & extension (+). e3: The axis coincident with the Y-axis of the thorax coordinate system. Rotation (γ_{GT}): axial rotation to the left (+) & to the right (-). e2: The common axis perpendicular to e1 and e3, the rotated X-axis of the thorax. Rotation (β_{GT}): lateral flexion to the right (+) & to the left (-).
Thoracohumeral	Rotation Sequence: Y-X-Y' e1: The axis coincident with the Y-axis of the thorax coordinate system. Rotation (γ_h): plane of elevation where 0° is abduction & 90° is forward flexion. e3: Axial rotation around the Y-axis of the humerus. Rotation (γ_h) ₂ : internal rotation (+) & external rotation (-). e2: The axis coincident with the X-axis of the humerus coordinate system. Rotation (β_h): elevation (-).
Elbow	Rotation Sequence: Z-X-Y e1: The axis coincident with the Z-axis of the humerus coordinate system. Rotation (α_{HF}): flexion (+) & hyperextension (-). e3: The axis coincident with the Y-axis of the forearm coordinate system. Rotation (γ_{HF}): pronation (+) & supination (-). e2: The common axis perpendicular to e1 and e3, the rotated X-axis of the forearm coordinate system. Rotation (β_{HF}): carrying angle.

All of the calculations for joints angles associated with movement cues for each exercise (Table 8) were completed using a custom MATLAB 2019a program (MathWorks, Massachusetts, USA). From the time-series joint angle data, the maximum and minimum joint angles was extracted for each 5th, 10th, and 15th repetition of each exercise. Range of motion for each movement cue was obtained by subtracting the minimum angle from the maximum angle for each extracted repetition, for each of the six rehabilitative shoulder exercises. Joint angles were computed for the torso and dominant arm of participants in the asymptomatic group and for the torso and affected arm of participants in the symptomatic group.

Table 8: Selected compensatory movement cues and their associated joint angles used for comparison between standard and simulated compensatory exercise performance by the asymptomatic group.

Exercise	Compensatory Movement Cues	Joint Angles
Active Assisted Shoulder Flexion	<ul style="list-style-type: none"> • raise the ‘affected’ arm to 90° of shoulder flexion • bend the trunk laterally towards the arm used to raise the ‘affected’ arm • shrug the shoulder of the ‘affected’ arm when approaching 90° 	<ul style="list-style-type: none"> • thoracohumeral elevation • torso lateral flexion • shoulder shrug
Active Assisted Shoulder Scaption	<ul style="list-style-type: none"> • raise the ‘affected’ arm to 90° of shoulder flexion • bend the trunk laterally towards the arm used to raise the ‘affected’ arm • shrug the shoulder of the ‘affected’ arm when approaching 90° 	<ul style="list-style-type: none"> • thoracohumeral elevation • torso lateral flexion • shoulder shrug
Shoulder Abduction with Weight	<ul style="list-style-type: none"> • raise the arm to 90° of shoulder abduction • internally rotate the upper arm • internally rotate the forearm • shrug the shoulder of the moving arm when approaching 90° 	<ul style="list-style-type: none"> • thoracohumeral elevation • thoracohumeral axial rotation • forearm axial rotation • shoulder shrug
Internal Rotation with Resistance Band	<ul style="list-style-type: none"> • let the elbow come off the torso • shrug the shoulder of the arm performing the movement • rotate the torso in the same direction as the forearm movement 	<ul style="list-style-type: none"> • thoracohumeral elevation • torso axial rotation • shoulder shrug
External Rotation with Resistance Band	<ul style="list-style-type: none"> • let the elbow come off the torso • shrug the shoulder of the arm performing the movement • rotate the torso in the same direction as the forearm movement 	<ul style="list-style-type: none"> • thoracohumeral elevation • torso axial rotation • shoulder shrug
Standing Rows with Resistance Band	<ul style="list-style-type: none"> • pull the band upwards in a diagonal motion towards the shoulders • shrug the shoulders 	<ul style="list-style-type: none"> • elbow flexion • shoulder shrug

3.4.2 Statistical Analysis

3.4.2.1 Statistical Parametric Mapping

For this study, an open-source MATLAB code for statistical parametric mapping (SPM) was used to perform statistical analyses of time-series joint angle data (Pataky, 2012). SPM is a technique used to compare smooth one-dimensional data and provide continuous topological statistical analysis (Pataky, 2010). SPM possesses the advantages of presenting results in the original time spectrum and decisively distinguishing between groups and tasks when interpreting kinematic data (Li et al., 2016). This technique was originally used to analyze cerebral blood flow in three-dimensional positron emission tomography (PET) scans and functional magnetic resonance imaging (fMRI) images (Friston et al., 1991; Worsley et al., 1992). To test hypothesis #1, a series of paired t-tests were used to determine differences between standard and simulated compensatory exercise movement patterns of the asymptomatic group for the time-series curves of each joint angle associated with compensatory cues for the trunk, thoracohumeral and elbow kinematics (MacLean & Dickerson, 2019). Statistical significance was set to $P < 0.05$.

3.4.2.2 Mann-Whitney U Test

Mann-Whitney U tests were used to test hypothesis #2 by comparing the mean differences of maximum angle and ROM measures for asymptomatic simulated compensatory movement and symptomatic movement for trunk, thoracohumeral, and elbow kinematics for each of the six exercises performed. The Mann-Whitney U test is a non-parametric test that was selected over the independent samples t-test due to the uncertainty in the normal distribution of the data (Mann & Whitney, 1947; Hinton, 2010). Statistical significance was set to $P < 0.05$. All Mann-Whitney U tests were performed using SPSS version 26.0 (IBM, Armonk, NY).

4.0 Results

The results of this study are presented by exercise in the order that they were performed during the experimental protocol. The results for each exercise begin with a focus on the time-series joint angle profiles of the mean 10th repetition of each exercise from the asymptomatic group performing standard and simulated compensatory exercise movement. Next, the results of the maximum angle and ROM measures compare the 5th, 10th, and 15th repetitions of exercise movement by the symptomatic group and the simulated compensatory exercise movement of the asymptomatic group. Each of the 17 participants completed 20 repetitions of the six exercises following the appropriate experimental protocol. Individual results for each participant's average maximum angle and ROM for each of the cues associated with each exercise are reported in Appendix B.

4.1 Active Assisted Shoulder Flexion

During the active assisted shoulder flexion exercise, differences occurred in the time-series data between the performance conditions of the asymptomatic group. Differences in exercise performance occurred during the comparison of the thoracohumeral elevation angles between 35% and 75% of the repetition cycle ($p < 0.05$) (Figure 8A). Although no statistical differences existed for the torso lateral flexion (Figure 8B) or shoulder shrug cues (Figure 8C), the simulated compensatory performance achieved a lower mean shoulder shrug angle equating to a higher shoulder shrug movement. When comparing the maximum angle and ROM measures for each cue, similar trends emerged across repetitions. Participants in the symptomatic group, achieved a higher maximum angle for thoracohumeral elevation (Figure 9), a lower ROM for

torso lateral flexion and a lower ROM for the shoulder shrug compared to asymptomatic participants that simulated compensatory cues. Significant differences existed in the torso lateral flexion ROM with differences of 8° ($p = 0.014$) at the 10th repetition and 8° ($p = 0.033$) at the 15th repetition (Figure 10). A difference of 6° ($p = 0.043$) emerged for the ROM of the shoulder shrug cue at the 15th repetition, between the two groups (Figure 11).

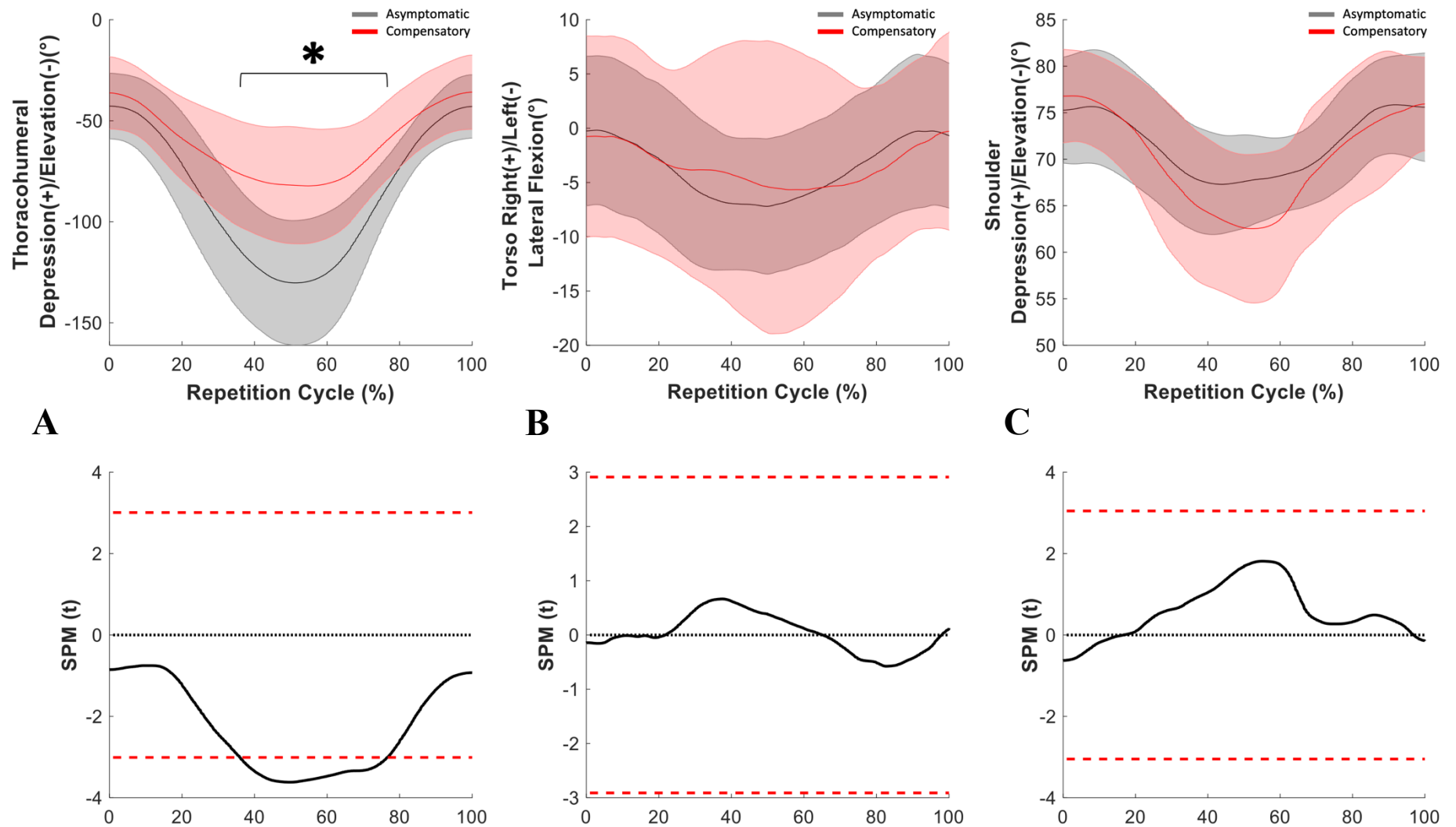


Figure 8: Averaged participant group thoracohumeral elevation angle (left), torso lateral flexion angle (middle) and shoulder shrug angle (right) for asymptomatic participants performing active assisted shoulder flexion standard exercise movement (grey) and simulated compensatory exercise movement (red), time normalized to a full repetition cycle (10th repetition). One standard deviation for each condition is represented by the shaded grey and red areas. Associated SPM z-scores are reported below the average time-series data, with critical z-scores represented by the red dashed lines. Z-scores that exceed the critical value represent significant differences between conditions and are marked with an asterisk (*) over the area(s) where they exist.

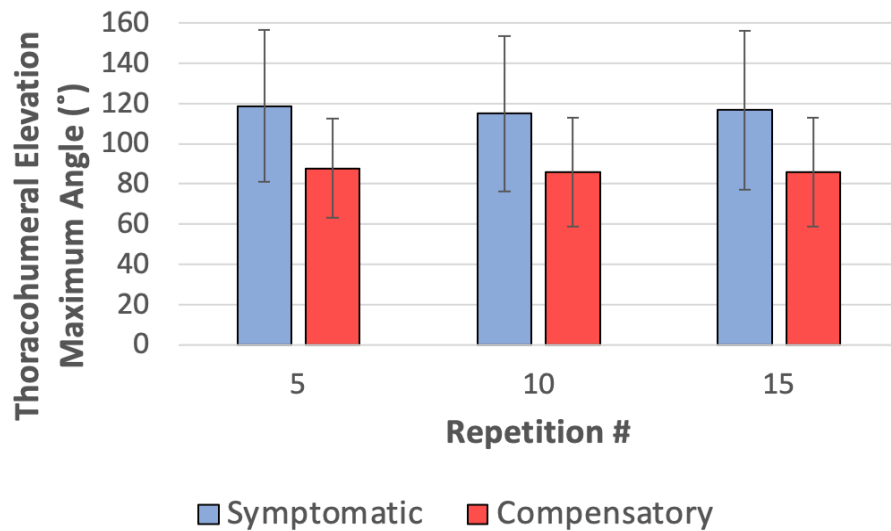


Figure 9: Thoracohumeral elevation maximum angle for the active assisted shoulder flexion exercise at the 5th, 10th and 15th repetitions. Error bars indicate standard deviation.

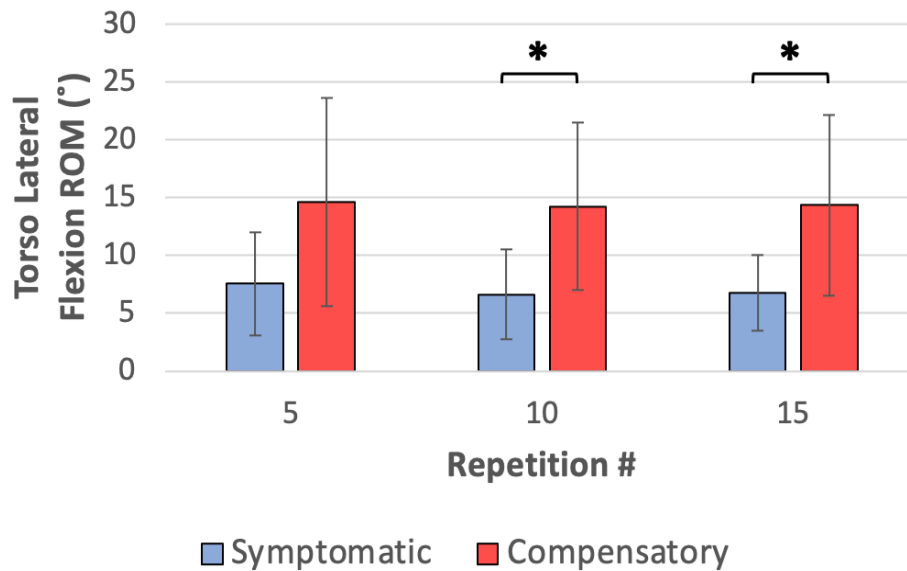


Figure 10: Torso lateral flexion ROM for the active assisted shoulder flexion exercise at the 5th, 10th and 15th repetitions. Error bars indicate standard deviation. An asterisk (*) indicates significance at $P < 0.05$ within a repetition.

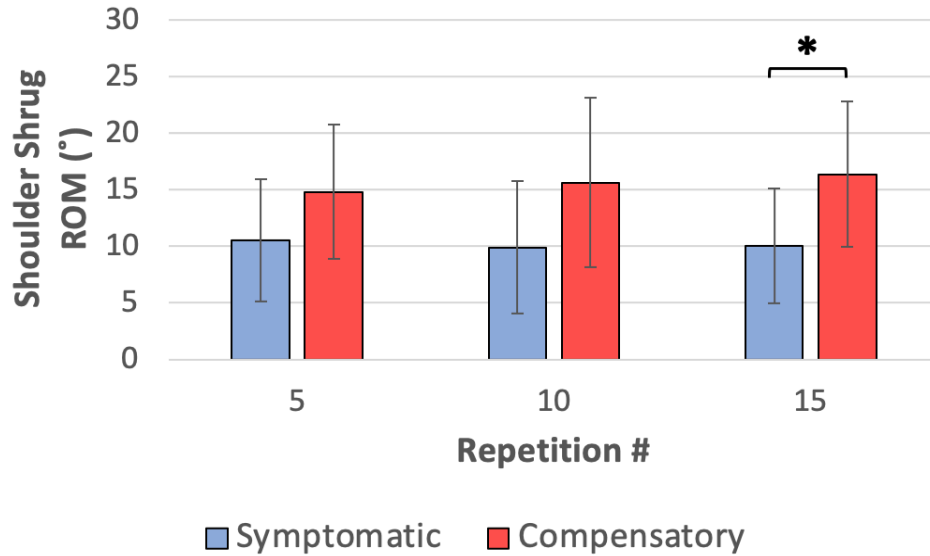


Figure 11: Shoulder shrug ROM for the active assisted shoulder flexion exercise at the 5th, 10th and 15th repetitions. Error bars indicate standard deviation. An asterisk (*) indicates significance at $P < 0.05$ within a repetition.

4.2 Active Assisted Shoulder Scaption

Throughout the active assisted shoulder scaption exercise, similar differences occurred in the time-series data comparison of the asymptomatic group. Differences in thoracohumeral elevation angle occurred between 30% to 60% of the repetition cycle ($p < 0.05$) (Figure 12A), but none for the torso lateral flexion (Figure 12B) or shoulder shrug (Figure 12C) time-series data. Asymptomatic participants once again achieved a lower mean shoulder shrug angle when simulating a compensatory shoulder shrug. Further, the maximum angle and ROM measures behaved similarly as in the active assisted shoulder flexion exercise. Symptomatic participants achieved a higher maximum angle for thoracohumeral elevation (Figure 13), a lower ROM for torso lateral flexion (Figure 14) and a lower ROM for the shoulder shrug when compared to the simulated compensatory movements of the asymptomatic participants. A significant difference only occurred in the 15th repetition for the shoulder shrug cue ROM with a difference of 6° ($p = 0.033$) between the two groups (Figure 15).

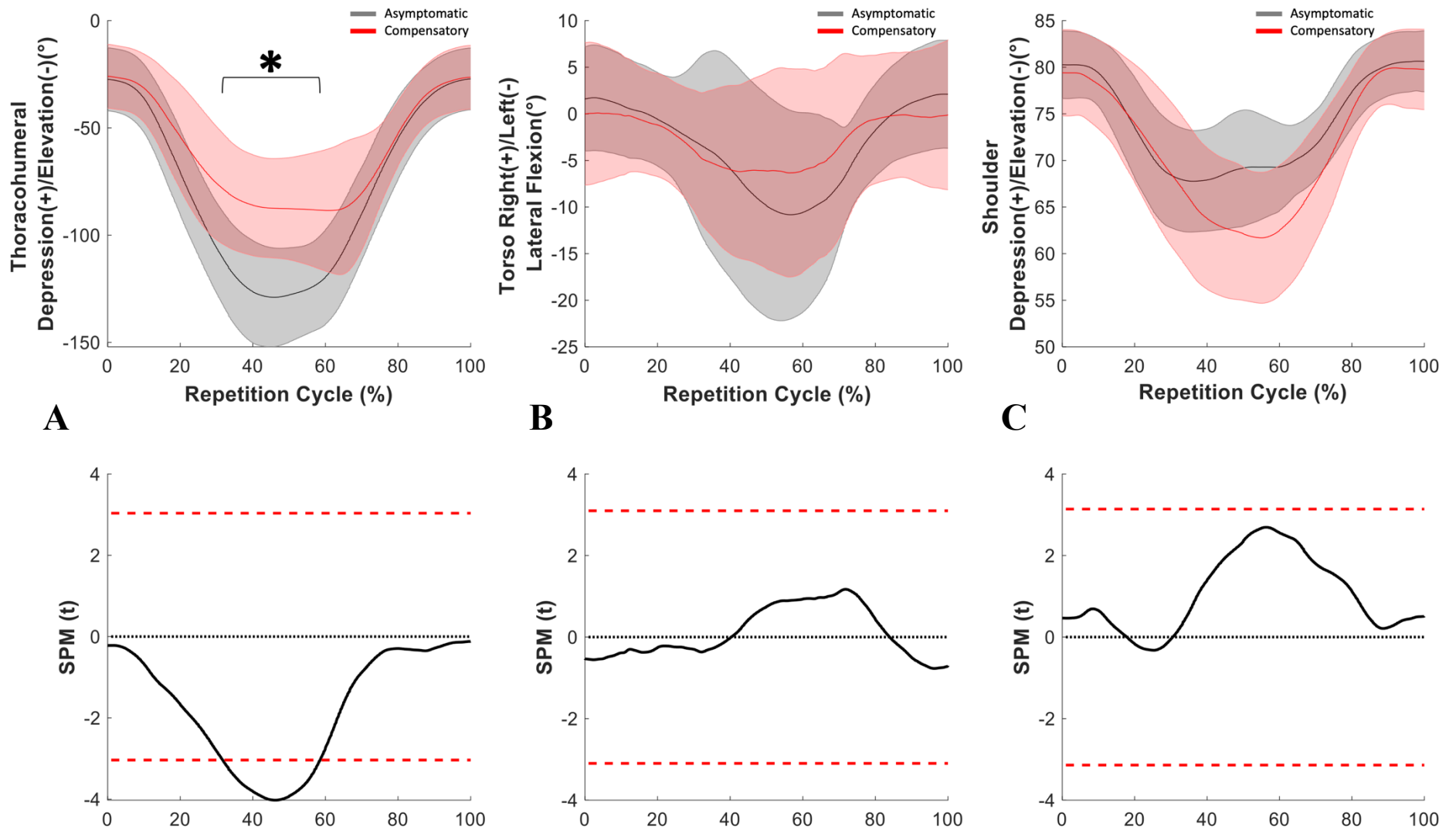


Figure 12: Averaged participant group thoracohumeral elevation angle (left), torso lateral flexion angle (middle) and shoulder shrug angle (right) for asymptomatic participants performing active assisted shoulder scaption standard exercise movement (grey) and simulated compensatory exercise movement (red), time normalized to a full repetition cycle (10th repetition). One standard deviation for each condition is represented by the shaded grey and red areas. Associated SPM z-scores are reported below the average time-series data, with critical z-scores represented by the red dashed lines. Z-scores that exceed the critical value represent significant differences between conditions and are marked with an asterisk (*) over the area(s) where they exist.

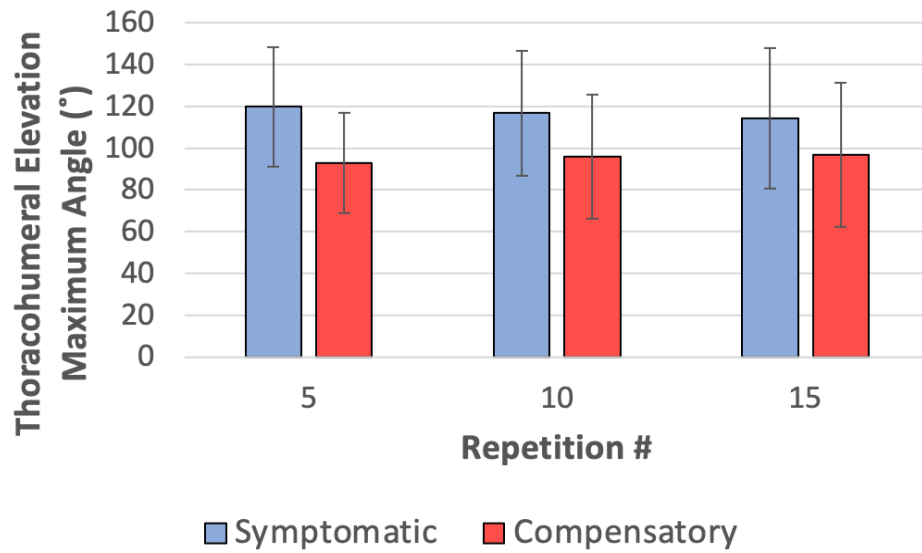


Figure 13: Thoracohumeral elevation maximum angle for the active assisted shoulder scaption exercise at the 5th, 10th and 15th repetitions. Error bars indicate standard deviation.

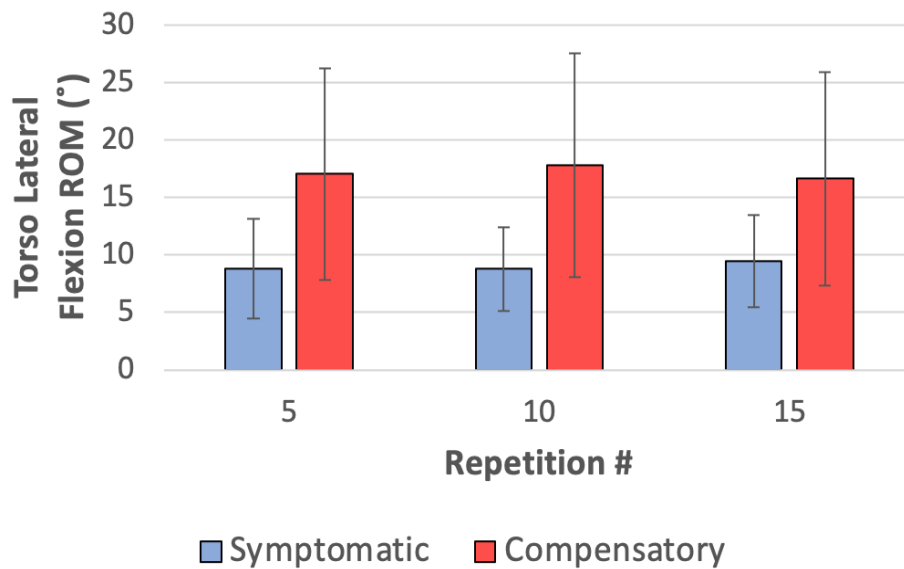


Figure 14: Torso lateral flexion ROM for the active assisted shoulder scaption exercise at the 5th, 10th and 15th repetitions. Error bars indicate standard deviation.

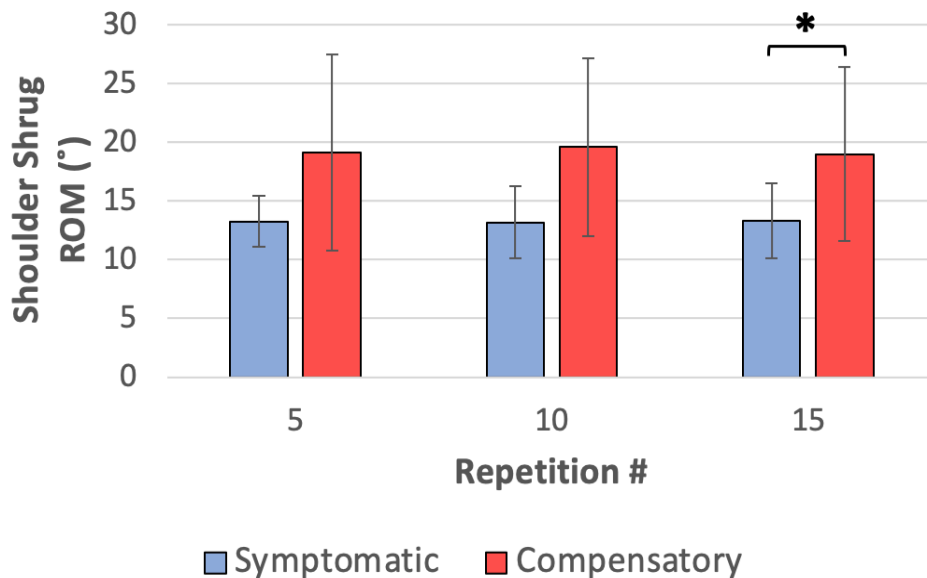


Figure 15: Shoulder shrug ROM for the active assisted shoulder scaption exercise at the 5th, 10th and 15th repetitions. Error bars indicate standard deviation. An asterisk (*) indicates significance at $P < 0.05$ within a repetition.

4.3 Shoulder Abduction

During the shoulder abduction exercise, there were differences in both the time-series and maximum angle data for thoracohumeral elevation. Differences in the time-series data for thoracohumeral elevation occurred between 35% and 60% of the repetition cycle ($p < 0.05$) (Figure 16A) with less thoracohumeral elevation in the compensatory performance. For the remainder of the cues, no differences existed but compensatory performances included more thoracohumeral internal rotation (Figure 16B), more elbow internal rotation (Figure 16C) from 20% to 65% of the repetition cycle and a lower shoulder shrug angle (Figure 16D) compared to the standard exercise movement performances. Moreover, differences persisted across repetitions assessed for thoracohumeral maximum angle with the symptomatic group attaining a higher maximum angle than the compensatory group. Differences of 39° ($p = 0.011$), 36° ($p = 0.022$), and 33° ($p = 0.042$) occurred for the 5th, 10th and 15th repetition respectively (Figure 17).

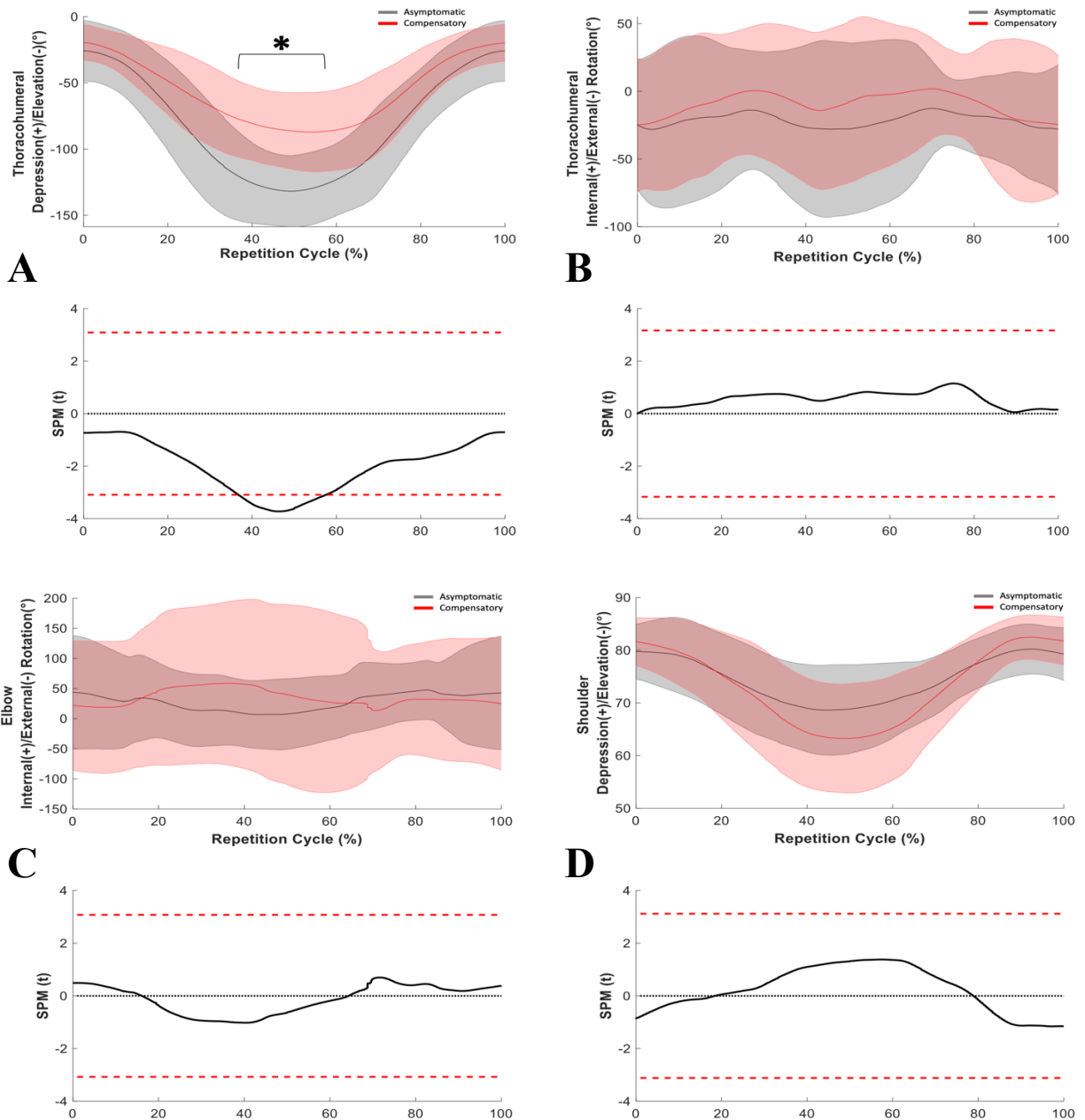


Figure 16: Averaged participant group thoracohumeral elevation angle (top left), thoracohumeral internal/external rotation (top right), elbow internal/external rotation (bottom left) and shoulder shrug angle (bottom right) for asymptomatic participants performing shoulder abduction standard exercise movement (grey) and simulated compensatory exercise movement (red), time normalized to a full repetition cycle (10th repetition). One standard deviation for each condition is represented by the shaded grey and red areas. Associated SPM z-scores are reported below the average time-series data, with critical z-scores represented by the red dashed lines. Z-scores that exceed the critical value represent significant differences between conditions and are marked with an asterisk (*) over the area(s) where they exist.

No differences emerged in the other cues, but symptomatic participants had more thoracohumeral axial rotation ROM (Figure 18), less forearm axial rotation ROM (Figure 19), and less shoulder shrug ROM (Figure 20) than the asymptomatic simulated compensatory movements.

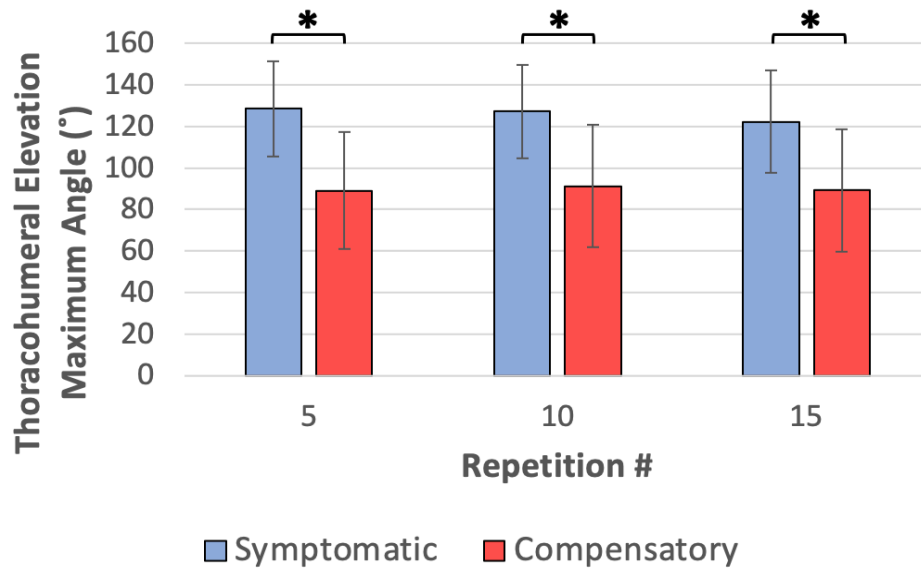


Figure 17: Thoracohumeral elevation maximum angle for the shoulder abduction exercise at the 5th, 10th and 15th repetitions. Error bars indicate standard deviation. An asterisk (*) indicates significance at $P < 0.05$ within a repetition.

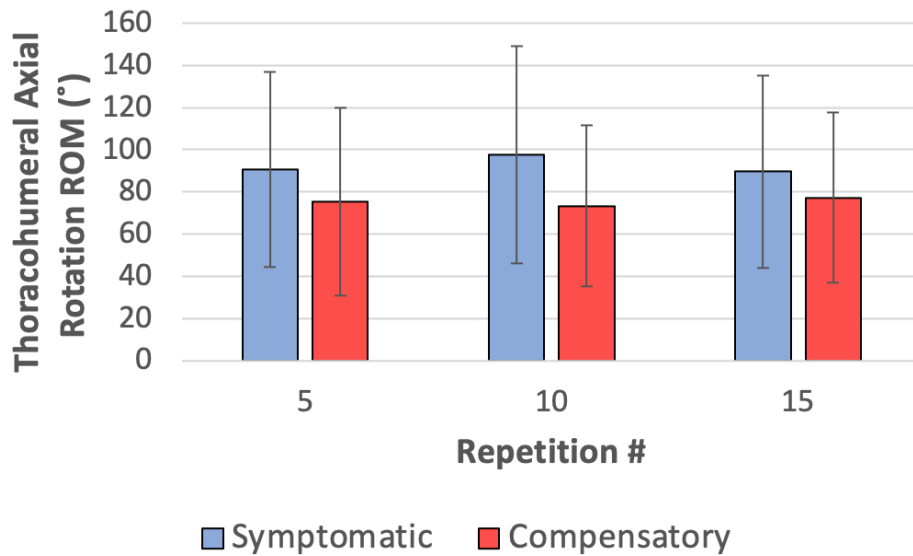


Figure 18: Thoracohumeral axial rotation ROM for the shoulder abduction exercise at the 5th, 10th, and 15th repetitions. Error bars indicate standard deviation.

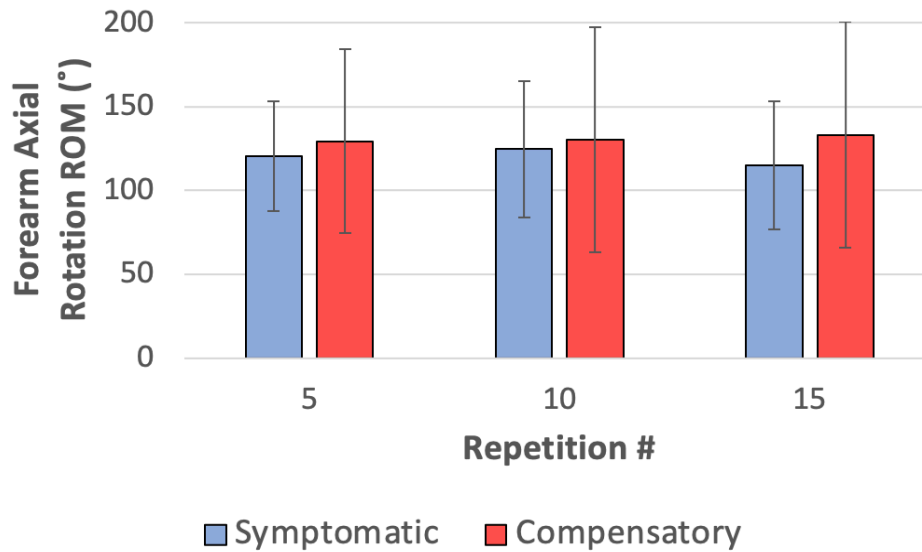


Figure 19: Forearm axial rotation ROM for the shoulder abduction exercise at the 5th, 10th, and 15th repetitions. Error bars indicate standard deviation.

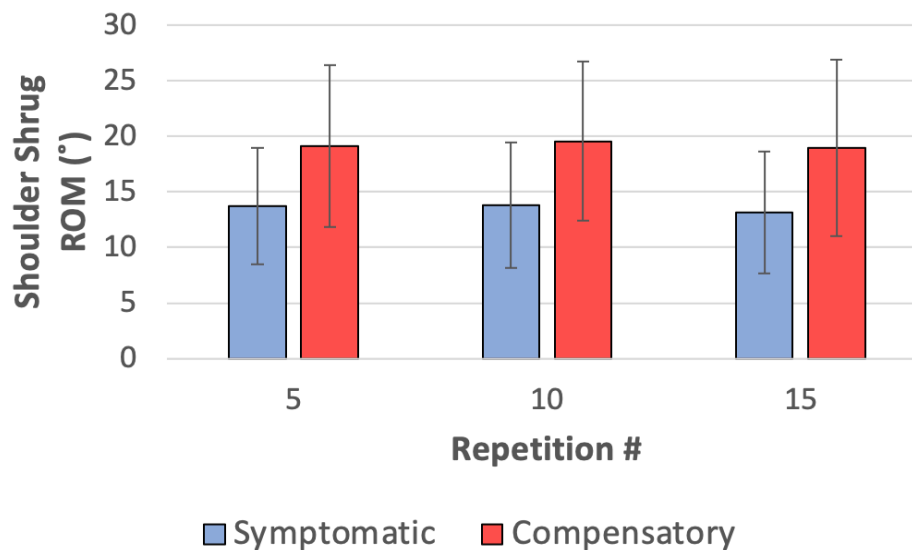


Figure 20: Shoulder shrug ROM for the shoulder abduction exercise at the 5th, 10th and 15th repetitions. Error bars indicate standard deviation.

4.4 Internal Rotation

Throughout the internal rotation exercise, no differences occurred in the time-series data while significant differences only emerged in the shrug ROM data. Although the time-series data of each cue included no significant differences in performance, the compensatory condition demonstrated higher thoracohumeral elevation angle (Figure 21A), less axial rotation of the torso (Figure 21B) and lower shoulder shrug angle (Figure 21C) throughout the repetition cycle, compared to the performance of standard exercise movement cues. For the symptomatic versus asymptomatic compensatory comparison, the symptomatic group had a lower maximum thoracohumeral elevation angle across all repetitions with no significant differences present (Figure 22). For torso axial rotation ROM, the symptomatic group had lower values across all repetitions with no significant differences (Figure 23). Finally, the shoulder shrug ROM showed differences between groups of 8° ($p = 0.005$), 5° ($p = 0.011$), and 6° ($p = 0.022$) at the 5th, 10th and 15th repetitions respectively (Figure 24).

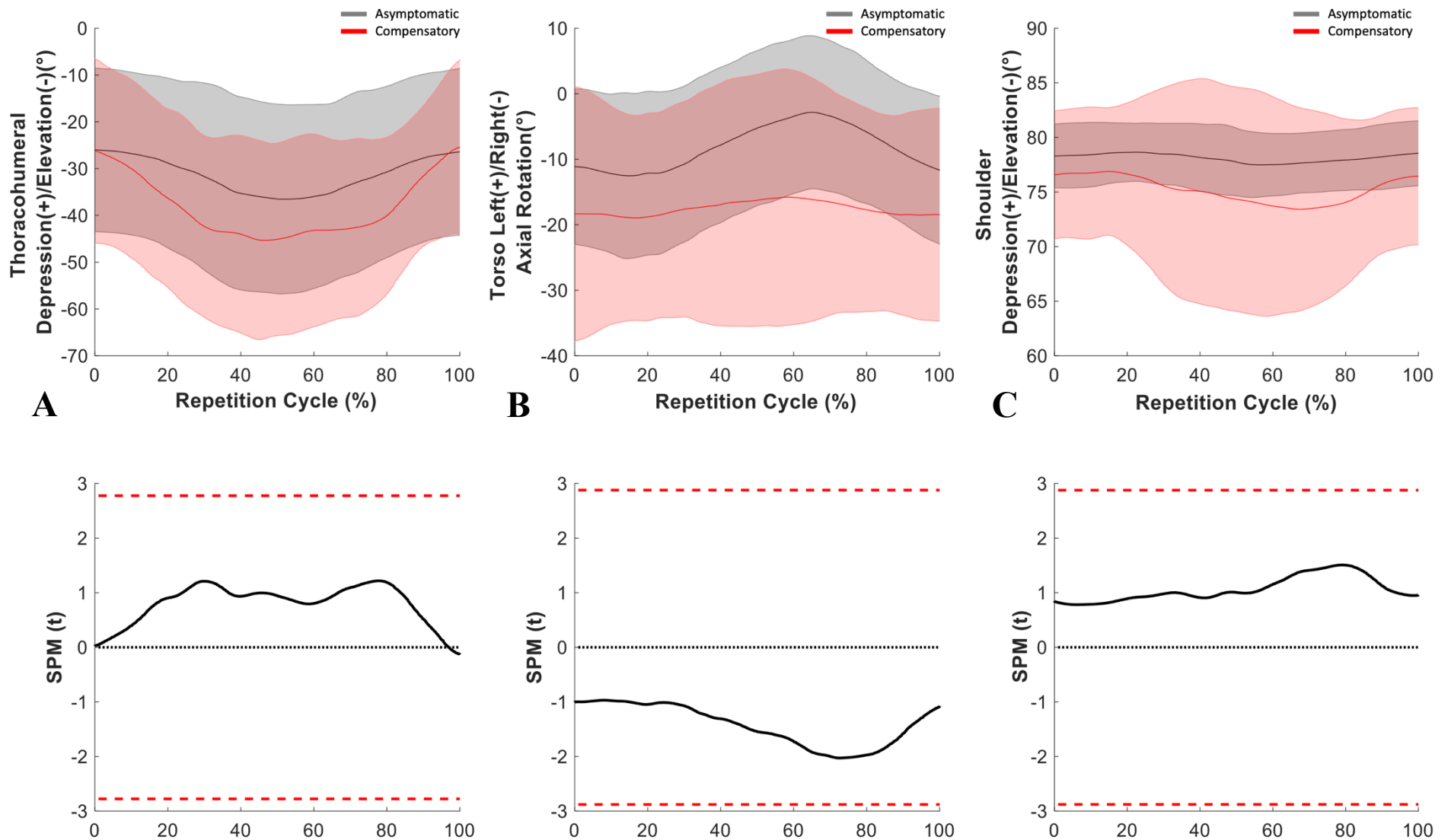


Figure 21: Averaged participant group thoracohumeral elevation angle (left), torso axial rotation angle (middle) and shoulder shrug angle (right) for asymptomatic participants performing shoulder internal rotation standard exercise movement (grey) and simulated compensatory exercise movement (red), time normalized to a full repetition cycle (10th repetition). One standard deviation for each condition is represented by the shaded grey and red areas. Associated SPM z-scores are reported below the average time-series data, with critical z-scores represented by the red dashed lines. Z-scores that exceed the critical value represent significant differences between conditions and are marked with an asterisk (*) over the area(s) where they exist.

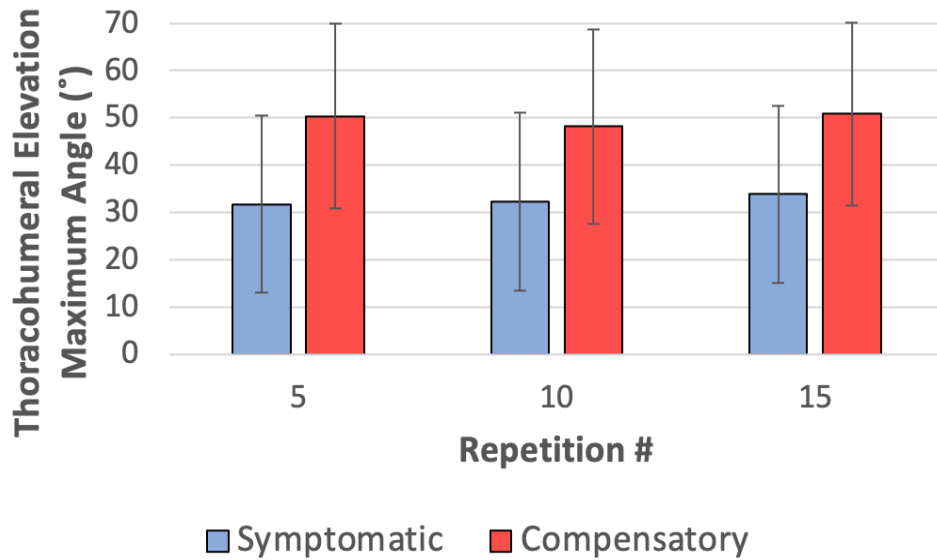


Figure 22: Thoracohumeral elevation maximum angle for the shoulder internal rotation exercise at the 5th, 10th and 15th repetitions. Error bars indicate standard deviation.

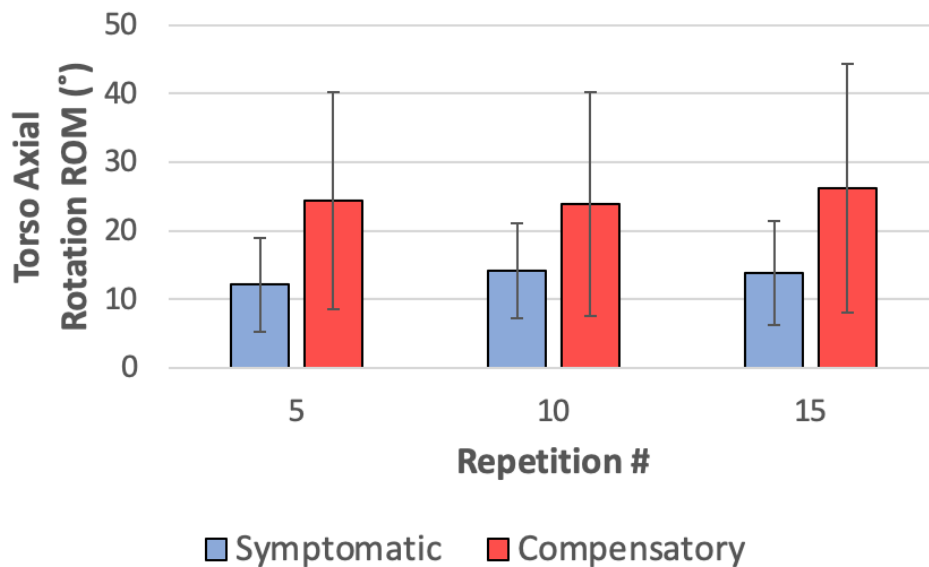


Figure 23: Torso axial rotation ROM for the shoulder internal rotation exercise at the 5th, 10th and 15th repetitions. Error bars indicate standard deviation.

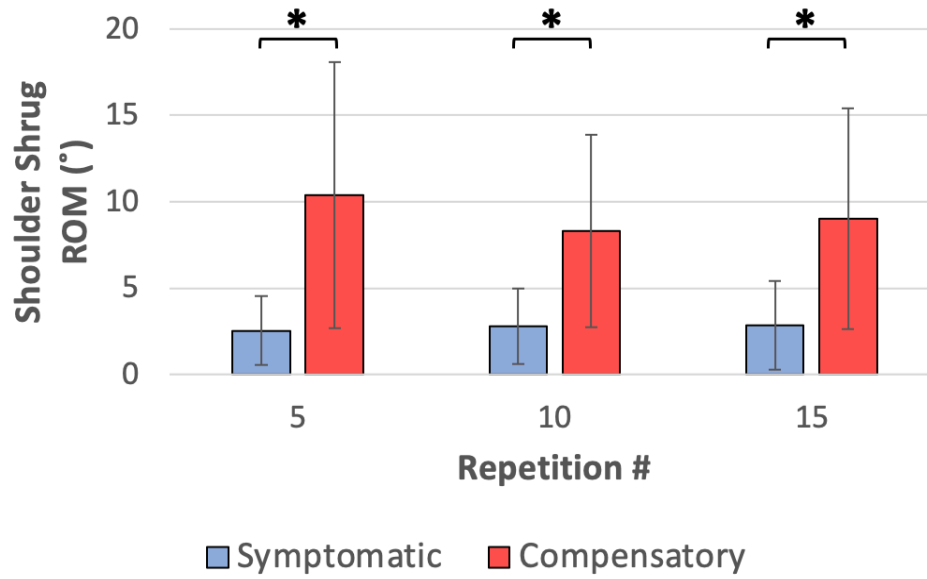


Figure 24: Shoulder shrug ROM for the shoulder internal rotation exercise at the 5th, 10th and 15th repetitions. Error bars indicate standard deviation. An asterisk (*) indicates significance at $P < 0.05$ within a repetition.

4.5 External Rotation

During the external rotation exercise, no differences occurred in the time-series data, while differences in maximum angle and ROM emerged between the symptomatic and asymptomatic groups. Although no differences emerged between the performance of both conditions by the asymptomatic group (Figure 25), participants had higher thoracohumeral elevation and achieved their maximum angle around 65% of the repetition cycle. When comparing between the symptomatic and asymptomatic compensatory groups, differences existed at each repetition for thoracohumeral elevation (5th repetition = 35°, $p = 0.005$; 10th repetition = 39°, $p = 0.003$; 15th repetition = 37°, $p = 0.003$) (Figure 26). For the axial rotation ROM of the torso, differences were only present during the 5th repetition (8°, $p = 0.040$) (Figure 27). Finally, differences occurred at each repetition for the shoulder shrug cue (5th repetition = 7°, $p = 0.001$; 10th repetition = 7°, $p = 0.001$; 15th repetition = 7°, $p = 0.001$) (Figure 28).

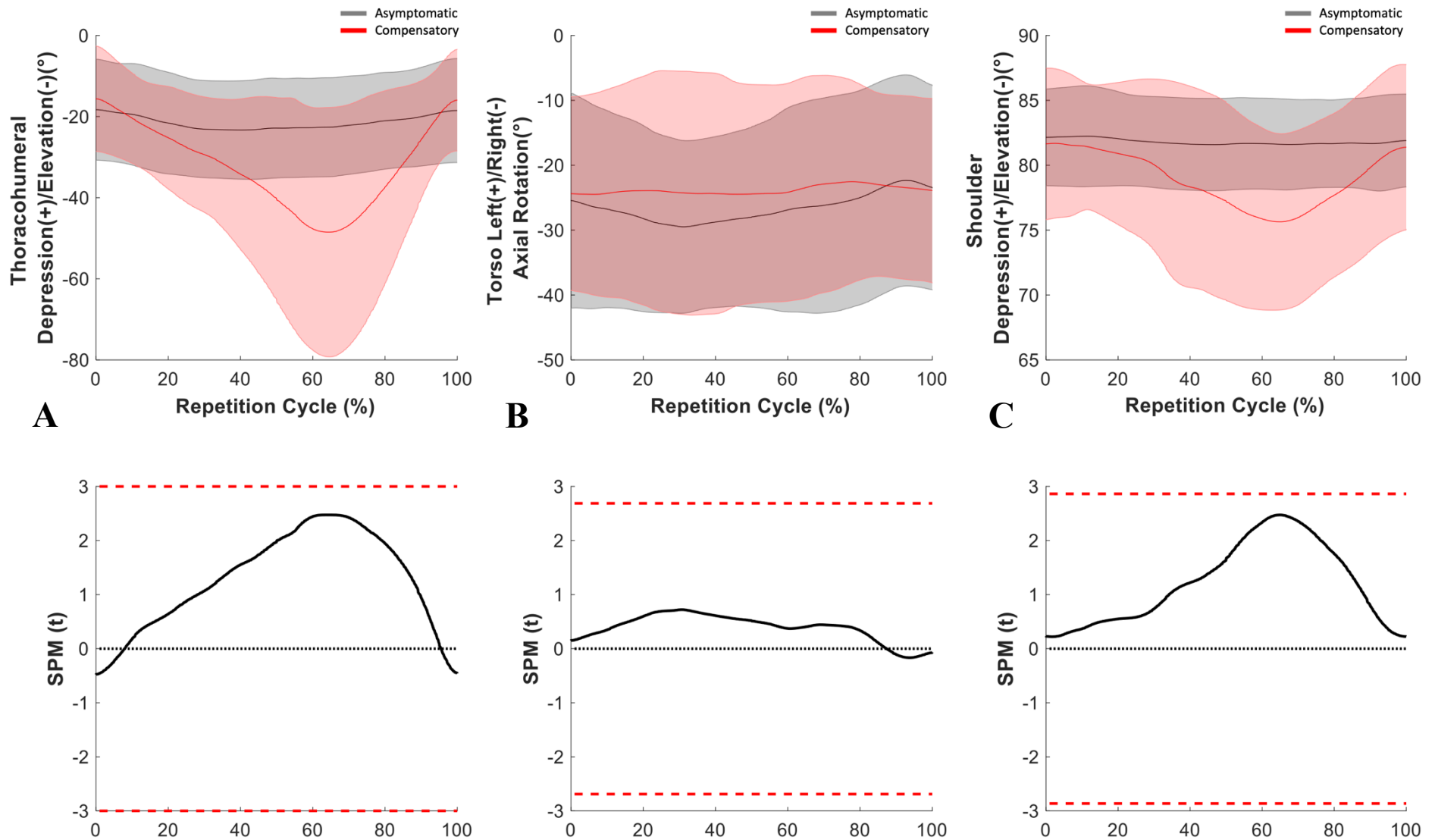


Figure 25: Averaged participant group thoracohumeral elevation angle (left), torso axial rotation angle (middle) and shoulder shrug angle (right) for asymptomatic participants performing shoulder external rotation standard exercise movement (grey) and simulated compensatory exercise movement (red), time normalized to a full repetition cycle (10th repetition). One standard deviation for each condition is represented by the shaded grey and red areas. Associated SPM z-scores are reported below the average time-series data, with critical z-scores represented by the red dashed lines. Z-scores that exceed the critical value represent significant differences between conditions and are marked with an asterisk (*) over the area(s) where they exist.

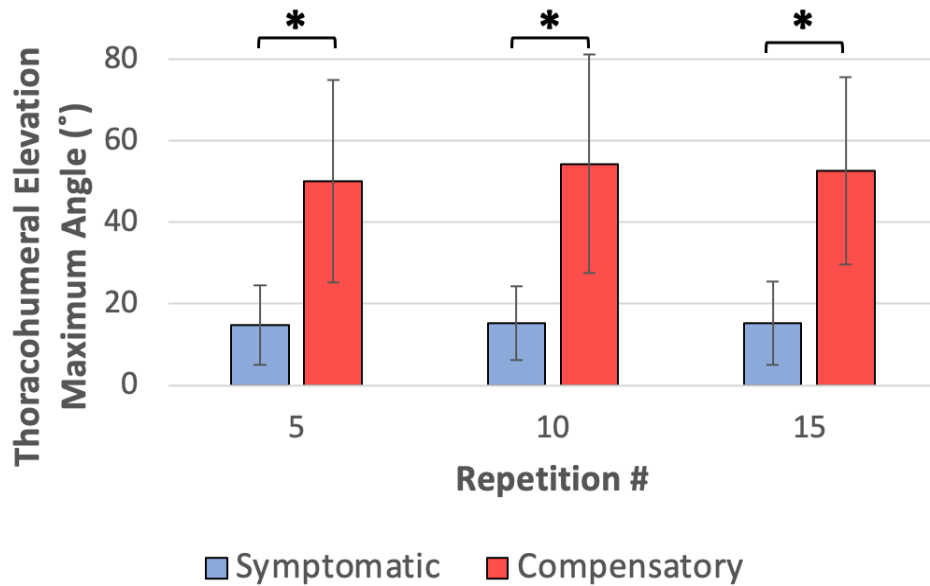


Figure 26: Thoracohumeral elevation maximum angle for the shoulder external rotation exercise at the 5th, 10th and 15th repetitions. Error bars indicate standard deviation. An asterisk (*) indicates significance at $P < 0.05$ within a repetition.

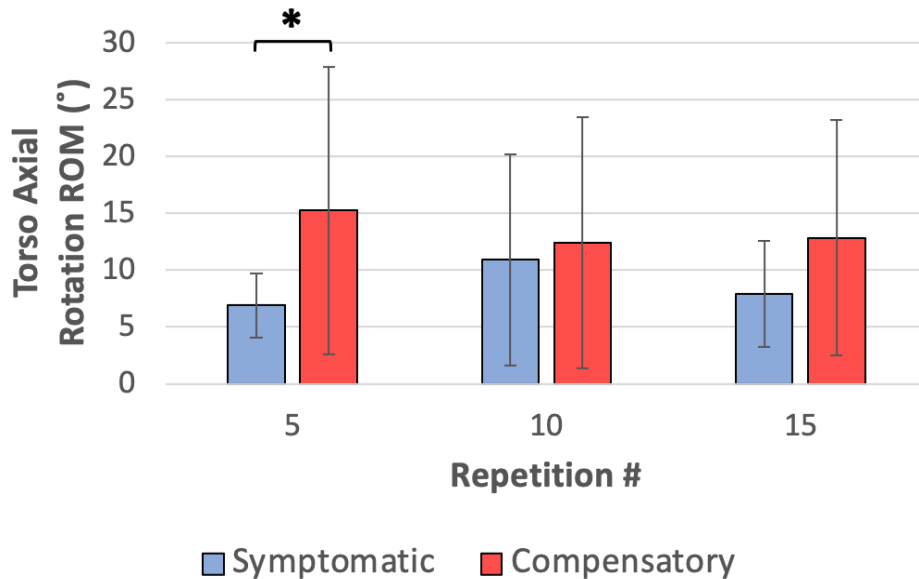


Figure 27: Torso axial rotation ROM for the shoulder external rotation exercise at the 5th, 10th and 15th repetitions. Error bars indicate standard deviation. An asterisk (*) indicates significance at $P < 0.05$ within a repetition.

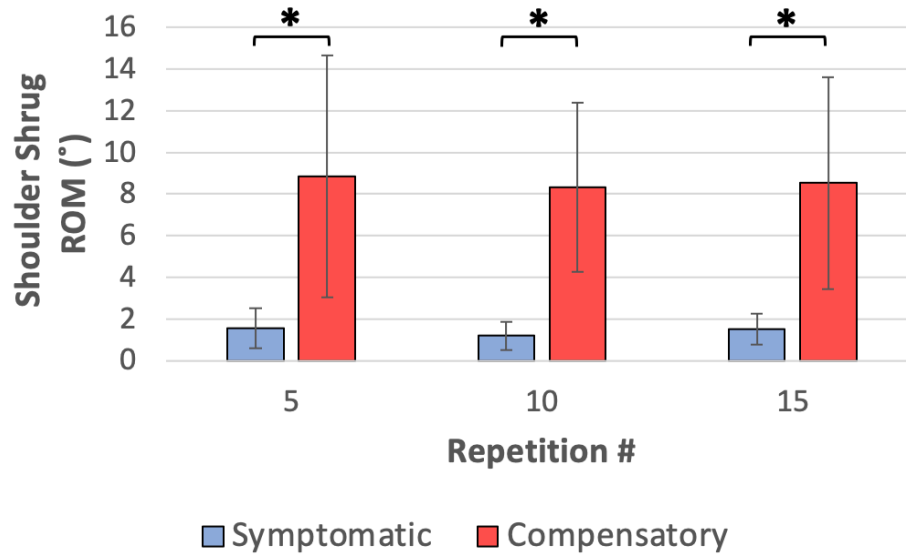
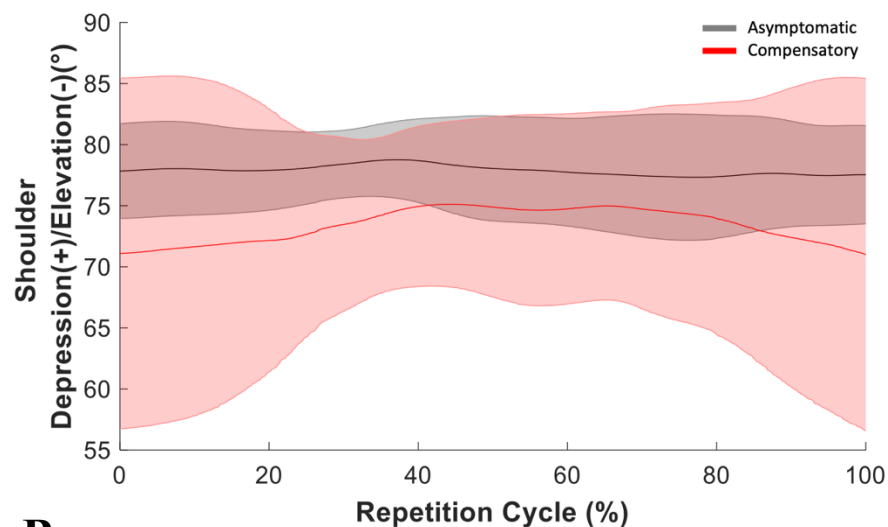
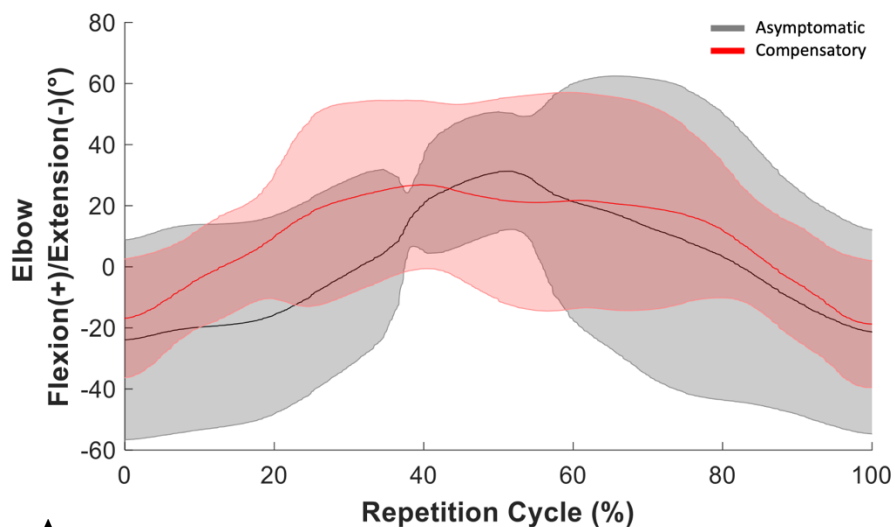


Figure 28: Shoulder shrug ROM for the shoulder external rotation exercise at the 5th, 10th and 15th repetitions. Error bars indicate standard deviation. An asterisk (*) indicates significance at $P < 0.05$ within a repetition.

4.6 Standing Row

Throughout the standing row exercise, only one difference emerged from the comparison of symptomatic and asymptomatic performance. The time-series data showed no differences between performance conditions for either cue during the repetition cycle. However, the simulated compensatory condition attained peak elbow flexion earlier in the repetition cycle and had a lower shoulder shrug angle throughout the entire cycle (Figure 29). Next, no differences emerged in the elbow flexion ROM data across all repetitions, but the symptomatic group consistently had less elbow flexion ROM than the asymptomatic compensatory performance (Figure 30). Finally, for the shoulder shrug ROM, the only between-group difference was for the 10th repetition of 8° ($p = 0.031$) (Figure 31).



A

B

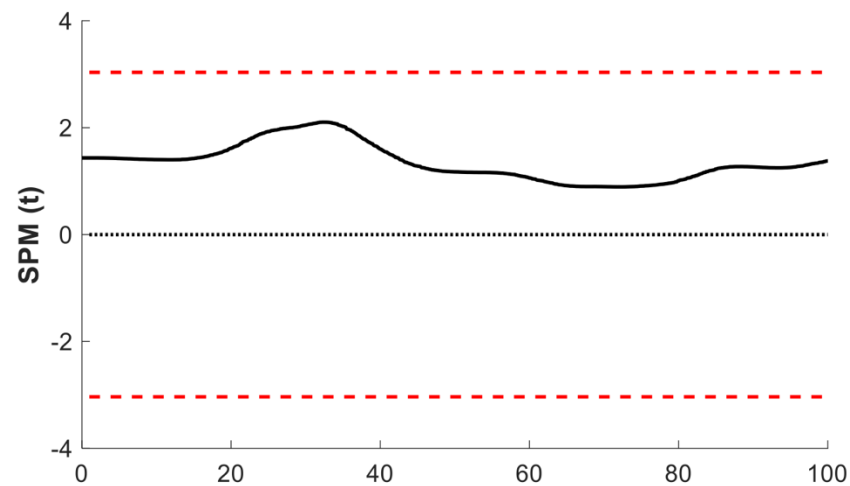
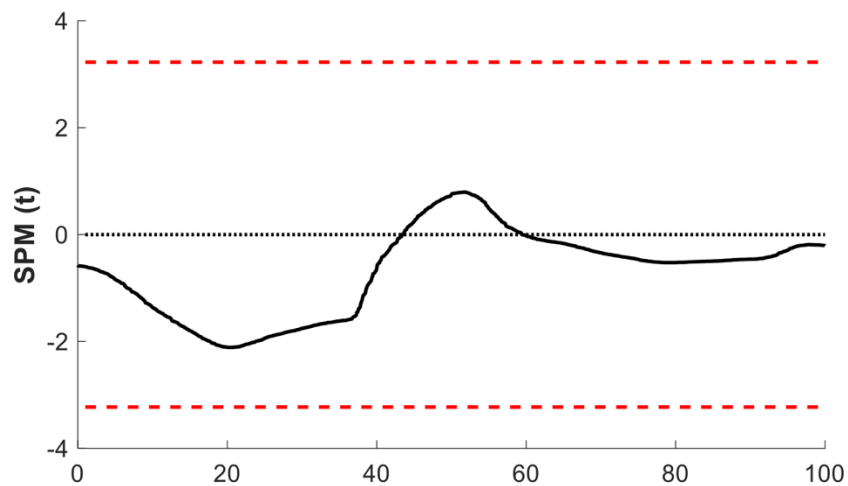


Figure 29: Averaged participant group elbow flexion/extension angle (left) and shoulder shrug angle (right) for asymptomatic participants performing standing row standard exercise movement (grey) and simulated compensatory exercise movement (red), time normalized to a full repetition cycle (10th repetition). One standard deviation for each condition is represented by the shaded grey and red areas. Associated SPM z-scores are reported below the average time-series data, with critical z-scores represented by the red dashed lines. Z-scores that exceed the critical value represent significant differences between conditions and are marked with an asterisk (*) over the area(s) where they exist.

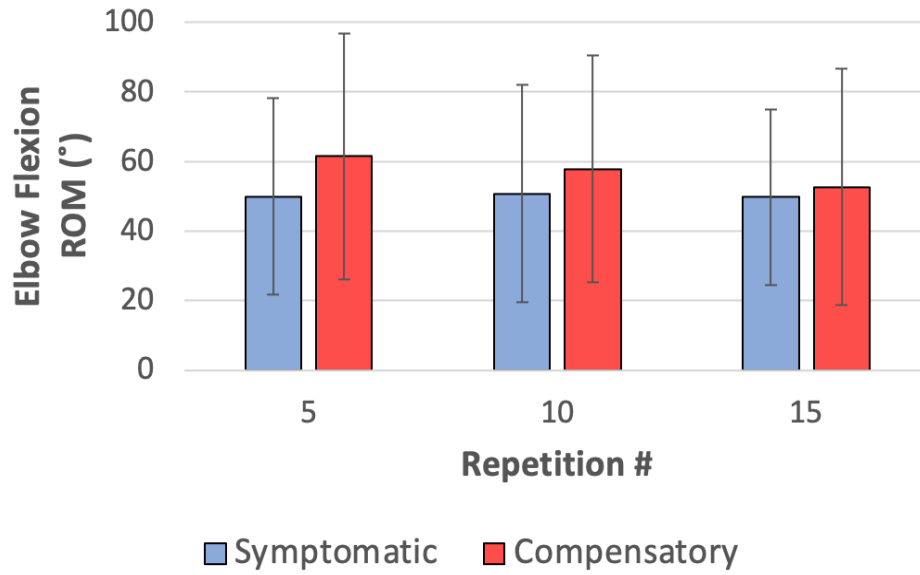


Figure 30: Elbow flexion ROM for the standing row exercise at the 5th, 10th and 15th repetitions. Error bars indicate standard deviation.

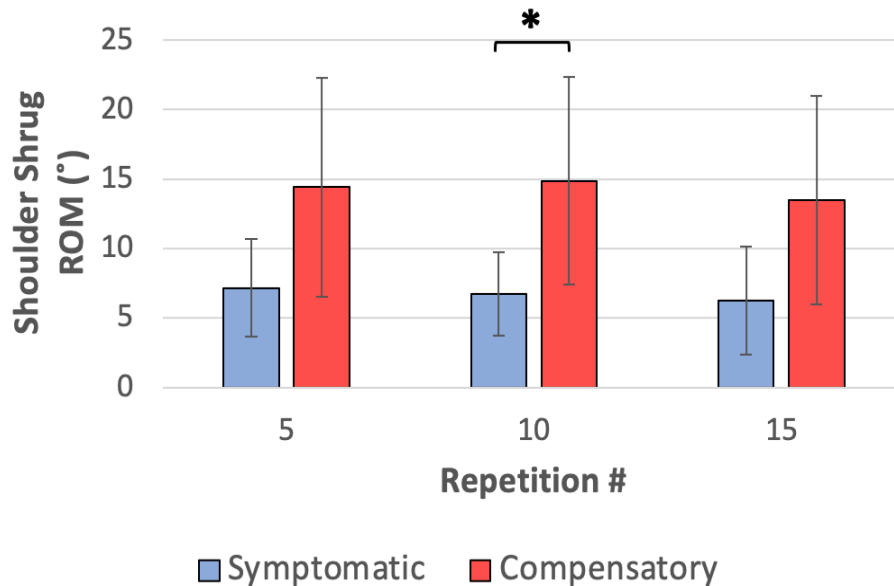


Figure 31: Shoulder shrug ROM for the standing row exercise at the 5th, 10th and 15th repetitions. Error bars indicate standard deviation. An asterisk (*) indicates significance at $P < 0.05$ within a repetition.

5.0 Discussion

The primary goal of this thesis was to systematically determine whether a healthy asymptomatic group of participants were capable of simulating compensatory exercise movement cues associated with subacromial impingement rotator cuff pathology. Comparisons were made between two conditions of movement cues (standard and compensatory) performed by the same group of asymptomatic participants, while symptomatic participants' exercise movements were compared to the simulated compensatory exercise movements of the asymptomatic group. The results suggest that asymptomatic individuals were successful in performing certain movement cues based on the changes of their time-series joint angle profiles. The results also suggest that the compensatory cues performed by the asymptomatic group represented an exaggerated or “worst-case” scenario of movement compensation, which was not representative of all collected individuals who were symptomatic for subacromial impingement syndrome. Yet, there was a wide spectrum of movement patterns recorded for the symptomatic group where participants fell within the exercise movement ranges of standard and compensatory performance of the asymptomatic group. For example, two symptomatic participants achieved a mean thoracohumeral elevation maximum angle that was below 80° and were among the asymptomatic simulated compensatory data, while three symptomatic participants were above 130° of elevation and were among asymptomatic standard exercise performances (Figure 32). The similarities and differences in kinematics between different groups and conditions encourages additional assessment of compensatory movements in rehabilitative shoulder exercises in order to better define the ranges that distinguish standard and compensatory performances. This study also showed that future investigations involving exercise tracking with ML algorithms may benefit from a broader shoulder kinematic dataset encompassing a wide

spectrum of exercise performances of both standard and compensatory movements to recognize individuals at various stages of rehabilitation.

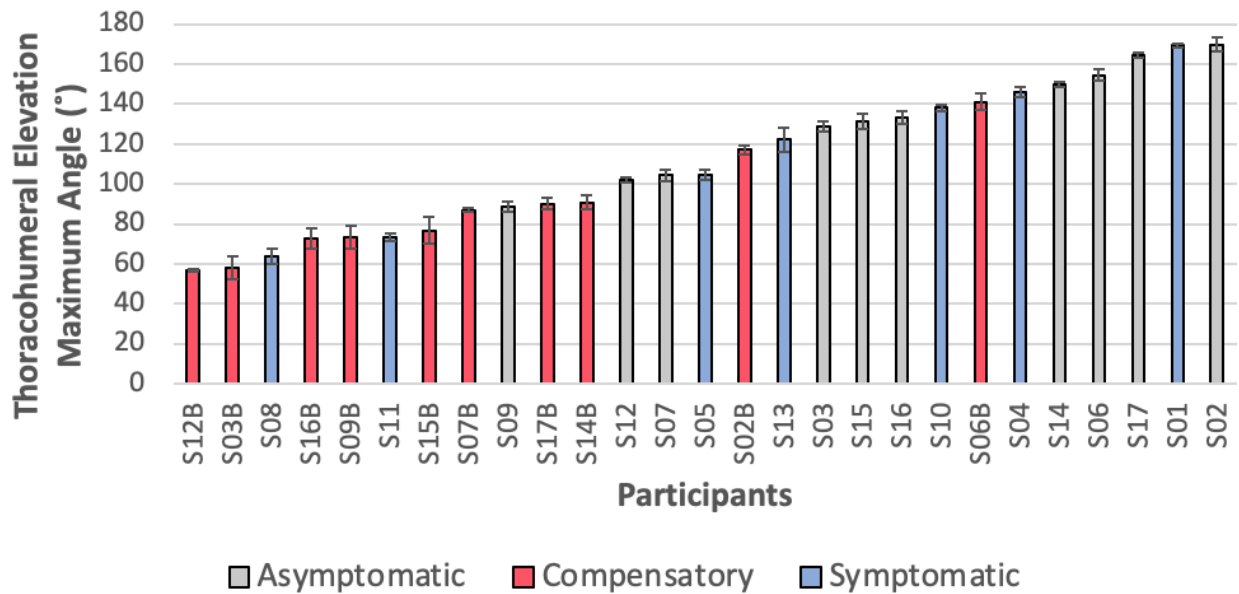


Figure 32: Mean thoracohumeral elevation maximum angle for the active assisted shoulder flexion exercise of all participants. Error bars indicate standard deviation. Participants with a “B” after their subject number signifies the same asymptomatic participant performing compensatory movement cues. Similar figures for other exercise movements are shown in Appendix B.

5.1 Hypotheses

5.1.1 Hypothesis #1

Hypothesis #1 stated that there would be detectable differences in trunk, thoracohumeral and elbow kinematic patterns between standard exercise movements and simulated compensatory exercise movements performed by the asymptomatic group. This hypothesis was partially accepted. Detectable differences were only present in three out of eighteen comparisons. The time-series joint angle profiles for thoracohumeral elevation during active assisted shoulder flexion, active assisted shoulder scaption and shoulder abduction had detectable differences

around the middle portion of the repetition cycle, as participants were instructed in the movement cues to elevate their arm to shoulder height (approximately 90° of elevation) for the compensatory condition and to the maximal height they could attain (approximately 180° of elevation) for the asymptomatic condition.

5.1.2 Hypothesis #2

Hypothesis #2 stated that asymptomatic individuals performing simulated compensatory shoulder exercise movement cues would have similar maximum angle and ROM outcomes for trunk, thoracohumeral and elbow movements compared to symptomatic individuals performing the same shoulder exercise movements. This hypothesis was partially accepted. Out of fifty-four comparisons, thirty-six repetitions were not significantly different when comparing the same exercise and repetition number between symptomatic and asymptomatic (compensatory) groups. The movement cues that had no similarity across any repetitions within the same exercise included: shoulder abduction – thoracohumeral elevation; shoulder internal rotation – shoulder shrug; and shoulder external rotation – thoracohumeral elevation and shoulder shrug.

5.2 Kinematics

5.2.1 Time-Series Data

Based on the analyzed time-series data, the results suggest that asymptomatic participants were capable of achieving two different targets and movement patterns for a specific movement cue for the same exercise. Differences were detected when comparing time-series joint angle profiles of specific movements cues during different rehabilitative shoulder exercises. As mentioned in section 5.1.1, differences emerged between standard and simulated compensatory movement performed by the asymptomatic group for thoracohumeral elevation during active

assisted shoulder flexion, scaption and shoulder abduction. This is reflected in the timing and manner in which they attained the desired cue and returned to the starting position of the exercise. The thoracohumeral elevation angle for each of the three exercises had participants achieve peak elevation angle around 90° of shoulder flexion and abduction later in the repetition cycle (around 60% to 65%) for the compensatory condition compared to a higher peak elevation angle of shoulder flexion and abduction at approximately 50% of the repetition cycle for the standard movement condition. For the time-series data that did not show detectable differences in the movement cues, the information provided from the means and standard deviations of the compensatory condition suggests that asymptomatic participants were still able to execute two different motions based on the visual trends. For example, in Figure 24, the compensatory conditions included increased thoracohumeral elevation and shoulder elevation (reaching the peak around 65% of the repetition cycle) while maintaining a steady axial rotation angle of the torso throughout the cycle. Additionally, use of the SPM approach to visualize and identify differences in the time-series movement patterns can help to confirm appropriate classification of the wrist-worn IMU data for the exercise performance conditions (standard and compensatory) of the asymptomatic group. This ability will benefit the development of ML models by providing more accurate labels of time-series sensor data towards the goal of improved exercise recognition and adherence tracking for health care providers. Being able to visualize how different movement cues are being performed simultaneously may also provide additional depth to movement training where patients can be given specific cues to correct potential compensatory movements at each segment, thereby enhancing the treatment plan of each patient (Santos et al., 2018). Additionally, this was the first study to apply SPM analysis to assess kinematic waveforms of the torso and upper limbs of individuals performing rehabilitative

shoulder exercises. This provided the advantage of using SPM to analyze the complexity of a movement in its entirety (Papi et al., 2020) throughout a movement cycle and gain insight into what was occurring simultaneously at different segments.

5.2.2 Maximum Angle & ROM Measures

Many of the maximum angle and ROM measures suggest that asymptomatic participants were able to closely simulate compensatory exercise movements associated with a symptomatic population from a statistical standpoint when differences were not identified between group means. For example, during the active assisted shoulder flexion exercise, there was no difference between the means from both groups if they were within 30° of thoracohumeral elevation, had a difference in torso lateral flexion below 7.5° or a difference in shrug ROM below 6°. This suggests that some of the compensatory cues performed by the asymptomatic group may depict compensatory movement in a symptomatic population suffering from SAIS or RCT. Although some of the differences found may not be statistically different, clinically relevant differences may be present within the data. Previous studies evaluating kinematics of patients with SAIS have focused on functional movements, activities of daily living (Ludewig & Cook, 2000; Kelly et al., 2005; Hall et al., 2011; Li et al., 2016) and on scapular kinematics as altered scapular movement has been reported in patients with SAIS (Saito et al., 2018). This study was an initial attempt to quantify torso and upper limb kinematics in asymptomatic and symptomatic populations which may provide important information on how other segments of the body may affect the effectiveness of rehabilitative shoulder exercises. Due to the age range of both sample groups in the current work, no direct comparisons to previous work on impingement kinematics was attempted. It has been suggested that younger populations with SAIS or RCT have decreased ROM in internal and external rotation movements (Senbursa et al., 2007; van Andel et

al., 2008) while older populations have decreased ROM in flexion, extension, abduction and external rotation movements (Hall et al., 2011). Additional analysis and comparison of the results may provide further agreement with the previous literature, while the current analysis suggests similar trends in movement for symptomatic individuals performing rehabilitative shoulder exercises.

Although the mean outcome measures of each movement cue may not describe the entirety of a symptomatic or asymptomatic population, analyzing each individual performance may provide insight into the variability of the movements captured as well as the range of movement that participants with and without symptoms will achieve. For example, individual performances of thoracohumeral elevation during active assisted shoulder flexion (Figure 32) illustrate that the symptomatic group had achieved thoracohumeral elevation angles between 60° to 170°, the asymptomatic group ranged from 90° to 170° and the asymptomatic simulated compensatory condition varied from 55° to 140°. By having asymptomatic participants perform both standard and compensatory movements as worst- and best-case scenarios for performance, all movements of the symptomatic group fell within the established spectrum of movement. This figure also demonstrates that asymptomatic individuals could attain target cues based on the movement instructions provided. Additionally, for the torso lateral flexion cue (Figure 33 – Appendix B), individual performances of compensatory movement by the asymptomatic group reflected symptomatic individual behaviors which included increased ROM in torso lateral flexion. Again, these results suggest that asymptomatic individuals could execute the movement cue properly as the compensatory values are grouped more towards the right of the graph indicating an increase in torso lateral flexion ROM. Therefore, the collected data is an important step towards understanding movement differences in rehabilitative shoulder exercises between

asymptomatic and symptomatic individuals and towards determining the feasibility of building an exercise movement dataset strictly from asymptomatic individuals that would include and capture asymptomatic and symptomatic movements within its spectrum.

5.3 Research Contributions and Applications

This thesis explored differences between asymptomatic and symptomatic torso and upper limb kinematics when performing rehabilitative shoulder exercises and helps to establish a foundation of kinematic knowledge regarding the torso and upper limb movement during therapeutic exercises. This complements previous kinematic studies which focused on scapulothoracic and thoracohumeral motion during functional movements and activities of daily living (Ludewig & Cook, 2000; Hall et al., 2011; Li et al., 2016; Vidt et al., 2016; Rossi et al., 2020). The current findings suggest that asymptomatic individuals can execute various movement cues associated with standard and compensatory exercise movements, and that by performing both types of motion, they produce movements that span a wide range of symptomatic movement associated with SAIS and RCT injuries. Further, the kinematic and IMU data collected will assist future development of ML algorithms for tracking the adherence of physical therapy exercise programs, provide distinguishing features between different exercise performances, and help refine movement cues for future data collections to closely match symptomatic behaviors. As demonstrated by Burns et al. (2018), smartwatches containing an IMU can recognize different rehabilitative shoulder exercises. New kinematic data collected in this thesis will improve future research efforts to achieve a more accurate and generalizable ML model that can be implemented in clinical settings to track patient progression in real-time while providing feedback to both the clinician and the patient.

5.4 Limitations

5.4.1 Kinematic Data Reduction

The work reported in this thesis should be considered with various limitations. First, the kinematic data reduction for the time-series, maximum angle and ROM measures may have obscured some nuanced results. Both maximum angle and ROM measures were evaluated at three repetitions out of a set of twenty and were further reduced to one number to represent group means and facilitate comparisons. An alternative approach would have been to average the values of each repetition for a set of exercises within participants to incorporate data from more repetitions. Adding additional repetitions would also increase the chance of capturing more of an individual's movement variability as five repetitions could capture up to 95% of an individual's variability (Frost et al., 2015). This would lower the potential sampling errors, but a minimum of three trials or repetitions was deemed adequate to capture a subject's variability at a given point in time. For the time-series kinematic data, examining additional collected repetitions would capture more of the movement variability throughout the repetition cycle. This could illustrate changes in the movement patterns within the exercise set as a participant performs more repetitions and begins to fatigue towards the end of the set.

5.4.2 Participant Sample

A second limitation to this thesis is the size of the participant sample. Due to the effect size used to calculate the minimum participant sample to yield a power value of 0.8, several potentially important group differences in the maximum angle and ROM measures may not be detected. Additional participants in both groups would improve sensitivity for identifying these potentially useful differences when it comes to statistical and clinical differences within the data. However, the complexity of the dataset collected retains value in the ML algorithm development.

Further, age differences, sex differences, and handedness were not considered for this sample. As suggested by previous literature, it is unlikely that sex differences or differences in hand dominance would affect performances (Milgrom et al., 1995; Tempelhof et al., 1999). However, age differences may influence movement strategies in both younger and older asymptomatic and symptomatic groups (Senbursa et al., 2007; van Andel et al., 2008; Hall et al., 2011). This occurs as the prevalence of RCT increases in part due to diminished quality of the muscles and tendons with increased age (Cooper & Ali, 2013). Finally, symptomatic classification was based on the result of two clinical impingement tests (Neer's and Hawkins-Kennedy impingement tests) performed by the lead researcher. Although care was taken to accurately assess participants, some previous literature recommends the use of three clinical tests as this may increase the reliability in classifying participants as symptomatic or asymptomatic for SAIS (Alquanaee et al., 2012). Future research could employ MRI or ultrasound imaging to formalize diagnoses of different rotator cuff pathologies.

5.5 Future Directions

Valuable future work could focus on collecting additional kinematic and IMU data of symptomatic patients with specific diagnoses at various stages of their recovery. This additional data would provide a larger sample of symptomatic movement to include into the dataset while tracking the movement changes as a patient returns to a healthy asymptomatic status with normal function. Additionally, collecting EMG and supplemental kinematic data of asymptomatic performances of standard and compensatory movement with refined compensatory movement cues may provide clear distinctions between different movement types in a generalized ML model.

Future work may also benefit from incorporating all collected repetitions into the dataset. This would provide some additional information on tracking the consistency of participant performances in the time-series, maximum angle and ROM measures. Additional repetitions would also confirm movement cue execution and ensure participants are not reverting to compensatory movements throughout a set of exercises. Also, a further breakdown in the comparisons when considering age and injury status may clarify if the origins of differences in kinematics relate to an individual's specific injury or generalized factors such as aging and the weakening of the rotator cuff muscles. Although one generalized ML model to track exercise adherence would be ideal, it may be practical to have models tailored for younger and older populations to account for consistent age-based differences.

6.0 Conclusions

In conclusion, this study generated a robust set of detailed kinematic data using both asymptomatic and symptomatic subjects that will help to assist the development of ML algorithms towards the goal of improved tracking of rehabilitative exercise program adherence. This study was the first to have an asymptomatic group simulate compensatory exercise movement of a symptomatic group, with the larger goal of creating a diverse and inclusive dataset of kinematic and IMU data. Asymptomatic participants were successful in executing movement cues for both standard and compensatory exercise performances. Data captured included movement variability that better represents a spectrum between worst-case compensatory and best-case proper movement for the shoulder exercises performed. When comparing the similarities between the asymptomatic compensatory and symptomatic performances, several movement cues for compensatory exercise performance were good indicators of symptomatic movement patterns, while other cues require additional refinement. Further research is needed to better understand the range of symptomatic exercise performance, preferably in clinical populations, in order to make the appropriate changes to movement cue instructions for asymptomatic individual performance.

References

- Alenabi, Talia, Whittaker, Rachel, Kim, Soo Y., & Dickerson, Clark R. (2018). Maximal voluntary isometric contraction tests for normalizing electromyographic data from different regions of supraspinatus and infraspinatus muscles: Identifying reliable combinations. *Journal of Electromyography and Kinesiology*, 41, 19-26.
<https://doi.org/10.1016/j.jelekin.2018.04.007>
- Alenabi, Talia, Whittaker, Rachel L., Kim, Soo Y., & Dickerson, Clark R. (2019). Arm posture influences on regional supraspinatus and infraspinatus activation in isometric arm elevation efforts. *Journal of Electromyography and Kinesiology*, 44, 108-116.
<https://doi.org/10.1016/j.jelekin.2018.12.005>
- Alqunae, Marwan, Galvin, Rose, & Fahey, Tom. (2012). Diagnostic Accuracy of Clinical Tests for Subacromial Impingement Syndrome: A Systematic Review and Meta-Analysis. *Archives of Physical Medicine and Rehabilitation*, 93, 229-236.
<https://doi: 10.1016/j.apmr.2011.08.035>
- Attal, Ferhat, Mohammed, Samer, Dedabrishvili, Mariam, Chamroukhi, Faicel, Oukhellow, Latifa, & Amirat, Yacine. (2015). Physical Human Activity Recognition Using Wearable Sensors. *Sensors*, 15(12), 31314-31338. <https://doi.org/10.3390/s151229858>
- Blasier, Ralph B., Soslowsky, Louis J., Makicky, David M., & Palmer, Mark L. (1997). Posterior Glenohumeral Subluxation: Active and Passive Stabilization in a Biomechanical Model. *The Journal of Bone & Joint Surgery*, 79(3), 433-440.
- Burkart, Andreas C., & Debski, Richard E., (2002). Anatomy and Function of the Glenohumeral Ligaments in Anterior Shoulder Instability. *Clinical Orthopaedics and Related Research*, 400, 32-39.

- Burke, Wendy S., Vangsness, C. Thomas, & Powers, Christopher M. (2002). Strengthening the Supraspinatus: A Clinical and Biomechanical Review. *Clinical Orthopaedics and Related Research*, 402, 292-298.
- Burns, David M., Leung, Nathan, Hardistry, Michael, Whyne, Cari, Henry, Patrick, & McLachlin, Stewart M. (2018). Shoulder Physiotherapy Exercise Recognition: Machine Learning the Inertial Signals from a Smartwatch. *Physiological Measurement*, 39(7), 075007. <https://doi.org/10.1088/1361-6579/aacfd9>
- Chang, K.-V., Hung, C.-Y., Han, D.-S., Chen, W.-S., Wang, T.-G., & Chien, K.-L. (2015). Early Versus Delayed Passive Range of Motion Exercise for Arthroscopic Rotator Cuff Repair: A Meta-analysis of Randomized Controlled Trials. *The American Journal of Sports Medicine*, 43(5), 1265–1273. <https://doi.org/10.1177/0363546514544698>
- Chopp, Jaclyn N., O'Neill, John M., Hurley, Kevin, & Dickerson, Clark R. (2010). Superior humeral head migration occurs after a protocol designed to fatigue the rotator cuff: A radiographic analysis. *Journal of Shoulder and Elbow Surgery*, 19(8), 1137-1144. <https://doi.org/10.1016/j.jse.2010.03.017>
- Chopp-Hurley, Jaclyn N., & Dickerson, Clark R. (2015). The potential role of upper extremity muscle fatigue in the generation of extrinsic subacromial impingement syndrome: a kinematic perspective. *Physical Therapy Reviews*, 20(3), 201-209. <https://doi.org/10.1179/1743288X15Y.0000000009>
- Chopp-Hurley, Jaclyn N., O'Neill, John M., McDonald, Alison C., Maciukiewicz, Jacquelyn M., & Dickerson, Clark R. (2016). Fatigue-induced glenohumeral and scapulothoracic kinematic variability: Implications for subacromial space reduction. *Journal of Electromyography and Kinesiology*, 29, 55-63. <http://dx.doi.org/10.1016/j.jelekin.2015.08.001>

- Codman, Ernest Amory. (1934). *The Shoulder: Rupture of the Supraspinatus Tendon and Other Lesions in or About the Subacromial Bursa*. Boston: (n.p.).
- Cohen, Jacob. (1992). Statistical Power Analysis. *Current Directions in Psychological Science*, 1(3), 98-101. <https://doi.org/10.1111/1467-8721.ep10768783>
- Cooper, Anthony, & Ali, Amjid. (2013). Rotator cuff tears. *Surgery (Oxford)*, 31(4), 168-171. <https://doi.org/10.1016/j.mpsur.2013.01.017>
- Cudlip, Alan C., & Dickerson, Clark R. (2018). Regional activation of anterior and posterior supraspinatus differs by plane of elevation, hand load and elevation angle. *Journal of Electromyography and Kinesiology*, 43, 14-20. <https://doi.org/10.1016/j.jelekin.2018.08.003>
- Engin, Ali Erkan. (1980). On the biomechanics of the shoulder complex. *Journal of Biomechanics*, 13(7), 575-590. [https://doi.org/10.1016/0021-9290\(80\)90058-5](https://doi.org/10.1016/0021-9290(80)90058-5)
- Friston, K. J., Frith, C. D., Liddle, P. F., & Frackowiak, R. S. J. (1991). Comparing Functional (PET) Images: The Assessment of Significant Change. *Journal of Cerebral Blood Flow and Metabolism*, 11, 690-699. <https://doi.org/10.1038/jcbfm.1991.122>
- Frost, David M., Beach, Tyson. A C., McGill, Stuart M., & Callaghan, Jack P. (2015). A proposed method to detect kinematic differences between and within individuals. *Journal of Electromyography and Kinesiology*, 25(3), 479–487. <https://doi.org/10.1016/j.jelekin.2015.02.012>
- Garcia-Ceja, Enrique, Brena, Ramon F., Carrasco-Jimenez, Jose C., & Garrido, Leonardo. (2014). Long-Term Activity Recognition from Wristwatch Accelerometer Data. *Sensors*, 14, 22500-22524. <https://doi.org/10.3390/s141222500>

Häberle, R., Schellenberg, F., List, R., Pluss, Michael, Taylor, William R., & Lorenzetti, Silvio.

(2018). Comparison of the kinematics and kinetics of shoulder exercises performed with constant and elastic resistance. *BMC Sports Science, Medicine and Rehabilitation*, 10(22).

<https://doi.org/10.1186/s13102-018-0111-7>

Hall, Laurie C., Middlebrook, Erin E., & Dickerson, Clark R. (2011). Analysis of the influence

of rotator cuff impingement on upper limb kinematics in an elderly population during activities of daily living. *Clinical Biomechanics*, 26(6), 579-584.

<https://doi.org/10.1016/j.clinbiomech.2011.02.006>

Hamada, Junichiro, Nimura, Akimoto, Yoshizaki, Kunio, & Akita, Keiichi. (2017). Anatomic

study and electromyographic analysis of the teres minor muscle. *Journal of Shoulder and Elbow Surgery*, 26(5), 870-877. <https://doi.org/10.1016/j.jse.2016.09.046>

Hawkins, R. J., & Kennedy, J. C. (1980). Impingement syndrome in athletes. *The American*

Journal of Sports Medicine, 8(3), 151-158. <https://doi->

[org.proxy.lib.uwaterloo.ca/10.1177/036354658000800302](https://doi-org.proxy.lib.uwaterloo.ca/10.1177/036354658000800302)

Hintermeister, Robert A., Lange, Gregory W., Schultheis, Jeanne M., Bey, Michael J., &

Hawkins, Richard J. (1998). Electromyographic Activity and Applied Load During Shoulder Rehabilitation Exercises Using Elastic Resistance. *The American Journal of Sports*

Medicine, 26(2), 210-220.

Hinton, Perry R. (2010). Mann-Whitney U Test. In *Encyclopedia of Research Design*. Thousand

Oaks, CA: SAGE Publications, Inc. <https://dx.doi.org/10.4135/9781412961288>

- Holden, Melanie A., Haywood, Kirstie L., Potia, Tanzila A., Gee, Melanie, & McLean, Sionnadh. (2014). Recommendations for exercise adherence measures in musculoskeletal settings: a systemic review and consensus meeting (protocol). *Systematic Review*, 3(1). <http://dx.doi.org.proxy.lib.uwaterloo.ca/10.1186/2046-4053-3-10>
- Huegel, Julianne, Williams, Alexis A., & Soslowsky, Louis J. (2015). Rotator Cuff Biology and Biomechanics: a Review of Normal and Pathological Conditions. *Current Rheumatology Reports*, 17(1), 1-9. <https://doi-org.proxy.lib.uwaterloo.ca/10.1007/s11926-014-0476-x>
- Kasten, Philip, Rettig, Oliver, Loew, Markus, Wolf, Sebastian, & Raiss, Patric. (2009). Three-dimensional motion analysis of compensatory movements in patients with radioulnar synostosis performing activities of daily living. *Journal of Orthopaedic Science*, 14, 307–312. <https://doi.org/10.1007/s00776-009-1332-0>
- Kelly, Bryan T., Kadrmas, Warren R., Kirkendall, Donald T., & Speer, Kevin P. (1996). Optimal Normalization Tests for Shoulder Muscle Activation: An Electromyographic Study. *Journal of Orthopaedic Research*, 14(4), 647-653. <https://doi-org.proxy.lib.uwaterloo.ca/10.1002/jor.1100140421>
- Kelly, Bryan T., Williams, Riley J., Cordasco, Frank A., Backus, Sherry I., Otis, James C., Weiland, Daniel E., Altchek, David W., Craig, Edward V., Wickiewicz, Thomas L., & Warren, Russell F. (2005). Differential Patterns of Muscle Activation in Patients with Symptomatic and Asymptomatic Rotator Cuff Tears. *Journal of Shoulder and Elbow Surgery*, 14(2), 165-171. <https://doi.org/10.1016/j.jse.2004.06.010>

- Kluczynski, M. A., Nayyar, S., Marzo, J. M., & Bisson, L. J. (2015). Early Versus Delayed Passive Range of Motion After Rotator Cuff Repair: A Systematic Review and Meta-analysis. *The American Journal of Sports Medicine*, 43(8), 2057–2063.
<https://doi.org/10.1177/0363546514552802>
- Kuhn, John E., Dunn, Warren R., Sanders, Rosemary, An, Qi, Baumgarten, Keith M., Bishop, Julie Y., Brophy, Robert H., Carey, James L., Holloway, Brian G., Jones, Grant L., Ma, C. Benjamin, Marx, Robert G., McCarty, Eric C., Poddar, Sourav K., Smith, Matthew V., Spencer, Edwin E., Vidal, Armando F., Wolf, Brian R., & Wright, Rick W. (2013). Effectiveness of Physical Therapy in Treating Atraumatic Full Thickness Rotator Cuff Tears. A Multicenter Prospective Cohort Study. *Journal of Shoulder and Elbow Surgery*, 22(10), 1371-1379. <https://doi.org/10.1016/j.jse.2013.01.026>
- Lara, Oscar D., Perez, Alfredo J., Labrador, Miguel A., & Posada, Jose D. (2012). Centinela: A human activity recognition system based on acceleration and vital sign data. *Pervasive and Mobile Computing*, 8(5), 717-729. <https://doi.org/10.1016/j.pmcj.2011.06.004>
- Leardini, Alberto, Chiari, Lorenzo, Croce, Ugo Della, & Cappozzo, Aurelio. (2005). Human movement analysis using stereophotogrammetry Part 3. Soft tissue artifact assessment and compensation. *Gait and Posture*, 21, 212-225. <https://doi:10.1016/j.gaitpost.2004.05.002>
- Lempereur, Mathieu, Brochard, Sylvain, Leboeuf, Fabien, & Rémy-Néris, Olivier. (2014). Validity and reliability of 3D marker based scapular motion analysis : A systematic review. *Journal of Biomechanics*, 47(10), 2219-2230.
<https://doi.org/10.1016/j.jbiomech.2014.04.028>

- Li, Xiaotong, Santago, Anthony C., Vidt, Meghan E., & Saul, Katherine R. (2016). Analysis of effects of loading and postural demands on upper limb reaching in older adults using statistical parametric mapping. *Journal of Biomechanics*, 49(13), 2806-2816.
<https://doi.org/10.1016/j.jbiomech.2016.06.018>
- Longo, Umile Giuseppe, Rizzello, Giacomo, Petrillo, Stefano, Loppini, Mattia, Maffulli, Nicola, & Denaro, Vincenzo. (2019). Conservative Rehabilitation Provides Superior Clinical Results Compared to Early Aggressive Rehabilitation for Rotator Cuff Repair: A Retrospective Comparative Study. *Medicina*, 55(8), 402-411. <https://doi.org/10.3390/medicina55080402>
- Ludewig, Paula M., & Cook, Thomas M. (2000). Alterations in Shoulder Kinematics and Associated Muscle Activity in People With Symptoms of Shoulder Impingement. *Physical Therapy*, 80(3), 276-291. <https://doi.org/10.1093/ptj/80.3.276>
- MacDermaid, Joy C., Ramos, Joanne, Drosdowech, Darren, Faber, Ken, & Patterson, Stuart. (2004). The impact of rotator cuff pathology on isometric and isokinetic strength, function, and quality of life. *Journal of Shoulder and Elbow Surgery*, 13(6), 593-598.
<https://doi.org/10.1016/j.jse.2004.03.009>
- MacLean, Kathleen F. E., & Dickerson, Clark R. (2019). Kinematic and EMG analysis of horizontal bimanual climbing in humans. *Journal of Biomechanics*, 92(19), 11-18.
<https://doi.org/10.1016/j.jbiomech.2019.05.023>
- Malanga, Gerard A., Jenp, Yue-Nan, Growney, Eric S., & An, Kai-Nan. (1996). EMG analysis of shoulder positioning in testing and strengthening the supraspinatus. *Medicine & Science in Sports & Exercise*, 28(6), 661-664.
- Mann, H. B., & Whitney, D. R. (1947). On a Test of Whether one of Two Random Variables is Stochastically Larger than the Other. *The Annals of Mathematical Statistics*, 18(1), 50-60.

- Maurer, Uwe, Smailagic, Asim, Siewiorik, Daniel P., & Deisher, Michael. (2006). Activity Recognition and Monitoring Using Multiple Sensors on Different Body Positions. *International Workshop on Wearable and Implantable Body Sensor Networks (BSN'06)*, Cambridge, MA. <https://doi.org/10.1109/BSN.2006.6>.
- McClure, Philip W., Michener, Lori A., & Karduna, Andrew R. (2006). Shoulder Function and 3-Dimensional Scapular Kinematics in People With and Without Shoulder Impingement Syndrome. *Physical Therapy*, 86(8), 1075-1090. <https://doi.org/10.1093/ptj/86.8.1075>
- Milgrom, C., Schaffler, M., Gilbert, S., Van Holsbeeck, M. (1995). Rotator-cuff changes in asymptomatic adults. The effects of age, hand dominance and gender. *The Journal of Bone and Joint Surgery*, 77(2), 296-298.
- Morag, Yoav, Jamadar, David A., Miller, Bruce, Dong, Qian, & Jacobson, Jon A. (2011). The subscapularis: anatomy, injury, and imaging. *Skeletal Radiology*, 40(3), 255-269. <https://doi.org/10.1007/s00256-009-0845-0>
- Myers, Joseph B., Pasquale, Maria R., Laudner, Kevin G., Sell, Timothy C., Bradley, James P., & Lephart, Scott M. (2005). On-the-Field Resistance-Tubing Exercises for Throwers: An Electromyographic Analysis. *Journal of Athletic Training*, 40(1), 15-22.
- Neer, Charles S. (1983). Impingement Lesions. *Clinical Orthopaedics and Related Research*, 173, 70-77.
- Nguyen, Minh, Fan, Liyue, & Shahabi, Cyrus. (2015). Activity Recognition Using Wrist-Worn Sensors for Human Performance Evaluation. *2015 IEEE International Conference on Data Mining Workshop (ICDMW)*, 164-169.

- Nussbaum, Maury A., & Zhang, Xudong. (2000). Heuristics for locating upper extremity joint centres from a reduced set of surface markers. *Human Movement Science*, 19(5), 797-816. [https://doi.org/10.1016/S0167-9457\(00\)00020-8](https://doi.org/10.1016/S0167-9457(00)00020-8)
- Osborne, Jeffrey D., Gowda, Ashok L., Wiater, Brett, & Wiater, J. Michael. (2016). Rotator cuff rehabilitation: current theories and practice. *The Physician and Sportsmedicine*, 44(1), 85-92. <https://doi.org/10.1080/00913847.2016.1108883>
- Otis, James C., Jiang, Ching-Chuan, Wickiewicz, Thomas L., Peterson, Margaret G. E., Warren, Russell F., & Santner, Thomas J. (1994). Changes in the Moment Arms of the Rotator Cuff and Deltoid Muscles with Abduction and Rotation. *The Journal of Bone and Joint Surgery*, 76(5), 667-676.
- Papi, Enrica, Bull, Anthony M. J., & McGregor, Alison H. (2020). Alteration of movement patterns in low back pain assessed by Statistical Parametric Mapping. *Journal of biomechanics*, 100, 109597. <https://doi.org/10.1016/j.jbiomech.2019.109597>
- Pataky, Todd C. (2010). Generalized n-dimensional biomechanical filed analysis using statistical parametric mapping. *Journal of Biomechanics*, 43(10), 1976-1982. <https://doi.org/10.1016/j.jbiomech.2010.03.008>
- Pataky, Todd C. (2012). One-dimensional statistical parametric mapping in Python. *Computer Methods in Biomechanics and Biomedical Engineering*, 15(3), 295-301. <https://doi.org/10.1080/10255842.2010.527837>
- Phadke, Vandana, Braman, Jonathan P., LaPrade, Robert F., & Ludewig, Paula M. (2011). Comparison of glenohumeral motion using different rotation sequences. *Journal of Biomechanics*, 44(4), 700-705. <https://doi.org/10.1016/j.jbiomech.2010.10.042>

- Picerno, Pietro, Viero, Valerio, Donati, Marco, Triossi, Tamara, Tancredi, Virginia, & Melchiorri, Giovanni. (2015). Ambulatory assessment of shoulder abduction strength curve using a single wearable inertial sensor. *Journal of Rehabilitation Research and Development*, 52(2), 171-180. <https://dx.doi.org/10.1682/jrrd.2014.06.0146>
- Raschhofer, Rudolf, Poulios, Nikos, Schimetta, Wolfgang, Kisling, Rudiger, & Mittermaier, Christian. (2017). Early active rehabilitation after arthroscopic rotator cuff repair: a prospective randomized pilot study. *Clinical Rehabilitation*, 31(10), 1332-1339. <https://doi.org/10.1177/0269215517694931>
- Rathi, Sangeeta, Taylor, Nicholas F., & Green, Rodney A. (2017). The upper and lower segments of subscapularis muscle have different roles in glenohumeral joint functioning. *Journal of Biomechanics*, 63, 92-97. <https://doi.org/10.1016/j.jbiomech.2017.08.007>
- Riboni, Daniele, & Bettini, Claudio. (2011). COSAR: hybrid reasoning for context-aware activity recognition. *Personal and Ubiquitous Computing*, 5, 271-289. <https://doi.org/10.1007/s00779-010-0331-7>
- Rossi, Denise M., Resende, Renan A., Hotta, Gisele H., da Fonseca, Sergio T., & de Oliveira, Anamaria S. (2020). Altered Scapular Time Series in Individuals With Subacromial Pain Syndrome. *Journal of Applied Biomechanics*, 36, 113-121. <https://doi.org/10.1123/jab.2019-0247>
- Ryösä, Anssi, Laimi, Katri, Äärimaa, Ville, Lehtimäki, Kaisa, Kukkonen, Juha, & Saltychev, Mikhail. (2017). Surgery or conservative treatment for rotator cuff tear: a meta-analysis. *Disability and Rehabilitation*, 39(14), 1357-1363. <https://doi.org/10.1080/09638288.2016.1198431>

- Saito, Hiroki, Harrold, Meg E., Cavalheri, Vinicius, & McKenna, Leanada. (2018). Scapular focused interventions to improve shoulder pain and function in adults with subacromial pain: A systematic review and meta-analysis. *Physiotherapy Theory and Practice*, 34(9), 653-670. <https://doi.org/10.1080/09593985.2018.1423656>
- Santos, Gabriela L., Russo, Thiago L., Nieuwenhuys, Angela, Monari, Davide, & Desloovere, Kaat. (2018). Kinematic Analysis of a Drinking Task in Chronic Hemiparetic Patients Using Features Analysis and Statistical Parametric Mapping. *Archives of Physical Medicine and Rehabilitation*, 99, 501-511.
- Senbursa, G., Baltaci, G., & Atay, A. (2007). Comparison of conservative treatment with and without manual physical therapy for patients with shoulder impingement syndrome: A prospective, randomized clinical trial. *Knee Surgery, Sports, Traumatology Arthroscopy*, 15, 915–921.
- Sher, Jerry S., Uribe, John W., Posada, Alejandro, Murphy, Brian J., & Zlatkin, Michael B. (1995). Abnormal Findings on Magnetic Resonance Images of Asymptomatic Shoulders. *The Journal of Bone and Joint Surgery*, 77(1), 10-15.
- Tempelhof, Siegbert, Rupp, Stefan, & Seil, Romain. (1999). Age-related prevalence of rotator cuff tears in asymptomatic shoulders. *Journal of Shoulder and Elbow Surgery*, 8(4), 269-299. [https://doi.org/10.1016/S1058-2746\(99\)90148-9](https://doi.org/10.1016/S1058-2746(99)90148-9)
- van Andel, C.J., Wolterbeek, N., Doorenbosch, C.A., Veeger, D.H., & Harlaar, J. (2008). Complete 3D kinematics of upper extremity functional tasks. *Gait Posture*, 27(1), 120–127. <https://doi.org/10.1016/j.gaitpost.2007.03.002>

- van Andel, Carolien, van Hutten, Kim, Eversdijk, Marielle, Veeger, Dirk Jan, & Harlaar, Jaap. (2009). Recording scapular motion using an acromion marker cluster. *Gait and Posture*, 29(1), 123-128. <https://doi.org/10.1016/j.gaitpost.2008.07.012>
- Veeger, H. E. J., & van der Helm, F. C. T. (2007). Shoulder function: The perfect compromise between mobility and stability. *Journal of Biomechanics*, 40(10), 2119-2129. <https://doi.org/10.1016/j.jbiomech.2006.10.016>
- Vidt, Meghan E., Santago II, Anthony C., Marsh, Anthony P., Hegedus, Eric J., Tuohy, Christopher J., Poehling, Gary G., Freehill, Michael T., Miller, Michael E., & Saul, Katherine R. (2016). The effects of a rotator cuff tear on activities of daily living in older adults: A kinematics analysis. *Journal of Biomechanics*, 49(4), 611-617. <https://doi.org/10.1016/j.jbiomech.2016.01.029>
- Vollans, Sam, & Ali, Amjid. (2016). Rotator Cuff Tears. *Surgery (Oxford)*, 34(3), 129-133. <https://doi.org/10.1016/j.mpsur.2016.01.005>
- Winter, David A. (2009). *Biomechanics and motor control of human movement (Fourth Edition)*. Hoboken: John Wiley & Sons, Inc. <https://doi.org/10.1002/9780470549148>
- Worsley, K. J., Evans, A. C., Marrett, S., & Neelin, P. (1992). A Three-Dimensional Statistical Analysis for CBF Activation Studies in Human Brain. *Journal of Cerebral Blood Flow and Metabolism*, 12(6), 900-918. <https://doi-org.proxy.lib.uwaterloo.ca/10.1038/jcbfm.1992.127>
- Wu, Ge, & Cavanaugh, Peter R. (1995). ISB recommendations for standardization in the reporting of kinematic data. *Journal of Biomechanics*, 28(10), 1257-1261. [https://doi.org/10.1016/0021-9290\(95\)00017-C](https://doi.org/10.1016/0021-9290(95)00017-C)

Wu, Ge, van der Helm, Frans C. T., Veeger, H. E. J., Makhsous, Mohsen, Van Roy, Peter, Anglin, Carolyn, Nagels, Jochem, Karduna, Andrew R., McQuade, Kevin, Wang, Xuguang, Werner, Frederick W., & Buchholz, Bryan. (2005). ISB recommendations on definitions of joint coordinate systems of various joints for the reporting of human joint motion – Part II: shoulder, elbow, wrist and hand. *Journal of Biomechanics*, 38(5), 981-992.
<https://doi.org/10.1016/j.jbiomech.2004.05.042>

Appendix A: QuickDASH Questionnaire



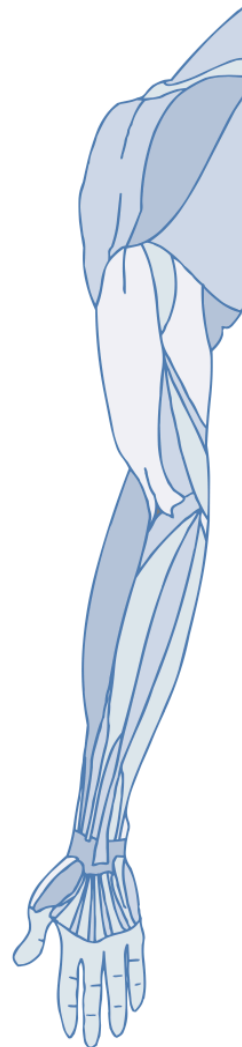
INSTRUCTIONS

This questionnaire asks about your symptoms as well as your ability to perform certain activities.

Please answer *every question*, based on your condition in the last week, by circling the appropriate number.

If you did not have the opportunity to perform an activity in the past week, please make your *best estimate* of which response would be the most accurate.

It doesn't matter which hand or arm you use to perform the activity; please answer based on your ability regardless of how you perform the task.



NAME _____

DATE _____

MR No. _____

QuickDASH

Please rate your ability to do the following activities in the last week by circling the number below the appropriate response.

	NO DIFFICULTY	MILD DIFFICULTY	MODERATE DIFFICULTY	SEVERE DIFFICULTY	UNABLE
1. Open a tight or new jar.	1	2	3	4	5
2. Do heavy household chores (e.g., wash walls, floors).	1	2	3	4	5
3. Carry a shopping bag or briefcase.	1	2	3	4	5
4. Wash your back.	1	2	3	4	5
5. Use a knife to cut food.	1	2	3	4	5
6. Recreational activities in which you take some force or impact through your arm, shoulder or hand (e.g., golf, hammering, tennis, etc.).	1	2	3	4	5

	NOT AT ALL	SLIGHTLY	MODERATELY	QUITE A BIT	EXTREMELY
7. During the past week, to what extent has your arm, shoulder or hand problem interfered with your normal social activities with family, friends, neighbours or groups?	1	2	3	4	5

	NOT LIMITED AT ALL	SLIGHTLY LIMITED	MODERATELY LIMITED	VERY LIMITED	UNABLE
8. During the past week, were you limited in your work or other regular daily activities as a result of your arm, shoulder or hand problem?	1	2	3	4	5

Please rate the severity of the following symptoms in the last week. (circle number)

	NONE	MILD	MODERATE	SEVERE	EXTREME
9. Arm, shoulder or hand pain.	1	2	3	4	5
10. Tingling (pins and needles) in your arm, shoulder or hand.	1	2	3	4	5

	NO DIFFICULTY	MILD DIFFICULTY	MODERATE DIFFICULTY	SEVERE DIFFICULTY	SO MUCH DIFFICULTY THAT I CAN'T SLEEP
11. During the past week, how much difficulty have you had sleeping because of the pain in your arm, shoulder or hand? (circle number)	1	2	3	4	5

QuickDASH DISABILITY/SYMPTOM SCORE = $\left(\left[\frac{\text{sum of } n \text{ responses}}{n} \right] - 1 \right) \times 25$, where n is equal to the number of completed responses.

A QuickDASH score may not be calculated if there is greater than 1 missing item.

QuickDASH

WORK MODULE (OPTIONAL)

The following questions ask about the impact of your arm, shoulder or hand problem on your ability to work (including homemaking if that is your main work role).

Please indicate what your job/work is: _____

I do not work. (You may skip this section.)

Please circle the number that best describes your physical ability in the past week.

Did you have any difficulty:	NO DIFFICULTY	MILD DIFFICULTY	MODERATE DIFFICULTY	SEVERE DIFFICULTY	UNABLE
1. using your usual technique for your work?	1	2	3	4	5
2. doing your usual work because of arm, shoulder or hand pain?	1	2	3	4	5
3. doing your work as well as you would like?	1	2	3	4	5
4. spending your usual amount of time doing your work?	1	2	3	4	5

SPORTS/PERFORMING ARTS MODULE (OPTIONAL)

The following questions relate to the impact of your arm, shoulder or hand problem on playing *your musical instrument or sport or both*. If you play more than one sport or instrument (or play both), please answer with respect to that activity which is most important to you.

Please indicate the sport or instrument which is most important to you: _____

I do not play a sport or an instrument. (You may skip this section.)

Please circle the number that best describes your physical ability in the past week.

Did you have any difficulty:	NO DIFFICULTY	MILD DIFFICULTY	MODERATE DIFFICULTY	SEVERE DIFFICULTY	UNABLE
1. using your usual technique for playing your instrument or sport?	1	2	3	4	5
2. playing your musical instrument or sport because of arm, shoulder or hand pain?	1	2	3	4	5
3. playing your musical instrument or sport as well as you would like?	1	2	3	4	5
4. spending your usual amount of time practising or playing your instrument or sport?	1	2	3	4	5

SCORING THE OPTIONAL MODULES: Add up assigned values for each response; divide by 4 (number of items); subtract 1; multiply by 25.

An optional module score may **not** be calculated if there are any missing items.

Appendix B: Individual Participant Results

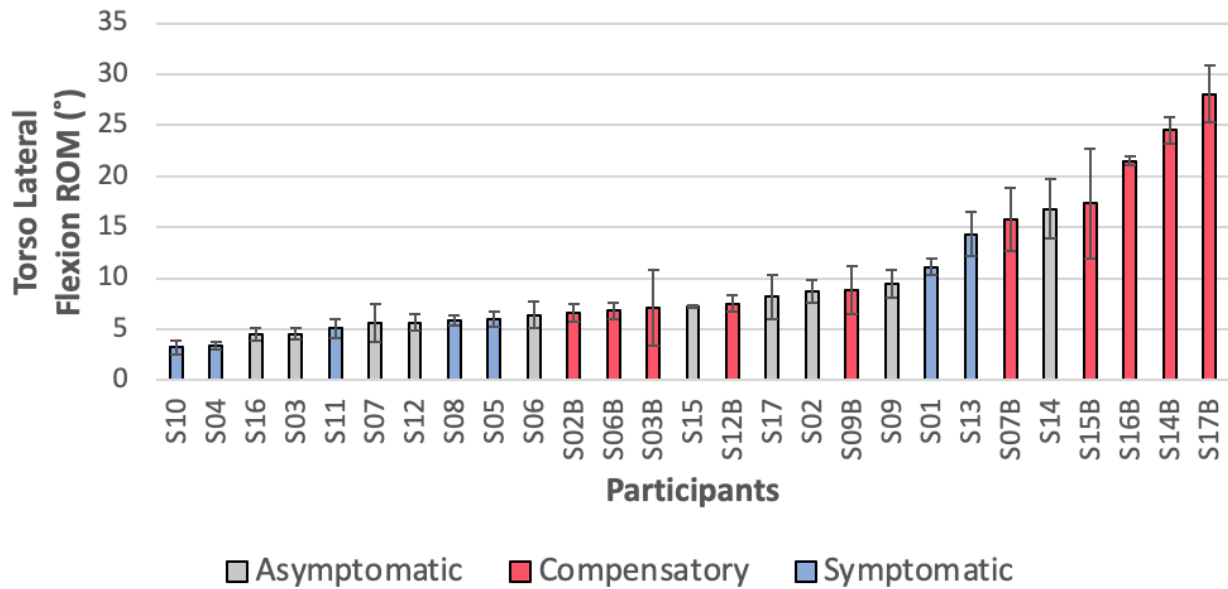


Figure 33: Mean torso lateral flexion ROM for the active assisted shoulder flexion exercise of all participants. Error bars indicate standard deviation. Participants with a “B” after their subject number signifies the same asymptomatic participant performing compensatory movement cues.

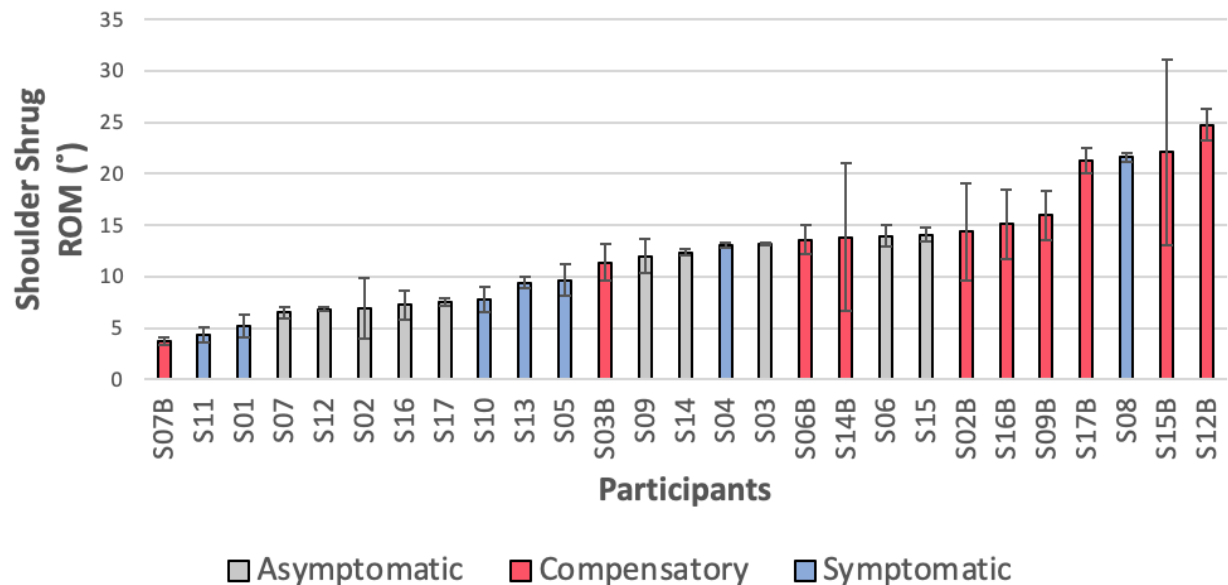


Figure 34: Mean shoulder shrug ROM for the active assisted shoulder flexion exercise of all participants. Error bars indicate standard deviation. Participants with a “B” after their subject number signifies the same asymptomatic participant performing compensatory movement cues.

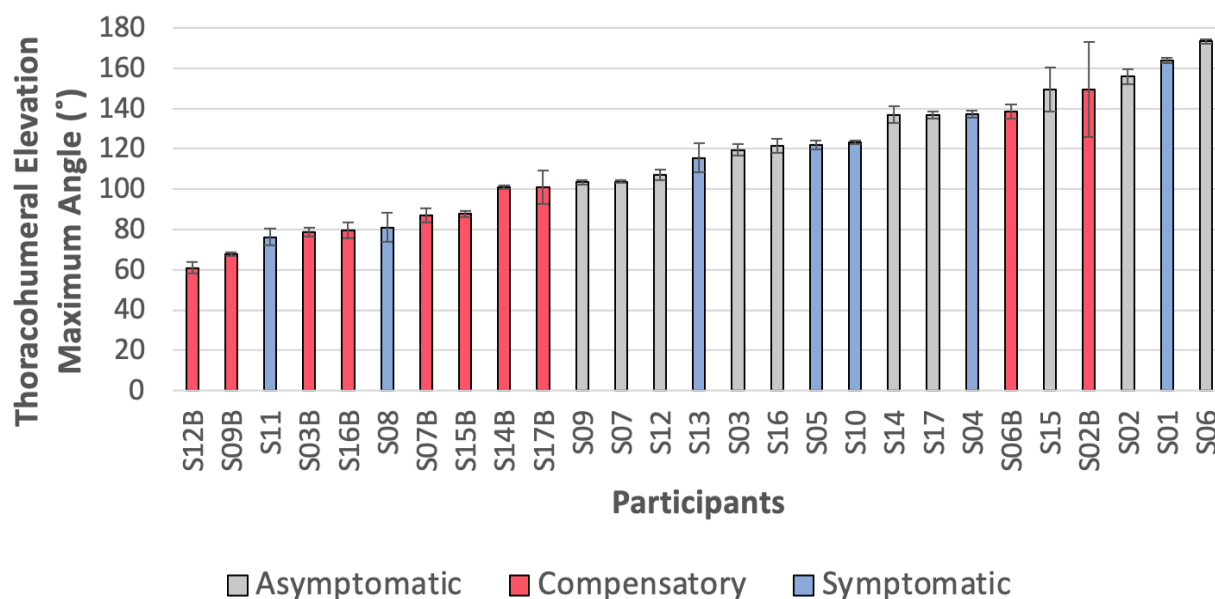


Figure 35: Mean thoracohumeral elevation maximum angle for the active assisted shoulder scaption exercise of all participants. Error bars indicate standard deviation. Participants with a “B” after their subject number signifies the same asymptomatic participant performing compensatory movement cues.

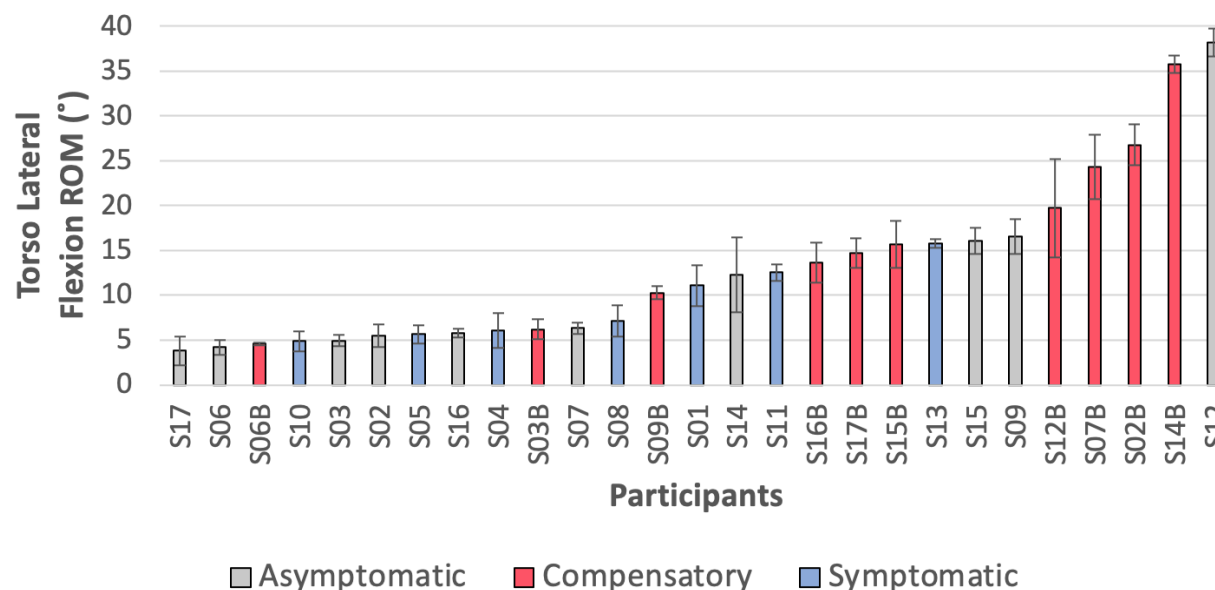


Figure 36: Mean torso lateral flexion ROM for the active assisted shoulder scaption exercise of all participants. Error bars indicate standard deviation. Participants with a “B” after their subject number signifies the same asymptomatic participant performing compensatory movement cues.

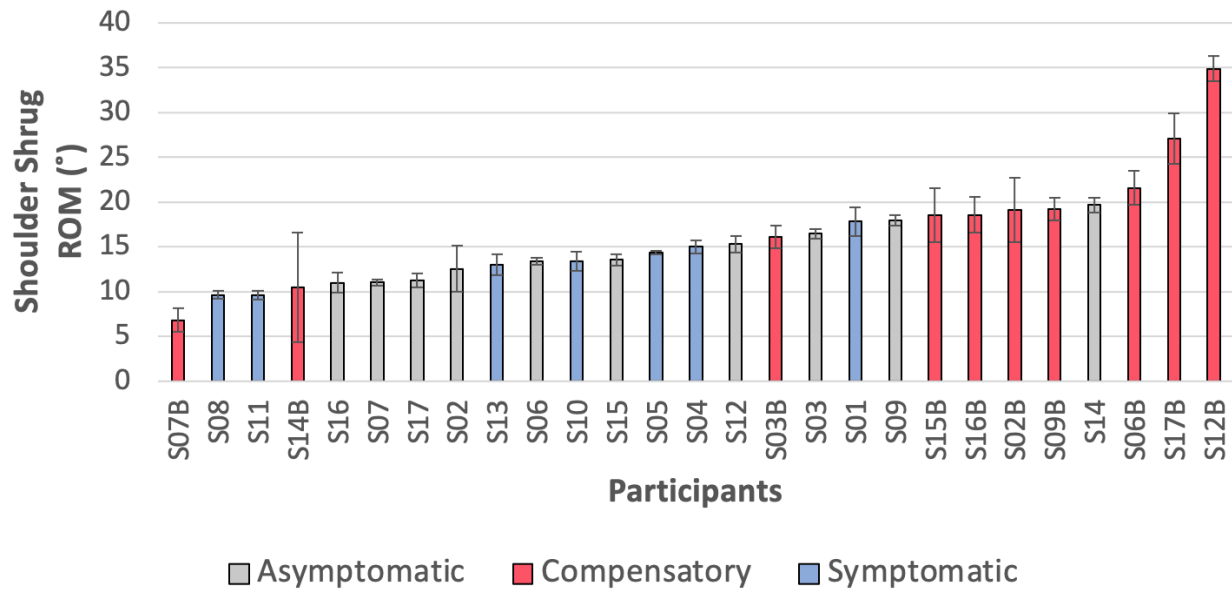


Figure 37: Mean shoulder shrug ROM for the active assisted shoulder scaption exercise of all participants. Error bars indicate standard deviation. Participants with a “B” after their subject number signifies the same asymptomatic participant performing compensatory movement cues.

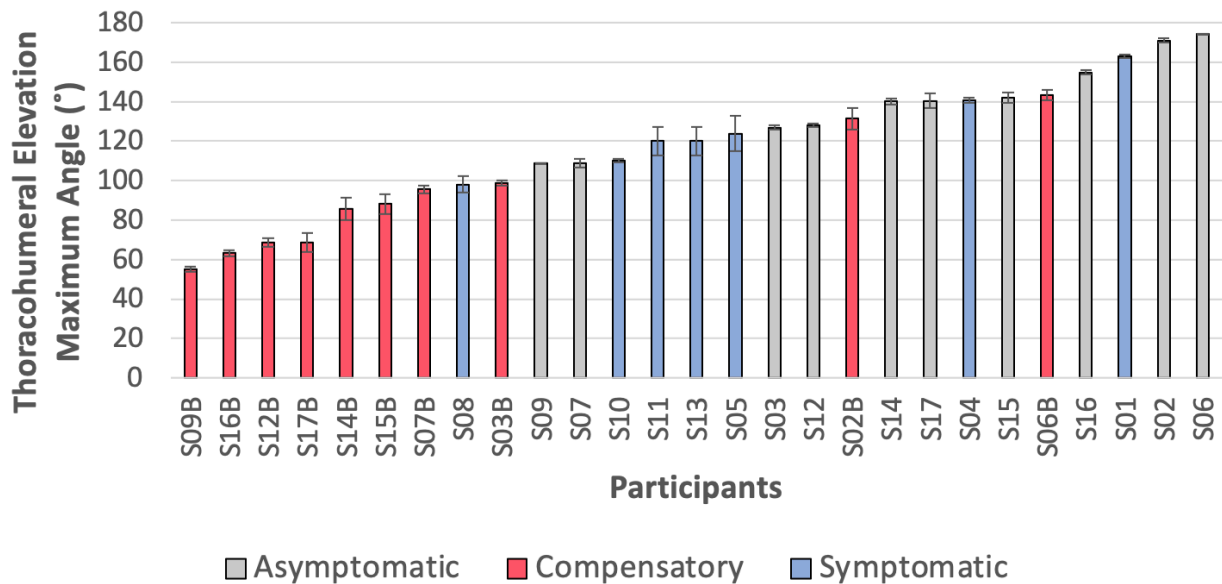


Figure 38: Mean thoracohumeral elevation maximum angle for the shoulder abduction exercise of all participants. Error bars indicate standard deviation. Participants with a “B” after their subject number signifies the same asymptomatic participant performing compensatory movement cues.

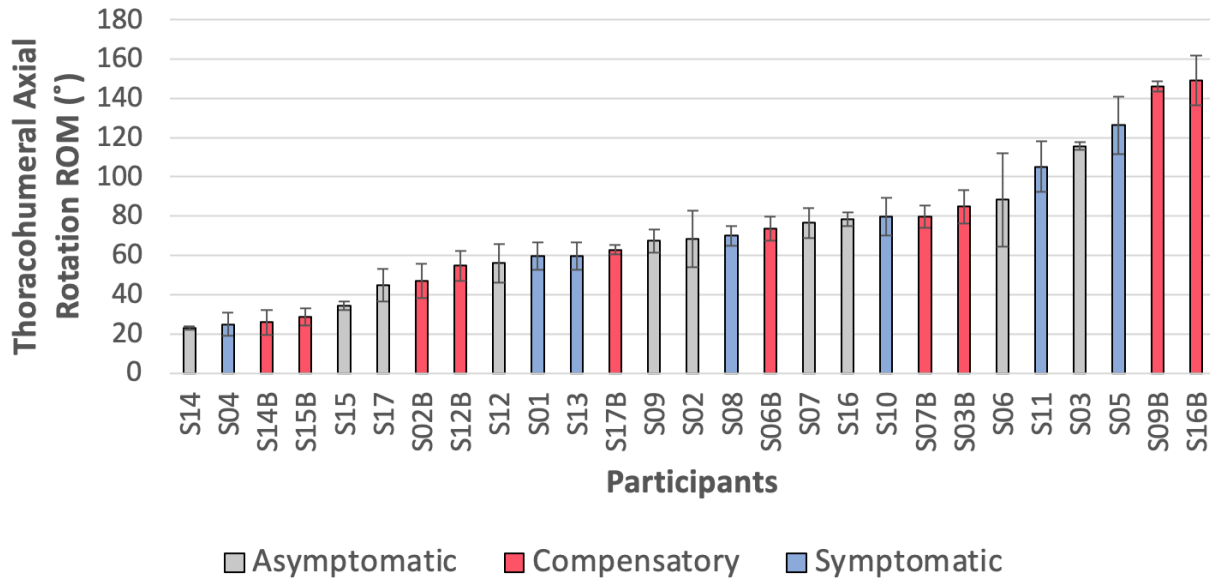


Figure 39: Mean thoracohumeral axial rotation ROM for the shoulder abduction exercise of all participants. Error bars indicate standard deviation. Participants with a “B” after their subject number signifies the same asymptomatic participant performing compensatory movement cues.

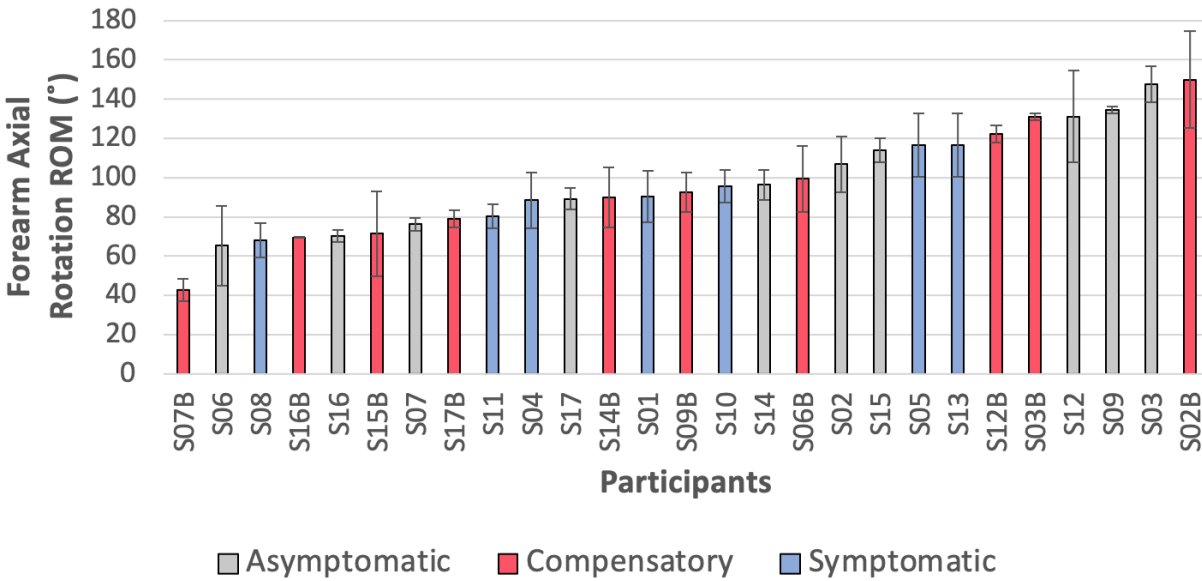


Figure 40: Mean forearm axial rotation ROM for the shoulder abduction exercise of all participants. Error bars indicate standard deviation. Participants with a “B” after their subject number signifies the same asymptomatic participant performing compensatory movement cues.

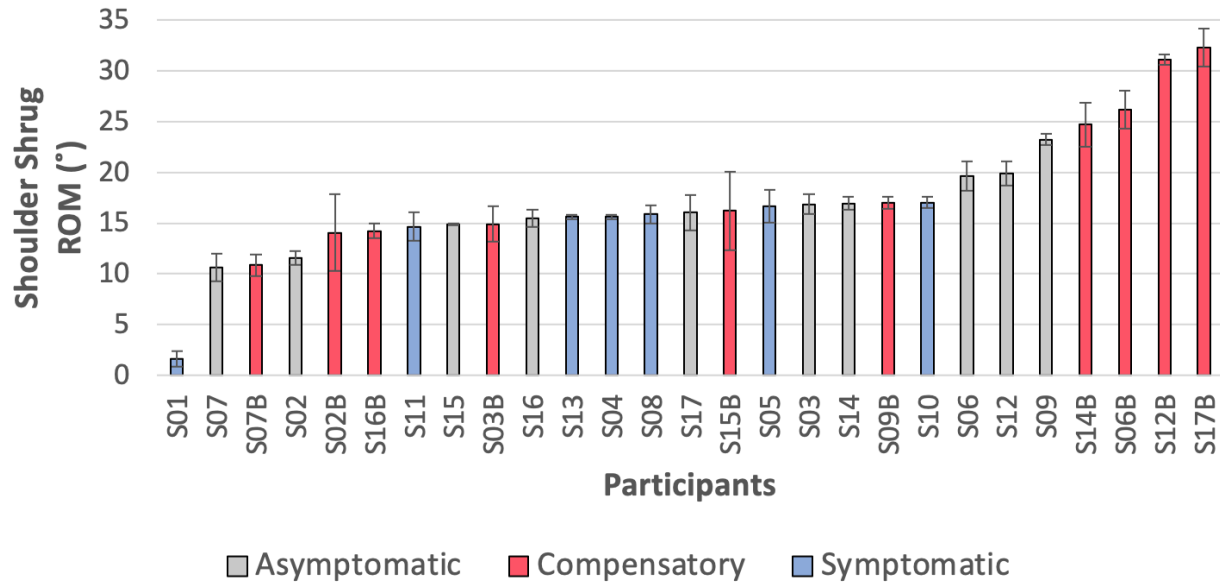


Figure 41: Mean shoulder shrug ROM for the shoulder abduction exercise of all participants. Error bars indicate standard deviation. Participants with a “B” after their subject number signifies the same asymptomatic participant performing compensatory movement cues.

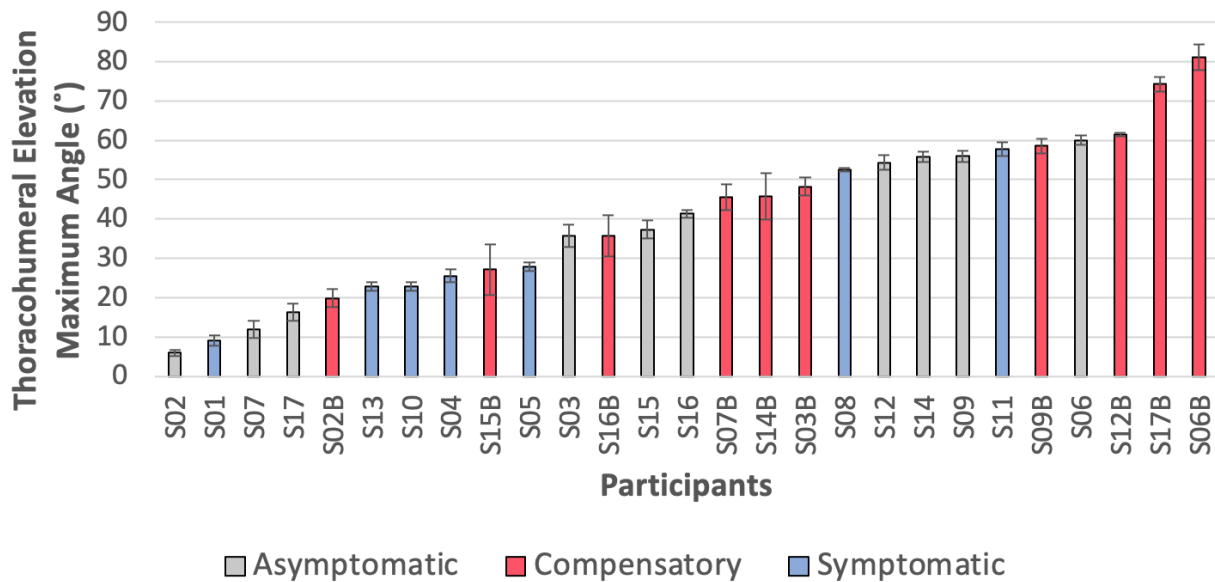
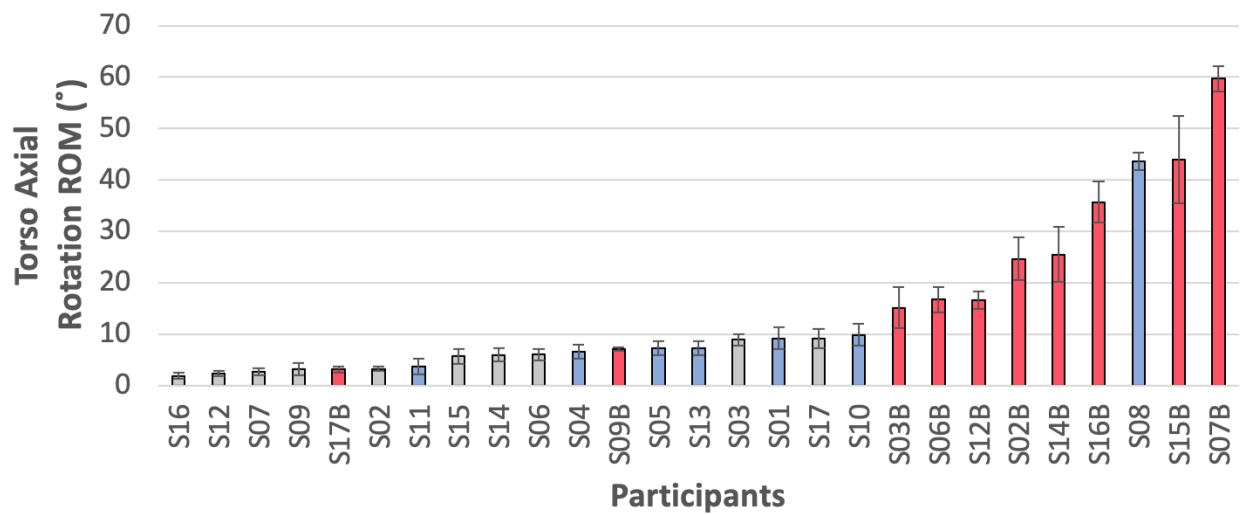
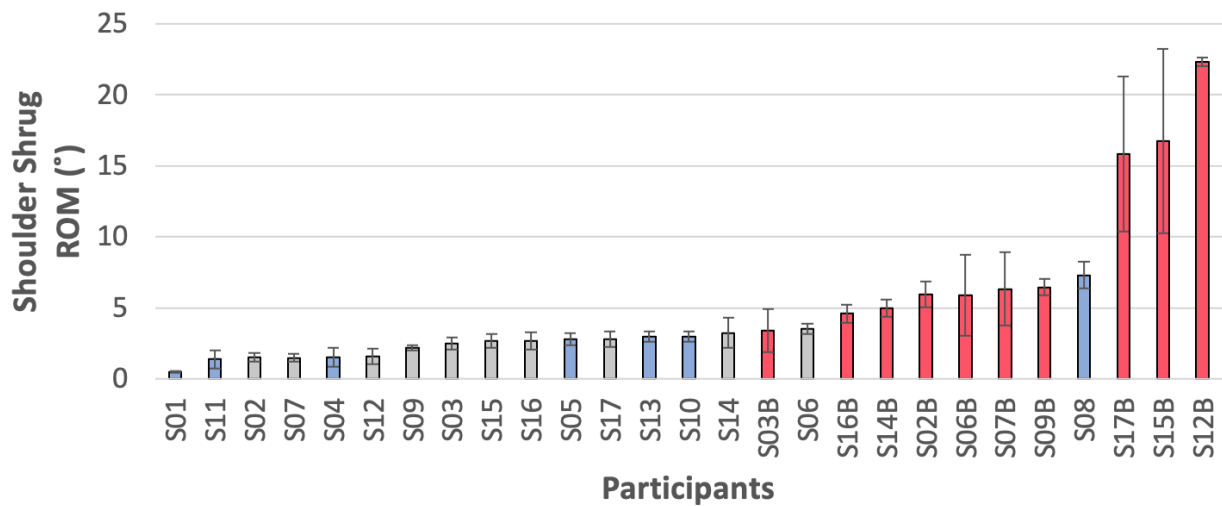


Figure 42: Mean thoracohumeral elevation maximum angle for the internal rotation exercise of all participants. Error bars indicate standard deviation. Participants with a “B” after their subject number signifies the same asymptomatic participant performing compensatory movement cues.



Asymptomatic
 Compensatory
 Symptomatic

Figure 43: Mean torso axial rotation ROM for the internal rotation exercise of all participants. Error bars indicate standard deviation. Participants with a “B” after their subject number signifies the same asymptomatic participant performing compensatory movement cues.



Asymptomatic
 Compensatory
 Symptomatic

Figure 44: Mean shoulder shrug ROM for the internal rotation exercise of all participants. Error bars indicate standard deviation. Participants with a “B” after their subject number signifies the same asymptomatic participant performing compensatory movement cues.

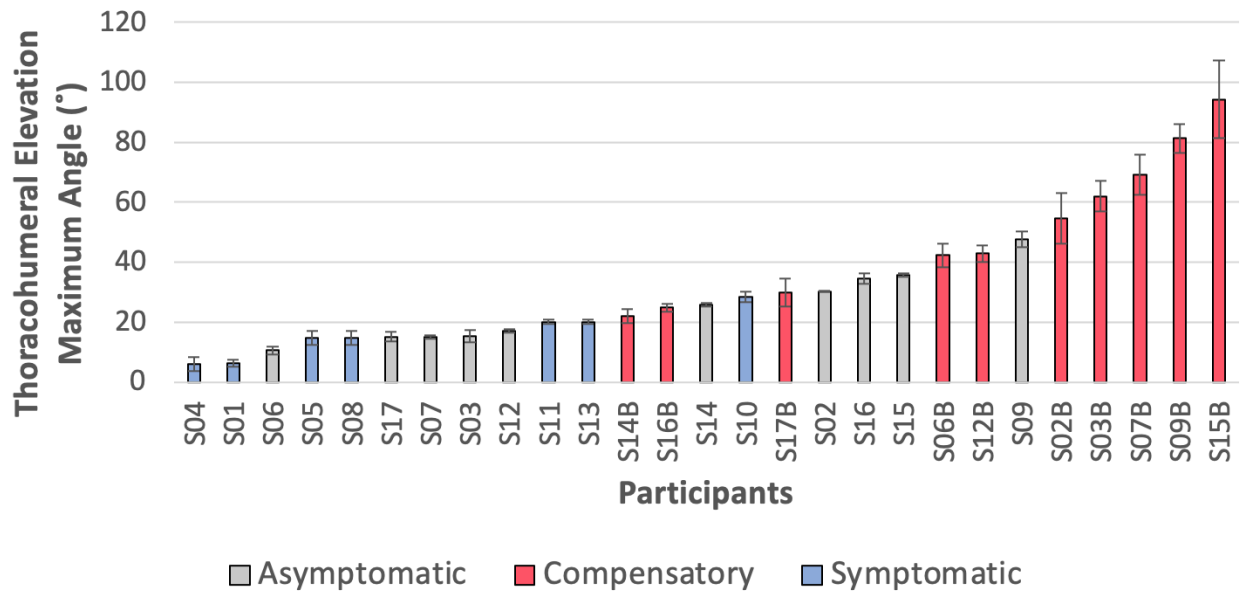


Figure 45: Mean thoracohumeral elevation maximum angle for the external rotation exercise of all participants. Error bars indicate standard deviation. Participants with a “B” after their subject number signifies the same asymptomatic participant performing compensatory movement cues.

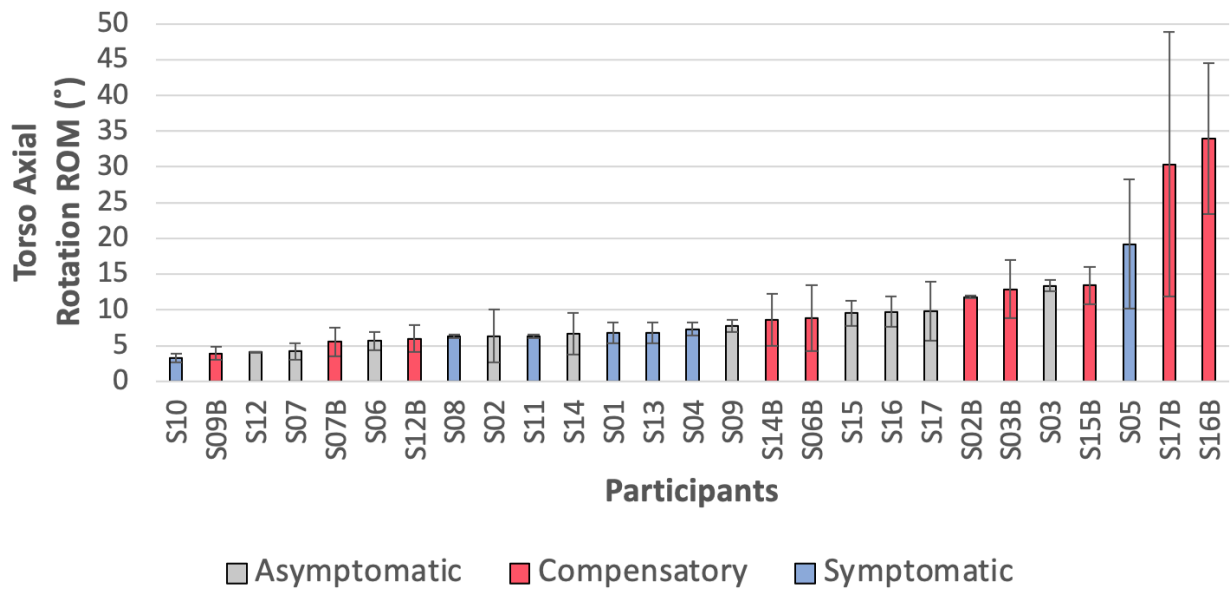


Figure 46: Mean torso axial rotation ROM for the external rotation exercise of all participants. Error bars indicate standard deviation. Participants with a “B” after their subject number signifies the same asymptomatic participant performing compensatory movement cues.

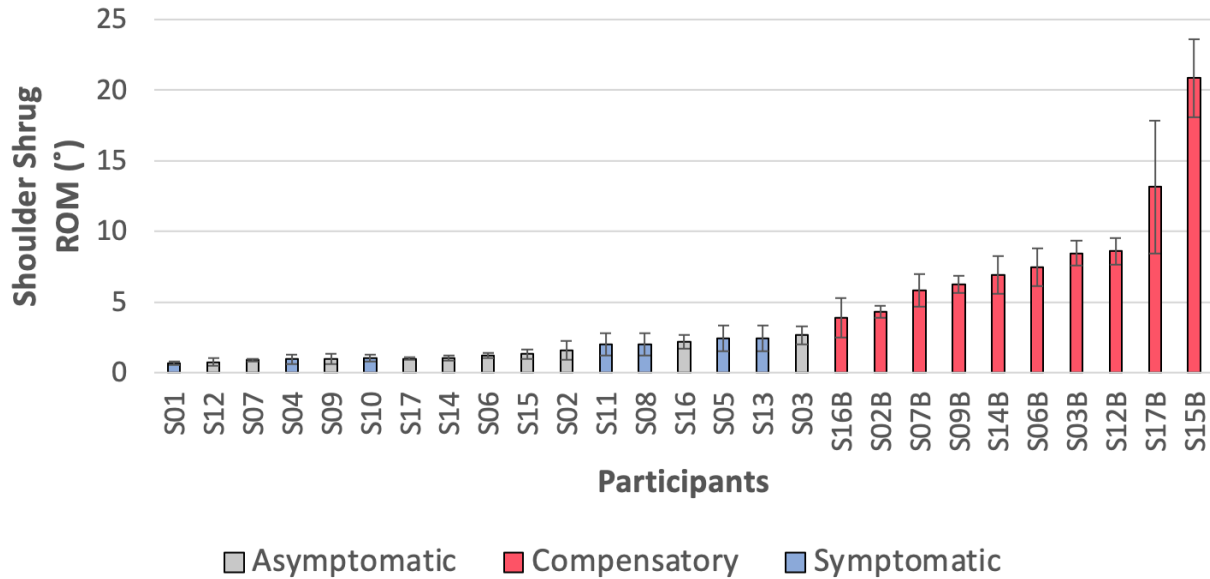


Figure 47: Mean shoulder shrug ROM for the external rotation exercise of all participants. Error bars indicate standard deviation. Participants with a “B” after their subject number signifies the same asymptomatic participant performing compensatory movement cues.

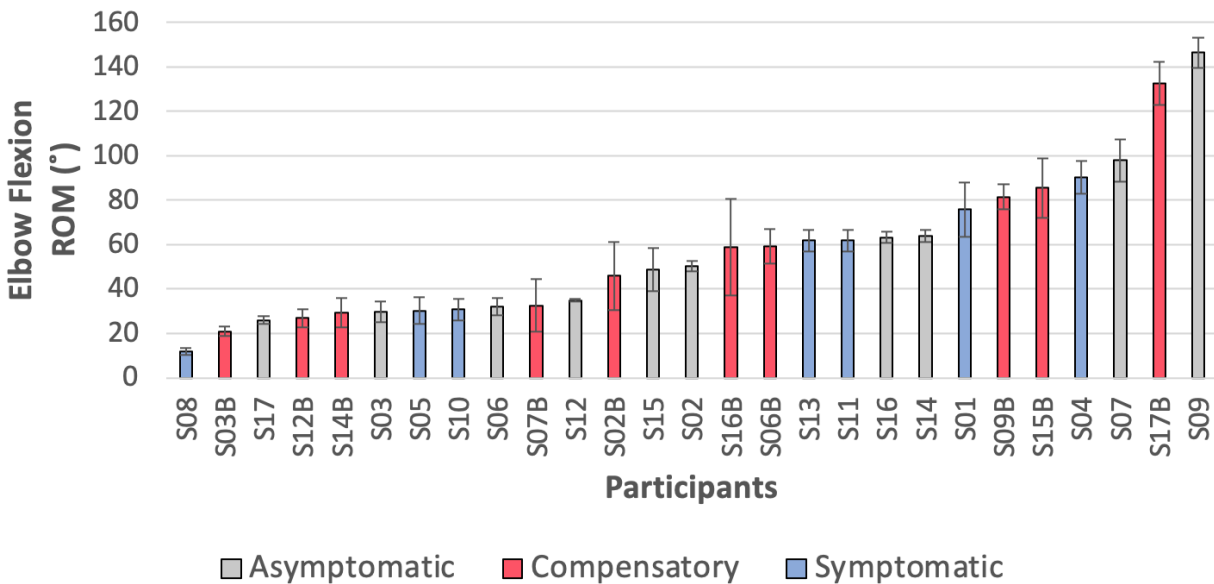


Figure 48: Mean elbow flexion ROM for the standing row exercise of all participants. Error bars indicate standard deviation. Participants with a “B” after their subject number signifies the same asymptomatic participant performing compensatory movement cues.

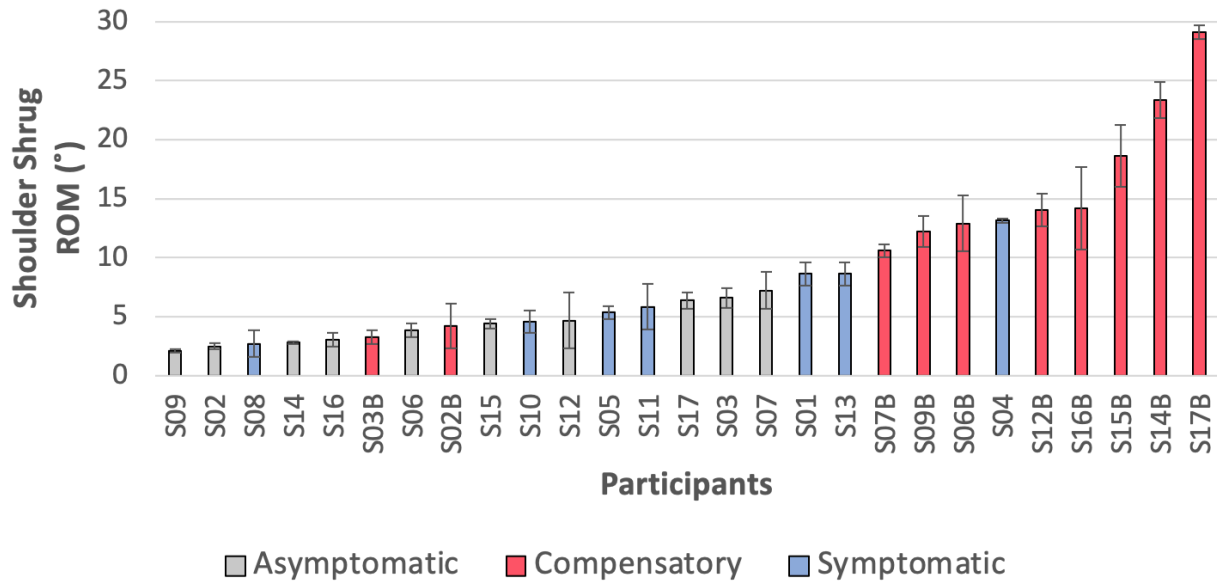


Figure 49: Mean shoulder shrug ROM for the standing row exercise of all participants. Error bars indicate standard deviation. Participants with a “B” after their subject number signifies the same asymptomatic participant performing compensatory movement cues.